Cellulose Nanocrystals/Polymer Nanocomposites for Application in Adhesives

Alexandra Ouzas

Thesis submitted in partial fulfillment of the requirements

for the degree of

Master of Applied Science in Chemical Engineering

Department of Chemical and Biological Engineering

Faculty of Engineering

uOttawa

Abstract

Cellulose nanocrystals (CNCs) are rod-shaped nanoparticles derived from cellulose, the most abundant polymer in the world. CNCs are as strong as Kevlar™, have a high aspect ratio (traditional nanoparticles are spherical) and thus, a higher surface area, which makes them ideal for use in nanocomposites. In addition, CNCs are considered the only safe nanomaterial according to Health Canada.

In this thesis, CNCs were used to produce nanocomposites via in situ semi-batch emulsion polymerization. The target application for these nanocomposites was as pressure sensitive adhesives (PSAs). In the past, CNCs have been blended with polymers rather than added in situ. Emulsion polymerization is considered a more sustainable method to synthesize polymers compared to say, solution polymerization. However, adhesives synthesized using this method tend to have a lower shear strength due to poor gel network formation. As a result, conventional emulsion-based PSAs suffer from the inability to increase certain adhesive properties (e.g., tack and peel strength) while simultaneously increasing shear strength. In this thesis, we demonstrate how the use of CNCs via in situ emulsion polymerization overcomes this classic problem.

Two polymer systems were tested: isobutyl acrylate (IBA)/n-butyl acrylate (BA)/methyl methacrylate (MMA) and 2-ethylhexyl acrylate (EHA)/BA/MMA. The use of CNC with IBA, a relatively hydrophilic monomer, rather than with EHA, a highly hydrophobic monomer, resulted in the simultaneous improvement of tack, peel strength and shear strength of the PSA films. Dynamic mechanical analysis (DMA) also indicated improved storage and loss moduli with increasing CNC content, further supporting the reinforcing effect of the CNCs within the PSA. EHA followed similar trends as IBA for conversion, particle size, viscosity, pH, glass transition temperature and gel content. On the other hand, the use of CNC with EHA yielded less improvement in adhesive properties due to poor dispersion of the CNCs because of the hydrophobic repulsion by the EHA.

Resumé

Les nanocristaux de cellulose (NCC) sont des nanoparticules en forme de tige dérivées de la cellulose, le polymère le plus abondant au monde. Les NCC sont aussi fortes que le Kevlar™, ont un rapport d'aspect élevé (les nanoparticules traditionnelles sont sphériques) et ont donc une aire de surface supérieure, ce qui les rend idéales pour les nanocomposés. En outre, les CNC sont considérés comme le seul nanomatériel non-hazardeux selon Santé Canada.

Dans cette thèse, les NCC ont été utilisés pour produire des nanocomposés via une polymérisation en émulsion semi-discontinue en situ. L'application cible de ces nanocomposés était comme adhésifs sensibles à la pression (ASP). Dans le passé, les CNC ont été mélangés avec des polymères plutôt que d'être ajoutés en situ. La polymérisation en émulsion est considérée comme une méthode plus durable pour synthétiser des polymères par rapport à la polymérisation en solution. Cependant, les adhésifs synthétisés à l'aide de ce procédé ont tendance à avoir une résistance au cisaillement plus faible en raison d'une mauvaise formation de réseau de gel. En conséquence, les ASP conventionnels à base d'émulsion souffrent de l'incapacité d'augmenter certaines propriétés adhésives (par exemple, l'adhérence et la résistance au pelage) tout en augmentant simultanément la résistance au cisaillement. Dans cette thèse, nous démontrons comment l'utilisation des NCC par polymérisation en émulsion en situ surpasse ce problème classique.

Deux systèmes polymères ont été testés: acrylate d'isobutyle (IBA)/acrylate de n-butyle (BA)/ méthacrylate de méthyle (MMA) et acrylate de 2-éthylhexyle (EHA)/BA/MMA. L'utilisation des NCC avec l'IBA, un monomère relativement hydrophile, plutôt qu'avec l'EHA, un monomère hautement hydrophobe, a entraîné une amélioration simultanée de l'adhérence, de la résistance au pelage et de la résistance au cisaillement des films ASP. L'analyse mécanique dynamique a également indiqué l'amélioration des modules de stockage et de perte avec l'augmentation du contenu NCC, en soutenant davantage l'effet de renforcement des NCC dans l'ASP. EHA a suivi des tendances similaires que l'IBA pour la conversion, la taille des particules, la viscosité, le pH, la température de transition vitreuse et la teneur en gel. D'autre part, l'utilisation des NCC avec l'EHA a donné moins d'amélioration des propriétés adhésives en raison de la faible dispersion des NCC en raison de la répulsion hydrophobe par l'EHA.

Statement of Contributions

I declare that I am the sole author of this thesis. All polymerizations, particle size, viscosity, glass transition temperature, gel content, NMR, adhesive testing and dynamic mechanical analysis tests were performed by myself. Dr. Elina Niinivaara from McMaster University kindly provided all AFM and TEM images. Editorial comments and technical guidance were provided by my thesis supervisor, Marc A. Dubé in the Department of Chemical and Biological Engineering.

Alexandra Ouzas Date: 05/10/2017

Acknowledgements

I would like to express my gratitude to my supervisor, Dr. Marc A. Dubé for all of his positive encouragement and help throughout my thesis work. I am also grateful for the patient advice and guidance from Dr. Emily D. Cranston from McMaster University, who helped with all CNC related issues. I would also like to thank all members of our research group: Yujie, Sara, Shidan, Shanshan, Vida and Amir. You have all been there to help with any minor (or major!) crises and for lab dance parties. Also, a big thank you to Elli, who was able to get amazing images of the latexes. I would also like to thank the "cool office"; you helped me discover my hidden talent (crosswords). Lastly, I would like to thank my boyfriend Alex and my family. You have always been there for me and you tolerate me!

Financial support through the Natural Sciences and Engineering Research Council (NSERC) of Canada, the Canada Foundation for Innovation (CFI), Celluforce and FPInnovations is also greatly appreciated.

Table of Contents

List of Figures

List of Tables

Nomenclature/Abbreviations

AA	Acrylic acid
AFM	Atomic force microscopy
BA	n-butyl acrylate
CMC	Critical micelle concentration
CNC	Cellulose nanocrystal
DDI water	Distilled, deionized water
DMA	Dynamic mechanical analysis
DSC	Differential scanning calorimetry
EHA	2-ethylhexyl acrylate
^{1}H-NMR	Proton nuclear magnetic resonance spectroscopy
IBA	Isobutyl acrylate
KPS	Potassium persulfate
MMA	Methyl methacrylate
PSA	Pressure sensitive adhesive
SDS	Sodium dodecyl sulfate
TEM	Transmission electron microscopy
T_g	Glass transition temperature [^{o}C]

Chapter 1: Introduction and Objectives

Pressure sensitive adhesives (PSAs) are polymers which can bond with a surface when light pressure is applied. Common examples are postage stamps, adhesive labels and tapes, and Post-it™ notes. PSAs must be sticky (or tacky) at room temperature to be used in these applications. The physical properties can be adjusted depending on the application; for example, a PSA used for a Post-it™ note should not leave residue behind on the surface it is being applied to and would require low peel strength. Well over 2400 kilotons of PSAs are made annually worldwide and are used in over 25000 products.[1], [2] However, as with many polymers, PSAs are made with non-renewable resources (originating primarily from fossil fuels) and there is significant interest in making their production more sustainable.[3]

Generally, PSA formulations use a mixture of monomers to exploit the qualities of each respective homopolymer. The polymer compositions can be tailored to specific applications and desired mechanical properties. A monomer with a low homopolymer glass transition temperature (T_g) (below 0 ^oC), which yields a soft polymer at room temperature, is often used in combination with a monomer with a higher homopolymer T_g, which provides strength and is considered a hard polymer. This combination creates the desired tack and strong mechanical properties of a PSA. The desired properties from particular homopolymers can be combined to form a copolymer with a blend of mechanical properties to obtain specific adhesive performance.[4] Regardless of the application, the T_g must be well below the application temperature.[5] Typical PSA formulations result in a polymer T_g between -50 and 0 ^oC which gives the polymer a certain degree of mobility; in other words, flowability. Various additives can be used to further influence the mechanical properties of adhesives. Chain transfer agents, tackifiers, peel modifiers and cross-linking agents are all commonly used. With a goal of producing more sustainable PSAs, it is essential to replace any of these additives that present toxicity. Alternatives to these substances should be renewable, non-toxic and should not sacrifice adhesive performance.

In this thesis, four monomers will be used in PSA formulations. These include: isobutyl acrylate (IBA), n-butyl acrylate (BA), methyl methacrylate (MMA), and 2-ethylhexyl acrylate (EHA)

(Figure 1-1). These are typical monomers used in PSA production where the hard monomer is MMA, and the soft monomer component is a mixture of BA, IBA or EHA.[1], [6], [7]

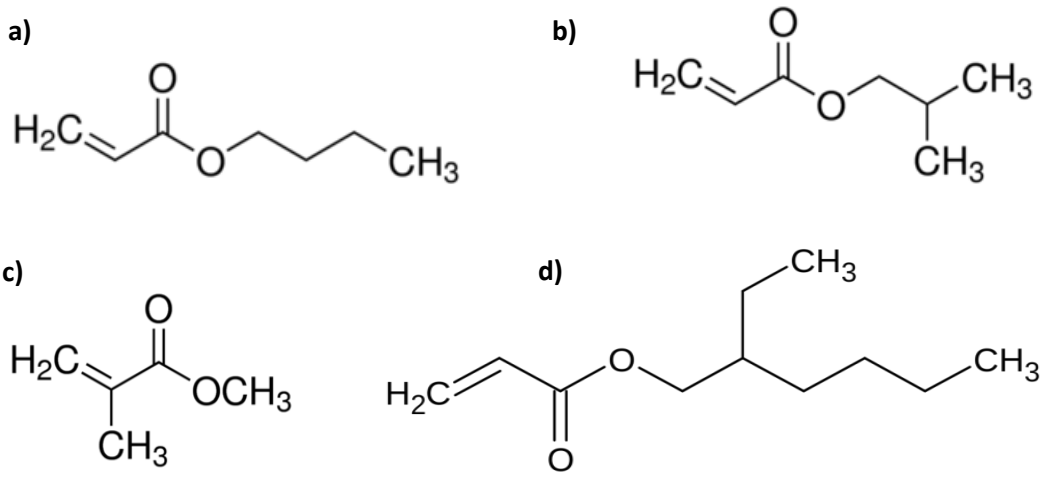

Figure 1-1: Structure of monomers: a) BA b) IBA c) MMA d) EHA

PSAs are used at ambient temperatures. Thus, the T_g of the PSA must be below the intended use temperature to avoid the transition from a tacky polymer to a hard, glassy one. The traditional target temperature is -15˚C to -5˚C, however even lower temperatures are used.[8] The selected T_g will have an impact on the flowability of the PSA and thus influence adhesive properties. The T_gs of all relevant homopolymers are summarized in Table 1-1.

Table 1-1: Homopolymer glass transition temperatures of monomers in this study (as reported from Sigma Aldrich)

Monomer	Homopolymer T_g [ºC]
MMA	105
BA	-54
IBA	-24
EHA	-50*

*Lower values of -70˚C have also been reported

MMA can be polymerized to poly(methyl methacrylate), a hard polymer with a high glass transition temperature. It is a glassy polymer whose properties can be manipulated with co-

polymerization.[9] As a homopolymer, MMA will not behave as a PSA due to its high glass transition temperature. However, it will improve the performance of a PSA when co-polymerized, due to its ability to impart high cohesive strength.

BA is used in toners, paints, and coatings.[10], [11] It can be co- and terpolymerized with many common monomers such as MMA, EHA, styrene, and butyl methacrylate.[11], [12] It has also been terpolymerized with styrene and conjugated linoleic acid for use in PSAs.[13] BA and MMA have also been used in paints used for art.[12] IBA is similar in structure and properties to BA (Figure 1-1) and is consequently used similar applications. EHA, BA and MMA have also been used in emulsion based PSAs to determine which blend of hard to soft monomers is required.

The solubility of each monomer is often important, especially when working in emulsion polymerization (Emulsion polymerization is increasingly preferred for PSA production because it uses a water-based medium and is therefore a "greener" process). The solubility in water of each monomer is shown in Table 1-2. Both BA and IBA can be considered slightly soluble in water and MMA, moderately soluble. EHA is considered highly hydrophobic.

Table 1-2: Solubility of monomers in water

Monomer	Solubility in water (g/L) at 20˚C
BA	1.4
MMA	15.9
IBA	2
EHA	<0.001

PSA Production

PSAs can be made by way of various polymerization methods: solution, hot melt and emulsion polymerization. Solution polymerization requires the use of a solvent which will dissolve the initiator and monomer, as well as the resulting polymer. It must be added in high enough quantities to allow for proper mixing of the reaction solution; otherwise, viscosity will interfere with the reaction.[4] Although an issue for other applications, solution polymerization does not require extra processing since the typical applications are in paints and adhesives. The solvent is typically evaporated at the film formation stage. Although this method provides good control over reaction conditions and requires little processing, it is not normally considered a "green" method. Typically,

harsh solvents are used for the solution polymerization, which pose health and safety problems. Typical solvents used are acetone, toluene and ethyl acetate.[14], [15] These solvents are very volatile, making the PSA unsafe when it is drying.

Hot melt PSAs are polymerized and removed using an extrusion process. The resulting polymer is a solid and does not have a carrier liquid, as with other PSA formation methods. To use the product, it must be melted. Although this is practical for automated processes, it can limit their use. A classic example of a hot melt adhesive is the glue used in a glue gun. The advantages are that they have a long shelf life and reduce the use of volatile solvents.

Emulsion polymerization is also used to formulate PSAs. Because the carrier is water rather than a solvent, it is a safer method for polymerization. Using emulsion polymerization also provides good temperature control (no risk of a runaway reaction).[4] The resulting PSA will not require processing before use; however it does requires time to cure and evaporate the water. Also, there is less process risk associated with this method since water is not harmful. This method is used commonly to produce PSAs.[1], [7], [16]–[18] Emulsion polymerization was the method used to perform all polymerizations in this thesis.

Emulsion Polymerization

Emulsion polymerization begins with formation of an emulsion – monomer, deionized water and surfactant are mixed. Surfactants are typically long-chain molecules having one end which is hydrophobic (usually a hydrocarbon chain) and the other end being hydrophilic. Sodium dodecyl sulfate (SDS) was used as the emulsifier in this thesis (Figure 1-2).

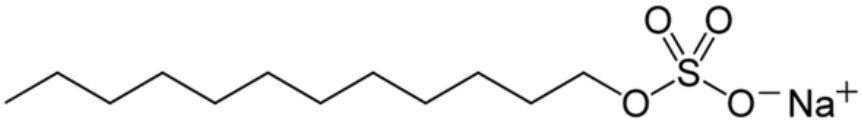

Figure 1-2: Sodium dodecyl sulfate (SDS) structure

When increasing the concentration of surfactant in an aqueous solution, a critical micelle concentration (CMC) is reached wherein the surfactant begins to form micelles (aggregates of surfactant) in which their hydrophilic ends point outwards and are in contact with the water phase

while their hydrophobic ends remain in the micellar core. When hydrophobic monomers are present, they will diffuse into the micelles. Thus, at the formulation stage of an emulsion polymerization, there will be small amounts of monomer dissolved in the water, large monomer droplets in suspension, and monomer-swollen micelles. A free-radical initiator is then needed to start the reaction.

When the initiator, typically a water-soluble compound such as potassium persulfate (Figure 1-3), is added, it will homolytically cleave due to heat and two radicals will form. The free radicals will react with monomer dissolved in the water phase to form oligomeric radicals. These oligomeric radicals will grow to a certain length until they become hydrophobic enough to enter the monomer-swollen micelles. Because of the higher surface area, polymerization will occur principally within the micelles as opposed to the monomer droplets. The entry of an oligomeric radical into a monomer-swollen micelle is referred to as particle nucleation. Once all the monomer-swollen micelles have been nucleated, no further particle formation is normally expected. Henceforth, oligomeric radicals enter the polymer particles to either terminate an existing polymer chain or initiate renewed polymerization within the particle. As monomer in the particle is consumed via propagation, monomer will diffuse from the droplets into the particles to maintain a thermodynamic equilibrium. Eventually, the monomer droplets will be depleted and polymerization will continue within the particles until the monomer has been fully consumed.[4]

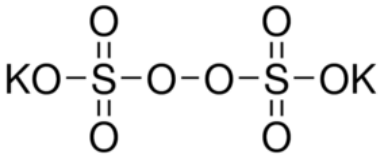

Figure 1-3: Potassium persulfate (KPS) structure

Additional reactions can occur in the polymer particles which include chain transfer, where the active chain can transfer to another molecule (e.g., monomer or polymer). This results in lower molecular weight polymer chains as the active reaction site moves to a new molecule and will continue to propagate. Cross-linking is another important reaction that can occur during

polymerization. This results in linked networks within the polymer matrix resulting in a strong, more reinforced material.[4]

Adhesive Properties

There are three main properties to monitor when measuring the performance of an adhesive: tack, peel strength and shear strength. Tack is a measure of the adhesive's ability to form a bond with a substrate when light pressure is applied. Peel strength is the amount of force required to remove the adhesives from a substrate at a specific angle (usually 90˚ or 180˚). Shear strength is a measure of the internal, or cohesive strength, of the adhesive. All three properties are interrelated and are influenced by the polymer properties. Depending on the application of the adhesive, the composition can be manipulated to achieve the desired performance. The chemical factors which affect each adhesive property can be found in Table 1-3.

Table 1-3: Chemical factors affecting adhesive properties. Adapted from [18] **Tables 7-9**

Factors	Tack	Peel Strength	Shear Strength
Soft Monomer	Increases	Decreases	Decreases
Hard Monomer	Decreases	Shows maximum	Increases
Polar Monomer	Decreases	Shows maximum	Increases
Cross-linking agents	Decreases	Show maximum	Increases

Typically, tack will increase when lower T_g monomers are used. The ability of the adhesive to form a quick bond with the surface will be better as the softer monomer will "flow" more at room temperature whereas using a harder monomer will have the opposite effect.[18] Adding a cross-linker will reduce the chain mobility of the polymer and therefore reduce the tack. Peel strength will be at a maximum when a harder monomer is used. This is caused by the increase in the stiffness of the adhesive; eventually a decrease will be seen if too much high T_g monomer is used as it will no longer form a bond with the substrate surface. Lastly, shear strength will improve if a network (i.e., cross-links) or strong entanglements are formed in the PSA film. Because these properties are all inter-related, a balance has to be found in order to optimize them.[18] The need for a balance to be struck between these properties, often means sacrificing performance in some way. For example, if shear strength is increased, the peel strength and tack will usually decrease. Therein lies a classic problem in emulsion-based adhesives. Ideally, it would be easier to tailor a PSA formulation to a specific application if there was no risk of limiting a particular property. This

phenomenon is especially true in emulsion polymerization where gel network formation in the resulting PSA films usually is not continuous, as it would be with solution polymerization. The network within each individual latex particle will be continuous, but during film formation, links between the latex particles do not form readily.[19]–[21] Thus, latexes prepared via emulsion polymerization typically have lower shear strengths than those prepared via solution polymerization.

Polymer Composites

A composite is made up of two materials with different mechanical properties to achieve a specific application performance. Polymer composites allow for fine tuning of desired performance by changing the composition of the materials added. Nanoparticles can be used in polymerization to reinforce a polymer structure and improve certain properties. Because nanoparticles have a high surface area, they will interact more effectively in a polymer.[4] Due to their size, nanoparticles do not have many imperfections. They will incorporate easily and more uniformly than a larger particle.[4] The resulting polymer is called a nanocomposite.

A lot of work has been done using nanoparticles to reinforce polymer matrices. For example, layered silicas have been used to reinforce coatings.[22] Nanosilica was used to act as a filler in rubber and poly(vinyl acetate).[23] Carbon nanotubes and nano-aluminum oxide have been used to reinforce epoxy phenol novolac resins and an improvement in mechanical properties, such as ultimate stress and stiffness, was observed.[24] PSAs have also been modified using nanoparticles. Yamamoto et al. (2015) synthesized PBA in the presence of nano-silica and found that tack increased 2.36 times and adhesion energy improved 1.36 times while using loadings up to 80%.[25] Nano-silica in loadings up to 4 wt% was also used to reinforce an EHA/AA/MMA PSA (where AA is acrylic acid) and was found to improve the adhesive properties as well as increase the elastic and loss modulus. An increase in latex viscosity was also noted with increasing nano-silica content.[26]

Striving towards a more environmentally friendly polymer is possible using nanoparticles. The nanoparticles themselves can also be “green”. Examples include nano-cellulose, nano-starch, and nano-silica.[4], [27] However, more traditional nanoparticles can require high energy inputs to be processed. Examples include nano-silica and carbon black.[28] Eliminating the need for high energy use would also make for a sustainable polymer. A “green” example of polymer

reinforcement used potato starch nanocrystals to reinforce natural rubber.[29] Mechanical properties such as tensile strength and modulus improved significantly with starch loadings of up to 20%. This was attributed to the formation of crystalline networks.

Nanoparticles can be used as property modifiers when bio-sourced feedstock is used to produce polymers in lieu of fossil-based resources. A common issue when replacing a polymer formulation component is a change in properties including starch based systems, polymers from cellulose derivatives and bacterial polyesters, for example.[30]–[32] However, a nanoparticle could be used to help regain any performance losses from a changing formulation. This may be particularly relevant when replacing fossil-based resources with "green" or renewable ones. The toxicity or safety of nanomaterials is under intense scrutiny. It would be anathema to use a toxic nanomaterial to help modify the properties of a so-called "green" polymer. Therefore, a "green" nanoparticle is required.

Cellulose Nanocrystals

Cellulose nanocrystals are made from cellulose, the most abundant polymer in the world.[33] They are made by subjecting cellulose to acid hydrolysis; typically, sulfuric acid is used. This dissolves the amorphous chains which leaves behind the stronger, more uniform and crystalline particles. The amount of imperfections on the particle is reduced in this process.[27] Cellulose is full of hydrogen bonds and these need to be removed in order to exploit their strength as the particles would be too rigid.[34] CNCs are rod-shaped particles with a high aspect ratio.[33] Because of their shape, CNCs have a large effect on the rheological properties of any solution they may be added to. The aspect ratio is dependent on the cellulose source as well as the hydrolysis method; the source can be plants, aquatic animals or even produced by specific strains of bacteria.[33], [35] In this work, the CNCs are $120 \pm 20 \times 4.3 \pm 0.7$ nm (Figure 1-4). CNCs are green, renewable materials produced in Canada and therefore are a Canadian solution to a challenging worldwide problem.

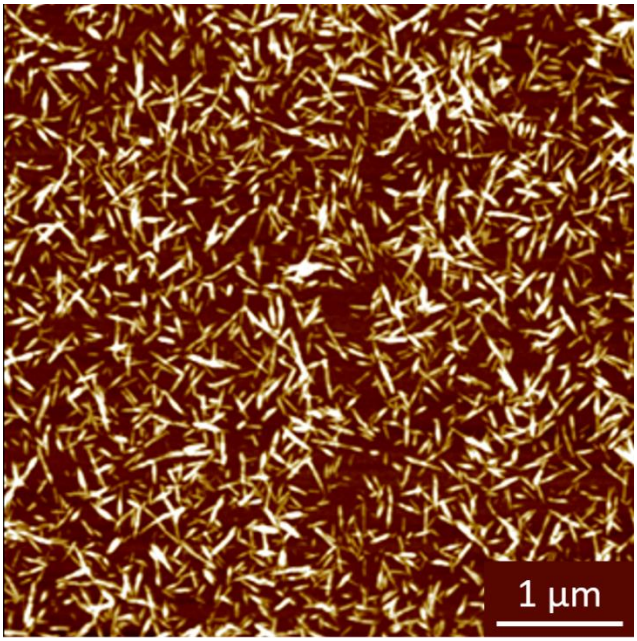

Figure 1-4: AFM image of CNCs

One of the first reports of using CNCs (then termed cellulose whiskers) in a polymer nanocomposite was in 1995 by Favier et al.[36] Styrene and BA were copolymerized and then blended with CNCs and a reinforcement affect was observed via dynamic mechanical analysis. Since then, CNCs have been widely used to reinforce polymer matrices. However, the use of cellulose (not at the nano scale) predates the use of CNCs as early as 1870 when the Hyatt Manufacturing Company synthesized celluloid, which is the first thermoplastic polymer.[33]

Nanocomposites of CNCs with a copolymer of styrene and BA were cast and it was shown that the CNCs provided structural reinforcement. The amount of reinforcement by the CNCs was shown to depend on the source of CNCs which differed in terms of their aspect ratios; a higher aspect ratio resulted in better reinforcement.[37] In another instance, modified CNCs (acetate and lactate modified) were used to reinforce polylactide via melt blending. An increase was observed in the storage modulus when 5 wt% loading was used. The lactate modified CNCs had the best dispersion in the polylactide.[35] CNCs synthesized from soy hulls have been used to reinforce natural rubber. They were dispersed in the natural rubber using a casting and evaporating method. The storage modulus was improved 21 times as compared to neat rubber using only 2.5 wt% CNCs.[28]

CNCs have been incorporated through an *in situ* polymerization in some cases. For example, they have been used in a ring-opening polymerization of L-lactide with CNCs present. Poly(L-lactide) (PLLA) was grafted onto the CNCs and could have further applications in tissue engineering with enhanced mechanical properties. The CNCs helped improve the barrier properties, which is important in applications of neat PLLA.[38] Hydrogels have also been prepared with CNCs used *in situ* rather than as a blend. Acrylamide was polymerized in the presence of CNCs. Up to 3 wt% CNC was used and a significant increase in tensile strength and elongation ratio was observed. This comparison was made to hydrogels which had otherwise been prepared with a cross-linker rather than using CNCs. An increase in viscosity was also noted.[39] In previous work in our laboratory, CNCs were polymerized *in situ* via batch emulsion polymerization with BA and MMA. The storage and loss moduli were increased with CNC loadings up to 2 wt% and the elasticity of the resulting polymer increased. The viscosity was also higher with increasing CNC content.[40]

CNCs have been used specifically in PSAs in two previous works. CNCs were added *in situ* to a suspension polymerization of EHA with loadings of up to 5 wt%. Tack and peel strength increased with increasing CNC content; shear strength was significantly increased with CNC loadings over 2 wt%. DMA supported the reinforcement through the use of CNCs; a low tan δ indicated a high shear strength at low frequencies, which was observed.[41] In addition, unpublished work in our laboratory showed that when CNCs are used in situ during the semi-batch emulsion polymerization of BA/MMA, simultaneous improvements in tack, peel strength and shear strength were noted.

There is an inherent challenge with incorporating CNCs into a polymer matrix; CNCs are hydrophilic, but polymers are hydrophobic. Also, due to their high aspect ratio, CNCs will have an influence on the rheological properties of the latex. It has been noticed previously that particles with high aspect ratios with have a stronger influence on viscosity. This is attributed to a higher surface area and volume fraction, as well as an increased probability of particle interactions.[42]–[45] Cylindrical particles generally lead to the highest viscosity increase out of platelet, blades, cylinders and brick shaped particles because of their high aspect ratio. [45] Ching et al. (2016) have noted this effect particularly for CNCs.[46] This sets a limit for the amount of CNCs that can be added to a polymer system.

Another issue is the requirement for water to make CNC solutions. To add CNCs to a polymerization, they must be dispersed in solution. Because CNC solutions also tend to be very

viscous, there is a minimum amount of water which must be used to ensure proper dispersion of the CNCs. Traditionally, 1 wt% solutions have shown to be the ideal fraction to avoid agglomeration.[47] This sets a limit to how many CNCs can be used in a system because more water also means a lower solids content for the PSA. If the solids content is too low, proper films will not form when the PSA is cast. In this work, CNC solutions of up to 1.65 wt% were used to maintain a higher solids content while respecting the need to use more water.

Hypothesis and Thesis Objectives

We hypothesize that the addition of CNCs to an emulsion based PSA formulation will improve adhesive properties. The objective of this thesis was to incorporate CNC nanoparticles into PSA formulations via free radical emulsion polymerization and study their effect on adhesive properties. While emulsion polymerization is a more sustainable process (it does not require any harsh solvents), it normally results in polymer films with a discontinuous gel network unlike the case in solution polymerization; this leads to weaker cohesion or shear strength. In many cases, if the shear strength is increased, the peel strength and tack will decrease. Finding a solution to this classic adhesive conundrum was also an objective.

A second objective was to verify the impact of system hydrophobicity on CNC nanocomposite production and resulting adhesive performance. Two terpolymer systems were investigated: System 1 was IBA/BA/MMA and system 2 was EHA/BA/MMA; IBA being slightly hydrophilic while EHA is highly hydrophobic.

Thesis Outline

This thesis contains 4 chapters. Chapter 1 presents an introduction and brief literature review, including background on emulsion polymerization, cellulose nanocrystals (CNCs), and adhesive properties. Chapter 2 reports on the effect of in situ CNCs in an IBA/BA/MMA adhesive synthesized using semi-batch emulsion polymerization. Chapter 3 presents a comparison of adhesive performance between the IBA/BA/MMA and EHA/BA/MMA systems. Chapter 4 concludes the thesis and offers suggestion of future work.

References

[1] W. Maaßen, S. Oelmann, D. Peter, W. Oswald, N. Willenbacher, and M. A. R. Meier, "Novel insights into pressure-sensitive adhesives based on plant oils," *Macromol. Chem. Phys.*, vol. 216, pp. 1609–1618, 2015.

[2] "Pressure Sensitive Adhesives Market Trends and Forecast 2013-2019," *Transparency Market Research*, 2014. [Online]. Available: http://www.transparencymarketresearch.com/psa-market.html.

[3] S. Salehpour and M. A. Dubé, "Applying the principles of green chemistry to polymer production technology," *Macromol. React. Eng.*, no. 8, pp. 7–28, 2014.

[4] R. J. Young and P. A. Lovell, *Introduction to Polymers*, Third. Boca Raton: CRC Press, 2011.

[5] A. Li and K. Li, "Pressure-sensitive adhesives based on soybean fatty acids," *RSC Adv.*, vol. 4, no. 41, pp. 21521–21530, 2014.

[6] A. Aymonier, E. Papon, J. J. Villenave, P. Tordjeman, R. Pirri, and P. Gérard, "Design of pressure-sensitive adhesives by free-radical emulsion copolymerization of methyl methacrylate and 2-ethylhexyl acrylate. 1. Kinetic study and tack properties," *Chem. Mater.*, vol. 13, no. 8, pp. 2562–2566, 2001.

[7] B. L. López, E. Murillo, and M. Hess, "Synthesis and characterization of a pressure-sensitive adhesive based on an isobutyl acrylate / 2-ethylhexyl acrylate copolymer," *e-Polymers*, vol. 4, no. 1, pp. 1–10, 2004.

[8] I. Benedek and L. J. Heymans, *Pressure-Sensitive Adhesives Technology*, CRC Press. New York: Marcel Dekker Inc., 1997.

[9] S. Özlem Gündoğdu, "The characterization of some methacrylate and acrylate homopolymers, copolymers and fibers via direct pyrolysis mass spectroscopy," Middle East Technical University, 2012.

[10] Y. Zang, M. Ye, A. Han, and Y. Ding, "Preparation of nano-encapsulated polyethylene wax particles for color toner by *in situ* emulsion polymerization," *J. Appl. Polym. Sci.*, vol. 134, no. 2, pp. 1–9, 2017.

[11] M. A. Dubé, A. Penlidis, and K. F. O'Driscoll, "A kinetic investigation of styrene/butyl acrylate copolymerization," *Can. J. Chem. Eng.*, vol. 68, pp. 974–987, 1990.

[12] O. Chiantore, D. Scalarone, and T. Learner, "Characterization of artists' acrylic emulsion

paints," *Int. J. Polym. Anal. Charact.*, vol. 8, no. 1, pp. 67–82, 2003.

[13] S. Roberge and M. A. Dubé, "Emulsion-based pressure sensitive adhesives from conjugated linoleic acid / styrene / butyl acrylate terpolymers," *Int. J. Adhes. Adhes.*, vol. 70, pp. 17–25, 2016.

[14] Z. Yan and Y. Deng, "Water-soluble/dispersible cationic pressure-sensitive adhesives. I. Adhesives from solution polymerization," *J. Appl. Polym. Sci.*, vol. 90, no. September 2002, pp. 1624–1630, 2003.

[15] T. F. Mckenna and A. Villanueva, "Effect of solvent on the rate constants in solution polymerization . Part II . vinyl acetate," *J. Polym. Sci. Part A Polym. Chem.*, vol. 37, pp. 589–601, 1999.

[16] J. Sakdapipanich, N. Thananusont, and N. Pukkate, "Synthesis of acrylate polymers by a novel emulsion polymerization for adhesive applications," *J. Appl. Polym. Sci.*, vol. 100, pp. 413–421, 2006.

[17] J. Lu, A. J. Easteal, and N. R. Edmonds, "Crosslinkable poly (vinyl acetate) emulsions for wood adhesive," *Pigment Resin Technol.*, vol. 40, no. 3, pp. 161–168, 2011.

[18] R. Jovanovic and M. A. Dubé, "Emulsion-based pressure-sensitive adhesives : A review," *J. Macromol. Sci.*, vol. C44, no. 1, pp. 1–51, 2004.

[19] S. Tobing, A. Klein, L. H. Sperling, and B. O. B. Petrasko, "Effect of network morphology on adhesive performance in emulsion blends of acrylic pressure sensitive adhesives," *J. Appl. Polym. Sci.*, vol. 81, pp. 2109–2117, 2001.

[20] S. D. Tobing and A. Klein, "Molecular Parameters and Their Relation to the Adhesive Performance of Acrylic Pressure-Sensitive Adhesives," pp. 2230–2244, 2001.

[21] L. Qie and M. A. Dubé, "Performance improvement of latex-based PSAs using polymer microstructure control," University of Ottawa, 2011.

[22] J. Yeh and K. Chang, "Polymer/layered silicate nanocomposite anticorrosive coatings," *J. Ind. Eng. Chem.*, vol. 14, pp. 275–291, 2008.

[23] A. Bandyopadhyay, M. D. E. Sarkar, and A. K. Bhowmick, "Polymer – filler interactions

in sol – gel derived polymer/silica hybrid nanocomposites," *J. Polym. Sci. Part B Polym. Phys.*, vol. 43, pp. 2399–2412, 2005.

[24] C. V Opelt, D. Becker, C. M. Lepienski, and L. A. F. Coelho, "Reinforcement and toughening mechanisms in polymer nanocomposites e Carbon nanotubes and aluminum oxide," *Compos. Part B*, vol. 75, pp. 119–126, 2015.

[25] Y. Yamamoto, S. Fujii, K. Shitajima, K. Fujiwara, and S. Hikasa, "Soft polymer-silica nanocomposite particles as fi ller for pressure-sensitive adhesives," *Polymer (Guildf).*, vol. 70, pp. 77–87, 2015.

[26] M. Khalina, M. Sanei, H. S. Mobarakeh, and A. Reza, "Preparation of acrylic / silica nanocomposites latexes with potential application in pressure sensitive adhesive," *Int. J. Adhes. Adhes.*, vol. 58, pp. 21–27, 2015.

[27] F. Chivrac, E. Pollet, and L. Avérous, "Progress in nano-biocomposites based on polysaccharides and nanoclays," *Mater. Sci. Eng. R Reports*, vol. 67, no. 1, pp. 1–17, 2009.

[28] W. P. Flauzino Neto, M. Mariano, I. S. V. da Silva, H. A. Silvério, J. L. Putaux, H. Otaguro, D. Pasquini, and A. Dufresne, "Mechanical properties of natural rubber nanocomposites reinforced with high aspect ratio cellulose nanocrystals isolated from soy hulls," *Carbohydr. Polym.*, vol. 153, pp. 143–152, 2016.

[29] K. R. Rajisha, H. J. Maria, L. A. Pothan, Z. Ahmad, and S. Thomas, "Preparation and characterization of potato starch nanocrystal reinforced natural rubber nanocomposites," *Int. J. Biol. Macromol.*, vol. 67, pp. 147–153, 2014.

[30] K. Leja and G. Lewandowicz, "Polymer biodegradation and biodegradable polymers - a review," *Polish J. Environ. Stud*, vol. 19, no. May, pp. 255–266, 2010.

[31] C. Irin Sheela and S. Begila David, "Photo and biodegradation of thermosetting polymers from linseed oil," *Int. J. Chem. Stud.*, vol. 2, no. 4, pp. 46–54, 2014.

[32] M. Van Der Zee, J. H. Stoutjesdijk, P. A. A. W. Van Der Heijden, and D. D. W. I, "Structure-biodegradation relationships of polymeric materials . 1 . Effect of degree of oxidation on biodegradability of carbohydrate polymers," *J. Environ. Polym. Degredation,*

vol. 3, no. 4, pp. 235–242, 1995.

[33] A. Dufresne, *Nanocellulose*. Saint Martin D'Heres cedex: De Gruyter, 2012.

[34] T. Heinze, "Cellulose : structure and properties," *Adv. Polym. Sci.*, vol. 271, pp. 1–52, 2016.

[35] S. Spinella, G. Lo Re, B. Liu, J. Dorgan, Y. Habibi, P. Leclère, J. M. Raquez, P. Dubois, and R. A. Gross, "Polylactide/cellulose nanocrystal nanocomposites: Efficient routes for nanofiber modification and effects of nanofiber chemistry on PLA reinforcement," *Polym. (United Kingdom)*, vol. 65, pp. 9–17, 2015.

[36] V. Favier, G. R. Canova, J. Y. Cavaillé, H. Chanzy, A. Dufresne, and C. Gauthier, "Nanocomposite materials from latex and cellulose whiskers," *Polym. Adv. Technol.*, vol. 6, no. 5, pp. 351–355, 1995.

[37] F. Bettaieb, R. Khiari, A. Dufresne, M. F. Mhenni, and M. N. Belgacem, "Mechanical and thermal properties of Posidonia oceanica cellulose nanocrystal reinforced polymer," *Carbohydr. Polym.*, vol. 123, pp. 99–104, 2015.

[38] C. Miao and W. Y. Hamad, "In-situ polymerized cellulose nanocrystals (CNC) poly(L-lactide) (PLLA) nanomaterials and applications in nanocomposite processing," *Carbohydr. Polym.*, vol. 153, pp. 549–558, 2016.

[39] J. Yang, C. R. Han, J. F. Duan, M. G. Ma, X. M. Zhang, F. Xu, and R. C. Sun, "Synthesis and characterization of mechanically flexible and tough cellulose nanocrystals-polyacrylamide nanocomposite hydrogels," *Cellulose*, vol. 20, no. 1, pp. 227–237, 2013.

[40] Z. Dastjerdi, E. D. Cranston, and M. A. Dubé, "Synthesis of poly (n -butyl acrylate / methyl methacrylate)/ CNC latex nanocomposites via in situ emulsion polymerization," *Macromol. React. Eng.*, pp. 1–8, 2017.

[41] J. Kajtna and U. Šebenik, "Novel acrylic / nanocellulose microsphere with improved adhesive properties," *Int. J. Adhes. Adhes.*, vol. 74, no. November 2016, pp. 100–106, 2017.

[42] K. B. Anoop, S. Kabelac, T. Sundararajan, and S. K. Das, "Rheological and flow

characteristics of nanofluids: Influence of electroviscous effects and particle agglomeration," *J. Appl. Phys.*, vol. 106, no. 3, 2009.

[43] Gaganpreet and S. Srivastava, "Influence of particle shape on viscosity of nanofluids," *AIP Conf. Proc.*, vol. 1512, no. 2013, pp. 984–985, 2013.

[44] M. C. Li, Q. Wu, K. Song, S. Lee, Y. Qing, and Y. Wu, "Cellulose nanoparticles: structure-morphology-rheology relationships," *ACS Sustain. Chem. Eng.*, vol. 3, no. 5, pp. 821–832, 2015.

[45] E. V. Timofeeva, J. L. Routbort, and D. Singh, "Particle shape effects on thermophysical properties of alumina nanofluids," *J. Appl. Phys.*, vol. 106, no. 1, 2009.

[46] Y. C. Ching, M. Ershad Ali, L. C. Abdullah, K. W. Choo, Y. C. Kuan, S. J. Julaihi, C. H. Chuah, and N. S. Liou, "Rheological properties of cellulose nanocrystal-embedded polymer composites: a review," *Cellulose*, vol. 23, no. 2, pp. 1011–1030, 2016.

[47] N. E. Marcovich, M. I. Auad, N. E. Bellesi, S. R. Nutt, and M. Aranguren, "Cellulose micro / nanocrystals reinforced polyurethane," *J. Mater. Res.*, vol. 21, no. 4, pp. 870–881, 2006.

Chapter 2: Synthesis of Poly(isobutyl acrylate/ n-butyl acrylate/ methyl methacrylate) CNC Nanocomposites for Adhesive Applications via In Situ Semi Batch Emulsion Polymerization

Alexandra Ouzas[1], Elina Niinivaara[2], Emily D. Cranston[2], Marc A. Dubé[1]

[1]Department of Chemical and Biological Engineering
Centre for Catalysis Research and Innovation
University of Ottawa
161 Louis Pasteur Pvt.
Ottawa, Ontario K1N 6N5, Canada

[2]Department of Chemical Engineering
McMaster University
1280 Main Street West
Hamilton, Ontario L8S 4L7, Canada

Pressure sensitive adhesive (PSA) films were prepared from in situ semi-batch emulsion polymerizations using isobutyl acrylate, n-butyl acrylate, and methyl methacrylate in the presence of cellulose nanocrystals (CNCs). The CNCs at loadings of up to 1 wt% with respect to monomer resulted in significant and simultaneous improvement in tack, peel strength and shear strength for the PSA films. While most latex properties were unchanged, the CNCs also led to increased latex viscosity. A range of varying compositions were used to test the limits of the application. Microscopy was used to demonstrate the location of the CNCs dispersed throughout the latex but outside of the polymer particles. Comparison to latex/CNC blends showed that the in situ technique provided higher shear strength PSA films.

Keywords: butyl acrylate, isobutyl acrylate, methyl methacrylate, cellulose nanocrystals, nanocomposites, emulsion polymerization, pressure sensitive adhesives

Introduction

The demand for sustainable, renewable polymers has been increasing in the face of growing concerns over the supply of fossil fuels, the pre-cursor for most monomers. The predominately used monomers are toxic, but provide good properties. Ideally, a bio-based monomer would be most environmentally friendly (and least toxic) but use of these monomers can affect the

mechanical and physical properties of the resulting polymer in an undesirable way.[1] Traditional fillers and reinforcing agents such as silica and carbon black require large energy consumption, so replacing them with an equally influential filler is desired.[2] Therefore, to improve the performance of the bio-based polymer, it would be reasonable to use a compound which is also bio-based and environmentally friendly but will also improve the polymer's performance properties. Thus, fully bio-based polymers would be one step closer to a possibility and there would be no trade-off in physical or mechanical properties

One way to modify the performance of polymers is through copolymerization. The properties from different monomers can be combined as a copolymer to achieve a broad range of application properties.[3] For example, a hard monomer (i.e., high polymer glass transition temperature, T_g) can be combined with a softer monomer (i.e., low polymer T_g) to manipulate adhesive properties in pressure sensitive adhesive (PSA) formulations. PSAs are polymers that adhere to surfaces on contact with minimal pressure. They have many applications (e.g., labels, tapes) and creating a greener way to modify their properties is desirable. There are three main properties that reflect the performance of an adhesive: tack, peel strength and shear strength. Tack is the measure of the adhesive's ability to form a bond to a substrate with no additional force applied. Peel strength is a measure of the force required to remove the adhesive from a substrate. Shear strength is the cohesive strength, which is measured by applying a weight to a test sample and measuring how long it takes to drop. Frequently, and particularly for emulsion polymerization (i.e., latex) based adhesives, increases in peel strength and tack result in a decrease in shear strength and vice-versa.[4] Finding a way to simultaneously improve all three characteristics would be ideal. Due to the compartmentalized nature of polymers produced through emulsion polymerization, the gel networks formed are not continuous as they would be for the case of solution polymerization based adhesives. In other words, the gel networks are continuous within each latex particle but the adhesive film formed from the latex may only be loosely connected via chain entanglements during the film formation process. Thus, weaker films will result in lower shear strength.[4] Of course, the emulsion-based approach provides a safer, less toxic and arguably more cost effective approach than a solution-based method for PSA production.[4]

Nanoparticles are often used to reinforce a polymer's microstructure while improving its performance properties. Using nanoparticles as opposed to larger scaled materials greatly increases

the surface area available for interaction or reaction with the polymer matrix.[3] Nanoparticles also tend to be more uniform in size and shape.[3] Examples of nanoparticles incorporated in polymer matrices include phyllosilicates, starch, cellulose, chitin, chitosan, pectin, nanosilica and clays, among many others.[3], [5]

Cellulose is the most readily available and abundant polymer on earth, present in plants and trees, is also produced by bacteria, algae and fungi, and can be found in some ocean animals.[6], [7]–[9] Because it is naturally occurring, cellulose is a renewable material with minimal environmental impact when used sustainably. Cellulose has a strong inter- and intramolecular hydrogen bonding capacity which allows it to self-assemble during biosynthesis into hierarchical ordered structures. However, large cellulosic structures, such as pulp fibres or fibril bundles tend to be inhomogeneous (containing both ordered and disordered regions) and non-uniform in size. Through acid hydrolysis of natural cellulose, the disordered cellulose chains, which act as a defects and impart flexibility in cellulose, are preferentially broken down.[6], [10] What remains are fairly uniform, highly crystalline, whisker-shaped cellulose nanocrystals (CNCs).

Once cellulose is deconstructed to CNCs, it has more desirable properties which can influence the mechanical performance of polymers (and therefore latexes). CNCs have a high aspect ratio, where the length is a few hundred nanometers and the width is a few nanometers.[6], [11], [12] The exact dimension of the CNCs depends on the source of cellulose as well as the acid hydrolysis procedure.[6] In this work, the CNC dimensions (provided by CelluForce) were 183±88 × 6±2 nm.[13] They also exhibit extraordinary strength and have low toxicity.[14] CNCs are reported to have a specific Young's modulus greater than that of Kevlar and have mechanical properties within the same range as other reinforcing materials.[6], [15]

Limitations for the use of CNCs as nanofillers include their inherent hydrophilic nature, which makes their dispersion within hydrophobic monomers difficult; their tendency towards aggregation; and the need for CNC surface modification to better incorporate them into the polymeric matrix.[7], [8], [10], [16], [17] Surface modification may improve the dispersion of CNCs within the polymer, but the additional process requirements may not be feasible on a larger scale for economic and perhaps, environmental reasons. These modifications are possible due to the presence of hydroxyl groups.[15] Nonetheless, CNCs have been used successfully as reinforcing fillers in nanocomposites, to improve waterborne epoxies, and as reinforcements in

thermoplastics.[7], [18]–[21] It has been suggested that the best method to incorporate CNCs into a polymer matrix is via melt-processing, largely for economic reasons; however, this generally requires modification of the CNCs and still tends to lead to CNC aggregation (and sometimes burning or discoloration due to heating).[7]

In this work, CNCs were incorporated in latex polymers using a seeded semi-batch emulsion polymerization. The use of a water-based system provides many advantages for CNC dispersion, lower cost, and less toxicity.[22] In addition, being able to add the CNCs directly to the polymerization as a one-pot synthesis improves their potential for industrial use. Furthermore, there is some evidence from previous work that CNCs can be used to modify adhesive properties and overcome the issues of increasing tack and peel strength vs. decreasing shear strength, as discussed above.[23] The use of CNCs in situ to modify adhesive properties is further investigated in this work by varying the polymer T_g to test the limits of the application. In addition, the location of the CNCs within the latex is discussed using microscopic imaging techniques.

Experimental

Materials

The monomers, n-butyl acrylate (BA), isobutyl acrylate (IBA) and methyl methacrylate (MMA) (all >99%, Sigma Aldrich) were used with no further purification. The initiator, potassium persulfate (KPS) (ACS Reagent, >99%, Sigma Aldrich), and the anionic surfactant, sodium dodecyl sulfate (SDS) (ACS Reagent >99%, Sigma Aldrich), were also used as received. CNCs produced by sulfuric acid hydrolysis were donated by CelluForce (Windsor, Quebec) as a spray-dried powder in the sodium salt form (183±88 × 6±2 nm) and were used to create aqueous CNC suspensions (1-1.65 wt%). Distilled, deionized (DDI) water was used as the suspension medium for the emulsion polymerizations and for the CNC suspensions. Hydroquinone (‘Baker’ grade, JT Baker Chemical Co.) was used as an inhibitor to quench the polymerizations. Tetrahydrofuran (THF, ACS grade, Sigma Aldrich) was used with no further purification, for gel content analysis.

CNC Suspension/Dispersion Preparation

The desired amount of CNC powder and DDI water were mixed on a magnetic stir plate for 1-3 h until the dispersion appeared uniform. The suspension was submerged in an ice bath and sonicated for 5 min at 75% Amp using a Fisher Scientific 550 sonic dismembrator; the suspension was then left to rest for 5 min. This process was repeated for a total of 3 times. The suspension was vacuum-

filtered (110 mm, particle retention of >2.7 µm) three times. The resulting CNC suspension was stored in a covered beaker overnight until the polymerization was performed.

Polymerization

A 1.25 L, stainless steel Labmax Automatic Lab Reactor (Mettler Toledo) with a cooling system, anchor stirrer, condenser and two feed lines was used for all polymerizations. A nitrogen blanket was maintained in the reactor at all times. A semi-batch procedure (i.e., a seed and feed procedure) was performed for all polymerizations. Three separate feed compositions (Table 2-1**)** were tested at three CNC loadings (0, 0.5 and 1 wt% based on total monomer) for a total of 9 runs. These formulations were used to achieve certain target T_g values appropriate for adhesive applications.[3], [24]The formulations for the feed and seed stages are shown in Table 2-2 and water allocation in the formulations is shown in Table 2-3. The base case runs were remade at a higher solids content to allow for appropriate film formation for consistent comparison to the nanocomposite films (Table 2-4).

Table 2-1: Monomer composition and theoretical T_g values for runs A, B and C

Run*	IBA/BA/MMA (wt%)	IBA/BA/MMA (mol%)	T_g (ºC)
A	70/20/10	68/20/12	-21
B	39/51/10	38/50/12	-31
C	8/82/10	8/80/12	-40

*Runs were identified by composition and CNC wt%; e.g., 0.5B represents formulation B with 0.5 wt% CNC.

Table 2-2: Seed and feed stage recipe

Component	Seed Stage Amount (g)	Feed Stage Amount (g)
CNC	0, 1.1 or 2.2	-
Monomer	22	198
KPS	0.06	0.54
SDS	0.7	2.6
Water	208*	122**

*Water was distributed between the CNC suspension, KPS solution and SDS solution depending on which loading of CNCs was used (see Table 2-3).
**54 g were used for the KPS solution and 68 g were used for the pre-emulsion (feed stage).

Table 2-3: Water allocation based on CNC loading

Suspension/solution	Water for 0 wt% CNC (g)	Water for 0.5 wt% CNC (g)	Water for 1 wt% CNC (g)
CNC	0	110	165
KPS	3	3	3
SDS	205	95	40

Table 2-4: Increased solids base case formulation

Component	Seed Stage Amount (g)	Feed Stage Amount (g)
Monomer	22	198
KPS	0.06	0.54
SDS	0.43	2.6
Water	115*/3**	122

* water used for the surfactant solution
** water used for the initiator solution

Seed Stage

To begin, the reactor was charged with the SDS solution; if CNCs were used, these were also charged as a single shot at the start. The reactor was then heated to 60℃ over 30 min while mixing at 250 rpm. During the initial heating period, nitrogen gas (Linde Canada) was used to purge the reactor. Next, the monomer was added to the reactor and allowed to adjust to the reactor temperature for 3 min. Finally, the initiator solution was added and the mixture was allowed to react for 30 min.

Feed Stage

At the conclusion of the seed stage, the pre-emulsion was fed to the reactor at 1.3 g/min for 210 min and the initiator solution was fed at 0.22 g/min for 240 min. The reactor was held at 60℃ and stirred at 250 rpm for the entire feed stage. Samples (~10 g) were taken periodically and quenched with a few drops of an aqueous hydroquinone solution (1% w/w). Once the feed stage was completed, the reaction was continued for 20 min and the resulting latex was stored at room temperature for characterization. The final solids content of each run was targeted to 40 wt%.

Characterization

All samples and the final latexes were characterized for conversion via gravimetry, particle size using dynamic light scattering (DLS) and pH. Final latexes were analyzed for viscosity, gel

content, and T_g using differential scanning calorimetry (DSC). Polymer molecular weights were not measured either due to high gel contents (i.e., samples could not be filtered for analysis) or due to the presence of CNCs which would likely clog the molecular weight columns. Shear strength, tack, peel strength and dynamic mechanical analysis were performed on films cast from all final latexes. All error bars presented represent the standard deviation of the measurement (only used when repeat measurements were performed).

Conversion

The overall conversion was measured for each sample using standard gravimetric techniques and was based on total dried polymer. The instantaneous conversion was calculated on the basis of monomer fed at the sampling time whereas overall conversion was calculated based on the monomer content in the entire reaction formulation.

Particle Size

The particle size and polydispersity for all samples and final latexes were measured using dynamic light scattering (Malvern NanoS Zetasizer). A drop of sample latex was added to ~2 g of DDI water. Then one drop of the resulting mixture was added to 2 g of DDI water in a plastic cuvette. Each sample was tested 3 times at an angle of 176 º.

pH

The pH of all samples and final latexes was measured using a pH probe (Fisher Scientific/ Accumet Research AR50 Dual Channel pH/Ion/ Conductivity meter)

Viscosity

The viscosity of all final latexes was tested using a Thermo Scientific HAAKE Viscotester (Model D). Depending on the viscosity, the appropriate spindle was used to provide the correct amount of drag. Each latex was tested at 200 rpm and at room temperature.

Glass Transition Temperature (T_g)

A TA Instruments Model Q100 DSC was used to determine the T_g of samples (~20 mg). All final latexes were tested. The system was calibrated and used a nitrogen blanket. The samples were heated to 100 ºC then cooled at 10 ºC/min to -80 ºC. Then they were heated to 20 ºC at 10 ºC/min to complete a cooling and heating cycle. The T_g was calculated from the reverse heat flow curve.

Gel Content

Gel content was measured for all final latexes. 0.2 g of polymer was placed in a poly(vinylidene fluoride) (PVDF) Durapore membrane pouch with a pore size of 0.5 μm and a diameter of 47 mm from Millipore and heat sealed. Each pouch was then soaked in tetrahydrofuran (THF, Sigma Aldrich) for 14 h and gently shaken for 8 h. Each pouch was dried to a constant weight and the gel content was calculated.

Adhesive Properties

Films were cast by spreading latex on a 12" x 14" (0.31 m x 0.36 m) Mylar sheet and drawing it down with a Meyer rod (#50). The films were left to dry for 48 h at 50 ±5 % relative humidity and 23 ±2 ˚C. All adhesive tests were performed at these conditions. All films were cast to a thickness of 30 μm. Additional base case runs were produced to 47.5% solids (as opposed to the original 40% solids runs) to ensure the same film thickness to make consistent and fair comparisons.

Loop tack was measured as per the PSTC-16 standard. From the cast film, a 1" x 5" (0.025 m x 0.13 m) strip was cut. The sample was formed into a loop with the adhesive side out and was secured with a strip of masking tape. The loop was placed in the Instron tester and was lowered at a constant rate of ~2 mm/s until 1" of the film was in contact with the test panel. The strip was then lifted by the tester at a rate of 5 mm/s and the maximum force required to remove the strip was recorded. At least 3 samples were tested per film.

Peel strength was measured as outlined in the PSTC-101 standard using Test A for 180^{o} peel. The adhesive film was cut into strips of 1" x 12" (0.025 m x 0.31 m). A piece of 1" masking tape was affixed to the end of the film to form a thicker edge for the Instron tester grips. The test strip was then flipped over so the adhesive side was facing down and was centered on the plate. Using a 2040 ± 45 g steel roller, the specimen was rolled twice in each lengthwise direction to apply the sample to the panel at 10 mm/s. If any air bubbles were visible, the sample was discarded. At least 5 samples were tested per film.

Shear strength was measured according to a modified PSTC-107A standard. A modification was made to the test area as the samples would not fall within a reasonable time frame. A 0.5" x 0.5" (0.013 m x 0.013 m) test area was used as opposed to a 1" x 1" (0.025 m x 0.025 m) area. The tape was cut into 0.5" x 5" strips. The sample was placed on the test panel and the area was ensured to be 0.5" x 0.5". The same roller used for peel tests was used to roll the sample onto the panel. The

sample was rolled twice in each direction, lengthwise at 100 mm/s. A 1 kg weight was affixed to each tape. The elapsed time until the sample fell was recorded along with the failure type.

Dynamic Mechanical Analysis

Dynamic mechanical analysis (DMA) was performed on all latexes used for adhesive testing. A TA Instruments RDA III rheometer was used. Samples were prepared on silicon release paper and cut into 25 mm diameter circles with a thickness of 1.8 ± 0.2 mm. Samples were dried for 1-2 days at room temperature, and then were heated to 35 ˚C under vacuum for 5-7 days. Frequency sweeps at 23 ˚C were used from 0.1 to 80 Hz.

Water Contact Angle

A VCA Optima (AST Products Inc.) was used to perform contact angle measurements. The DMA samples were used as the testing material. A 1 µL water droplet was lightly dropped onto the polymer surface and the contact angle was estimated (within 30 s) by VCA OptimaXE software. At least 3 measurements per sample were performed.

Microscopy

Both atomic force microscopy (AFM) and transmission electron microscopy (TEM) were used to image selected latex samples. Samples were diluted (1000x) prior to testing. For the AFM measurements, a pristine silicon wafer was prepared using a UV/ozone treatment. Samples were spin coated onto the wafer by spinning at 4000 rpm (7 s of acceleration) for 30 s (G3P spin-coater, Specialty Coating Systems Inc., Indianapolis, IN, USA). AFM cantilevers used were rectangular (NCHR, Nanoworld) with a nominal spring constant of 21 – 78 N/m and resonant frequency of 250 – 390 kHz. An Asylum MFP-3D AFM instrument (Asylum Research, Santa Barbara, CA) was used to collect the images in alternating current (AC) mode (also called "tapping mode"). The height images were processed using Igor Pro 6.0 running Asylum Research AFM software (version 13.17) using a second order flattening routine.

For the TEM measurements, a drop casting method was used. The latex was placed on Formvar coated copper TEM grids and was air dried for 24 h. A JEOL 1200 EX TEMSCAN microscope using 80 kV collected the TEM images. No staining was used in TEM measurements.

Results and discussion

Conversion

Conversion results for formulation A runs are shown in Figure 2-1. CNC loadings had no significant impact on reaction rate. The results of all other runs using formulations B and C showed similar trends (Appendix A).

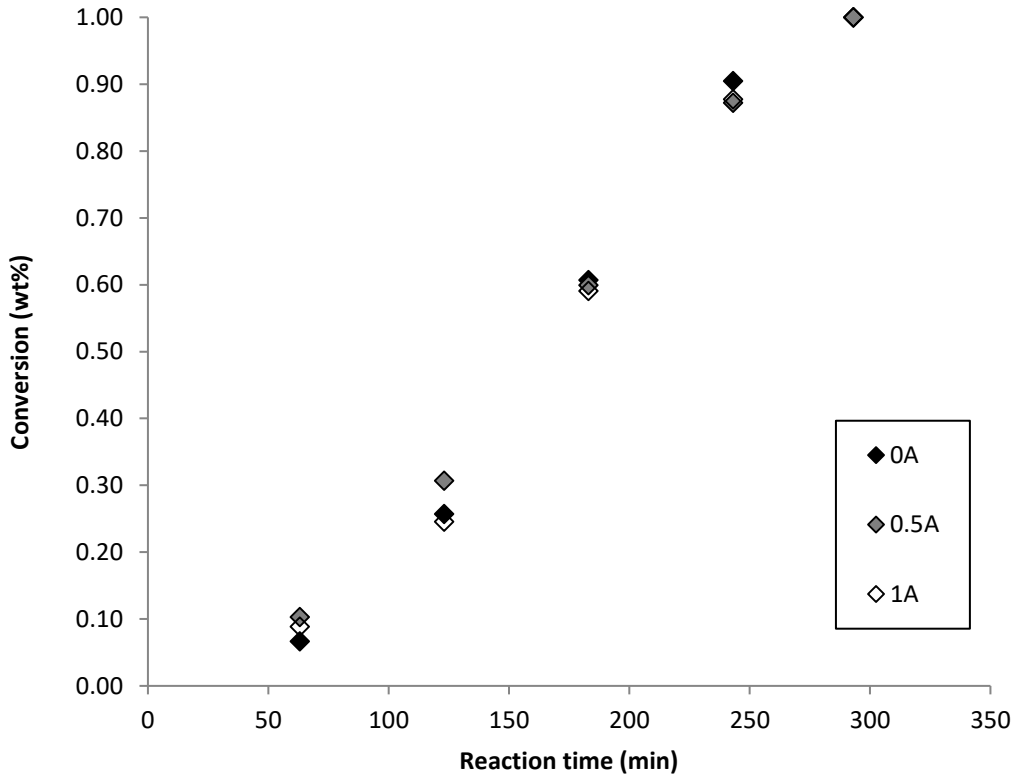

Figure 2-1: Overall conversion for runs 0A, 0.5A and 1A (runs using formulation A with 0, 0.5 and 1 wt% CNC loading, respectively)

The instantaneous and overall conversion trends for run 0A are shown in Figure 2-2. All runs exhibited similar trends. The difference between the instantaneous and overall conversion confirms that the runs were not at monomer-starved conditions. The seed stage began at time 0 min; the feed stage is also denoted in the figure.

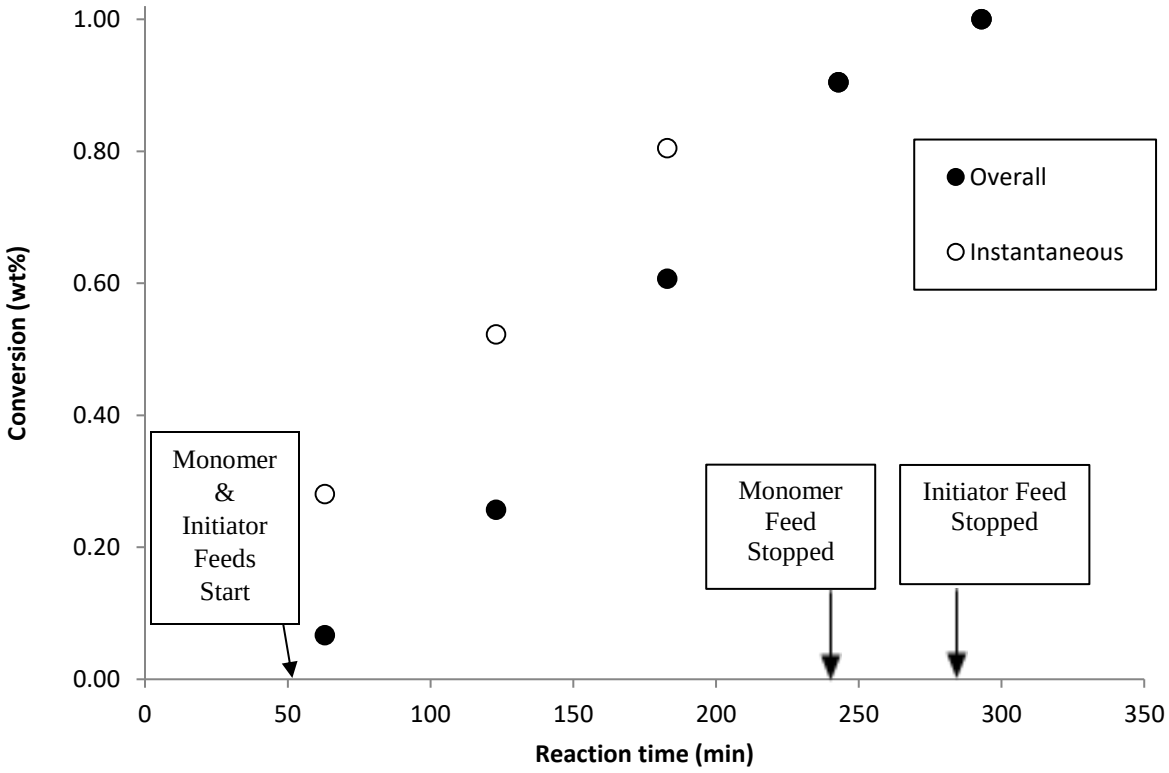

Figure 2-2: Instantaneous and overall conversion of latex formulation 0A

Particle Size

The particle size distribution (PSD) for all samples including the final latexes was considered to be narrow (all values were below 0.1) and thus, essentially monodisperse. The particle diameters for formulation A runs can be seen in Figure 2-3. Consistent with the conversion results, CNCs did not interfere with particle nucleation. Results for the other two formulations showed similar trends (Appendix A).

Because the PSD for all samples were narrow, the CNCs were most likely not located within the particles. The average particle size for runs 0.5A and 1A would have become increasingly larger if the CNCs were inside the particles because the CNCs themselves were almost the same size as the particles. However, one must consider that the samples for DLS analysis were diluted twice (to ca. 10,000x). Thus, the chances of a CNC particle being present in the analyzed samples was

low and therefore, while unlikely for other reasons (to be discussed later), it was still possible that the CNCs could be located inside some of the latex particles.

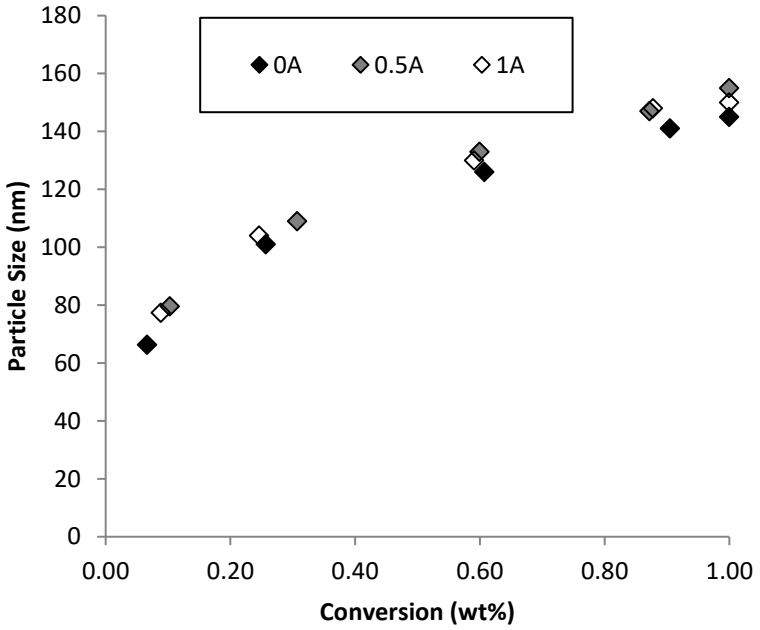

Figure 2-3: Average particle size of latex formulation A

Microscopy

Select latex samples were characterized via TEM and AFM imaging (Figures 2-4 a-f). Each final latex was imaged to determine the location of the CNCs in the latex. There are three possible locations for the CNC particles. They could have been in the aqueous solution between the latex particles, they could have acted as reinforcers or stabilizing agents surrounding the latex particles (and perhaps bonded to the polymer), or they could have resided within the latex particles. As noted above, particle size analysis suggests that the CNCs were not located within the latex particles. Comparing the TEM images of the final latexes from runs 0A (no CNC) and 1A (1 wt% CNC), latex particles are visible and CNCs are evident in Figures 2-4 c and d. The CNCs are located closely around the latex particles, but do not appear to be located within (or protruding from) the particles. Similar conclusions can be drawn from the AFM images in Figures 2-4 e and f. TEM imaging for the other formulations (latexes B and C) gave similar results. The method of sample preparation may have affected the location of the CNCs. For instance, because all images

were of low T_g polymers, with a tendency for some albeit limited flow, the latex particles tended to flatten out which is observed in the TEM images, which have a slightly larger particle size than that measured via DLS. When imaging soft polymers, the electron beam used in TEM may cause some sample melting. This melting would also contribute to the flattening effect of the latex particles.

It is possible that the CNCs were associated (bound or crosslinked) with the latex, but were displaced into the gaps between the latex particles during TEM sample preparation and imaging. On the other hand, the AFM images (Figures 2-4 e and f) indicate that some CNCs are associated with the latex particles and no CNC aggregates were detected away from the latex particles. In fact, it appears that the CNCs were closely associated with the latex particles and well dispersed along with the particles. This close contact with the latex particles would be a key factor in mechanical property modification. CNCs do have the ability to graft and what was observed in the AFM and TEM images perhaps implies crosslinking or at the very least, hydrogen bonding. TEM and AFM images for formulations B and C showed similar results (Appendix A).

It has been previously reported that it is possible for CNCs to undergo a grafting mechanism.[25] In fact, Gurdag et al. reported that KPS is the best initiator for hydrogen abstraction.[26] The abstraction of the hydrogen from the hydroxyl groups on the CNCs forms a radical on the CNC, allowing for polymerization to propagate from it. They also showed that grafting percentage improves at a pH of 4, which is similar to the conditions in our polymerizations.[25] Thus, we conclude that the CNCs were not located within the latex particles but may have grafted to the particles or at least had a strong association with the latex particles. The AFM and TEM imaging methods did not allow us to look within the latex particles. If the CNCs were inside the particles, the imaging would have most likely provided evidence of CNCs protruding from them because of their size relative to that of the particles. Because this was not the case, we surmise that the CNCs were only located outside of the particles.

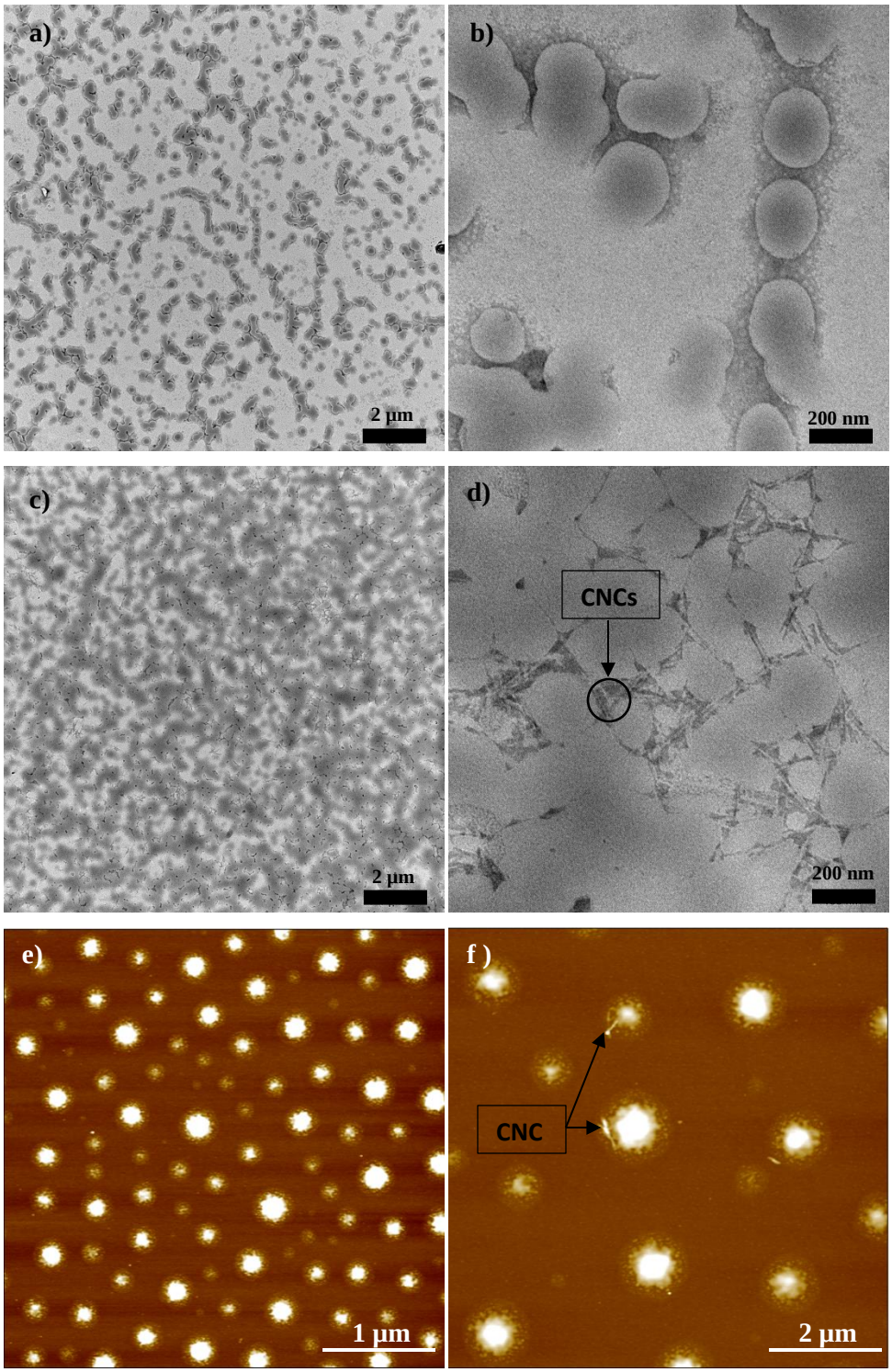

Figure 2-4: TEM images of latex 0A (a, b), latex 1A (c, d) and AFM images of formulations 0A (e) and 1A (f)

Viscosity

The latex viscosity was greatly affected by the presence of CNCs in the formulation. This was easily observed during sampling and at the time of discharging the reactor. Viscosities of the final latexes were measured using a rheometer and the increase in viscosity with CNC loading was confirmed (Figure 2-5). At 1 wt% CNC loading, latex viscosity was essentially doubled compared to the base case formulations. This viscosity increase supports the notion that CNCs were not located within the latex particles; had they been, the viscosity would not have changed so significantly. In addition, such a drastic viscosity increase suggests a strong association of the CNCs with the latex particles via grafting or at the very least hydrogen bonding.

CNCs are whisker-shaped particles which have a strong influence on the rheological properties of the resulting suspension and therefore, of the polymer latex. In general, suspensions with non-spherical particles (i.e., larger aspect ratios) will have a higher viscosity due to the increase in surface area, a higher volume fraction of particles in suspension, potential to orientate and an increase in particle interactions (higher probability of collisions occurring).[27]–[30] Out of various non-spherical shapes (platelets, blades, cylinders and bricks), cylindrical particles lead to the highest increases in viscosity because they have the highest aspect ratio.[30] This characteristic has also been noted specifically for CNCs.[31] The similarity in particle size for all of the runs in this study (Figure 2-3) confirm that the viscosity increases were due solely to the presence of CNCs in the formulations. When CNC suspensions have been studied for their rheological properties, the reported viscosity for a 1 wt% solution (considering a shear rate of 0.3 s^{-1}) is ~100 cP.[29], [32] The viscosity of a CNC solution will increase with the concentration because there is more likelihood of a collision occurring.[29] The latex viscosities reported for the 1 wt% CNC runs were more than double the original CNC solution viscosity. Considering the viscosity of the base case runs was also lower than 100 cP, the CNCs must be interacting with the latex to cause the difference in viscosity. It is suspected that the CNCs could be cross-linking or grafting with the particles, which has been seen previously in the preparation of hydrogels.[18] Our results are therefore consistent with the fact that CNCs were located outside of the spherical latex particles but were still interacting with the particles in a significant way.

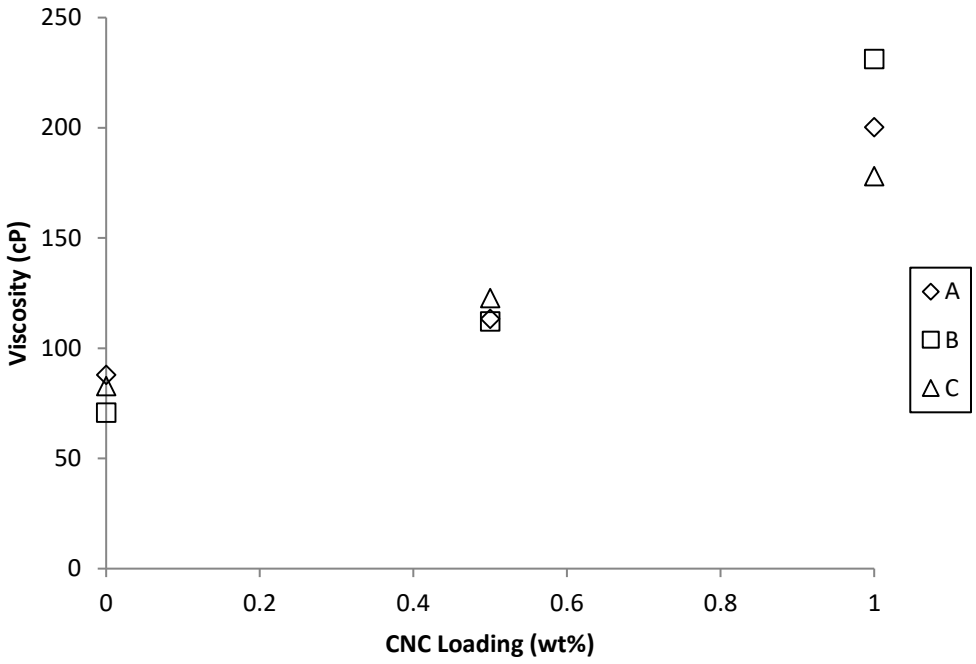

Figure 2-5: Viscosity of final latexes for all runs

These results also illustrate the difficulty of including even higher CNC loadings in latex formulations, as further viscosity increases could lead to coagulation. Finally, for the purposes of PSA applications, the viscosities achieved in these latexes permitted a reasonably straightforward film formation but further viscosity increases could lead to non-uniform film formation.

pH

pH was tracked for all runs and final latexes. All runs had a higher initial pH (between 3.6 and 4). As the reaction proceeded, the pH lowered to 3.3-3.5. This trend is expected as the initiator builds up as the reaction progresses causing a lower pH; it decreased the most between the last sample and the final latex. Recall that no buffer was added to the formulations to keep the ionic strength low and avoid colloidal destabilization of the CNCs. The addition of CNCs did not have a noticeable effect on the pH as compared to the base case formulations; given their low concentration, their small contribution to charge is not surprising.

Glass Transition Temperature

The T_g of each run was measured and can be found in Table 2-5. Recall that theoretical T_g targets were reported in Table 1. The actual T_g values trend in the same direction but differ somewhat

from the theoretical predictions. This is not surprising given that the simple equation used to predict T_g does not account for cross-linking and degree of hydration of the samples. The microscopy and viscosity measurements imply interactions between the polymer and the CNCs. Grafting or crosslinking of the CNCs would lead to more rigid polymer chains and an increase in T_g.[33] In this study, differences in T_g appear to have been due solely to changes in composition (compare formulations A, B and C); the effect of CNC loading was non-significant (within experimental error of the DSC). Previous studies have reported increases in T_g with increasing CNC loadings using weight fractions of CNCs as high as 30 to as low as 0.25.[33], [34] However, others have reported no change in T_g when using CNCs in situ.[17]

Table 2-5: Measured glass transition temperature

Run	T_g [ºC]
0A	-22
0.5A	-21
1A	-20
0B	-29
0.5B	-28
1B	-26
0C	-35
0.5C	-36
1C	-37

Gel Content

The gel content was very high for all formulations, regardless of CNC loading (Figure 2-6). Only in composition C (which had the highest BA content, Table 2-1) was there a prominent increase in gel content with CNC content. However, for this system, the gel contents for the base case formulations were already very high (formulations A and B, Table 2-1). There was little room to increase the gel content any higher as it was approaching 100%. In previous work, the gel content

increased significantly with CNC content.[23] This was expected as the CNCs could be causing more cross-linking or grafting.

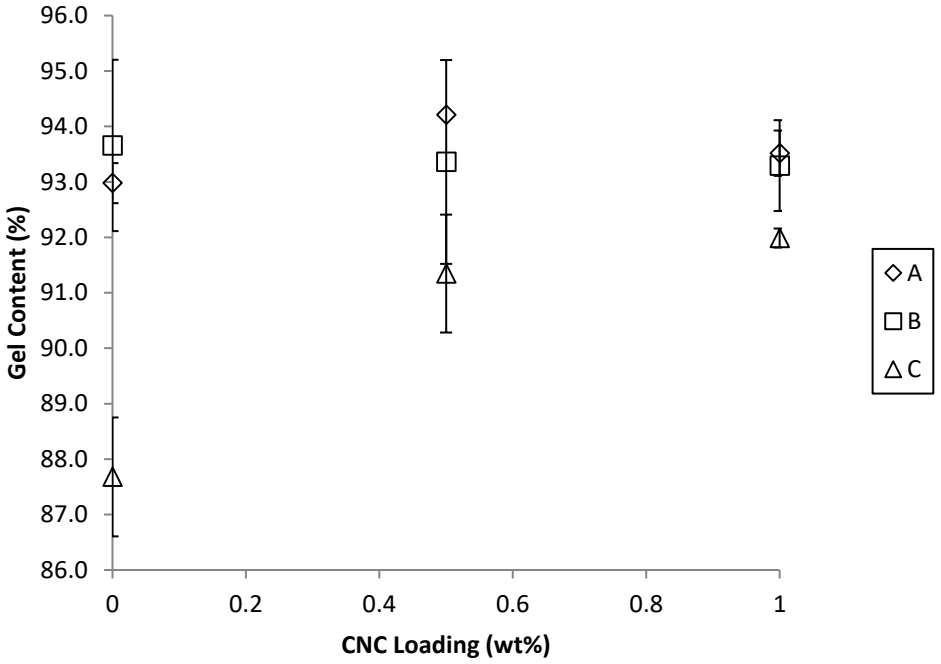

Figure 2-6: Gel content for all latexes

Adhesive Properties

Loop tack, peel strength, and shear strength were measured for all final latexes. Results for run 0.5B are from a replicate run as the peel strength results from the original run showed high variability.

For each formulation, loop tack increased with increasing CNC content (Figure 2-7). If CNCs were acting as a cross-linking agent, the tack for all formulations should have decreased. However, it increased regardless of formulation. CNCs improved the film forming ability of the PSAs due to the increase in viscosity, leading to the formation of a more uniform film. The clear influence of CNC content on tack can be explained by the improved contact of the PSA films with the testing panels due to the presence of more hydroxyl groups, in turn also improving the hydrophilicity of the PSAs. The improved wettability implies better contact between the PSA and test substrate (in

this case, stainless steel). The improved wettability relates to the increase in the presence of hydroxyl groups, which was observed via water contact angle measurements (Figure 2-8); hydroxyl groups are polar and improved the hydrophilicity.

The ability of the PSA to form a uniform bond with the stainless-steel testing plates was also improved by the addition of CNCs. It is possible that the polar hydroxyl groups present on the CNCs arranged themselves when in contact with the polar groups present on the test panel so as to improve the work of adhesion.[35]

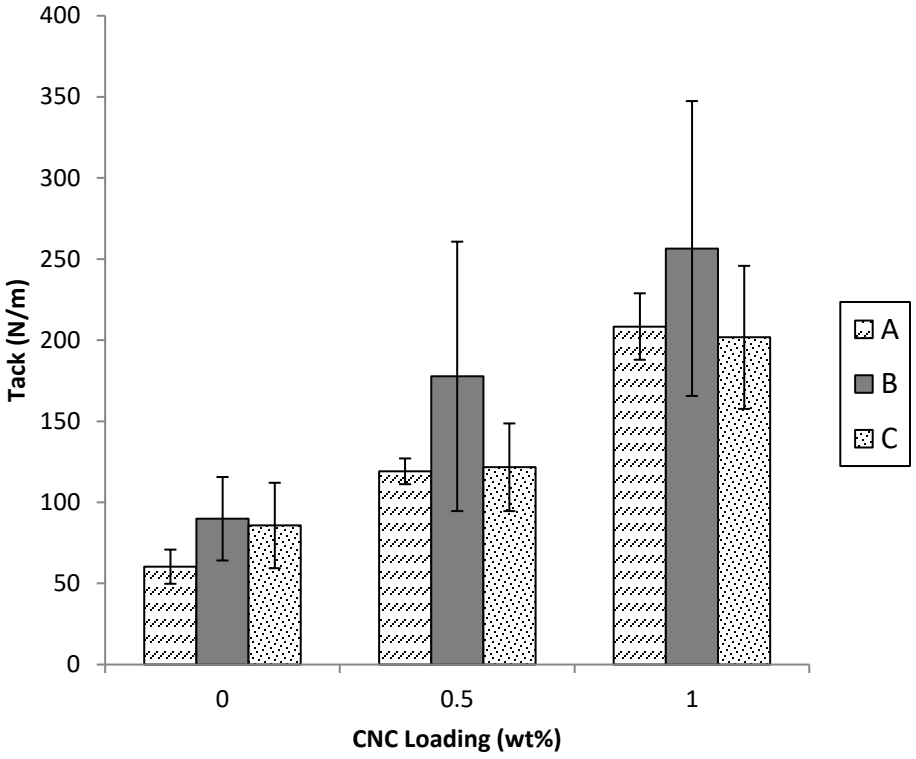

Figure 2-7: Loop tack vs. CNC content for the three latex formulations

Peel strength increased with increasing CNC content (Figure 2-9). As with the loop tack results, increasing CNC content resulted in increased peel strength. The increase in peel strength was also attributed to improved PSA film wettability. By improving the work of adhesion between the testing panel and the PSA (the initial formation of the bond), the peel strength was also improved. This effect was likely noticeable because of the low peel strength of the base case formulations. With a higher base case peel strength, one would not expect an increase in the work of adhesion

to affect the peel strength.[35], [36] Peel strength should have been higher for formulation A as it had the highest T_g. Higher T_g monomers result in improved stiffness and therefore a higher peel strength.[4]

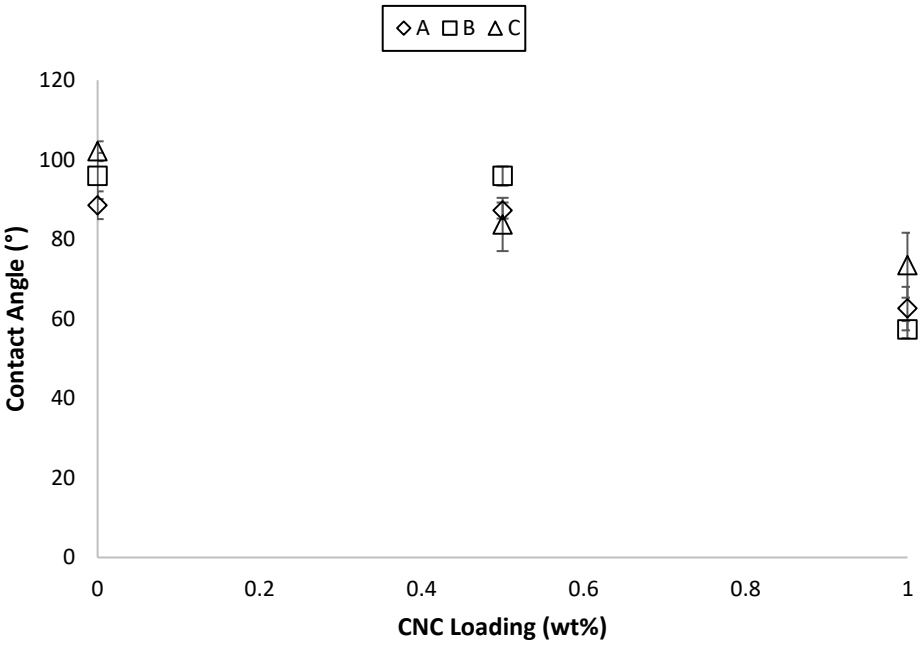

Figure 2-8: Water contact angle of latex films cast on Mylar

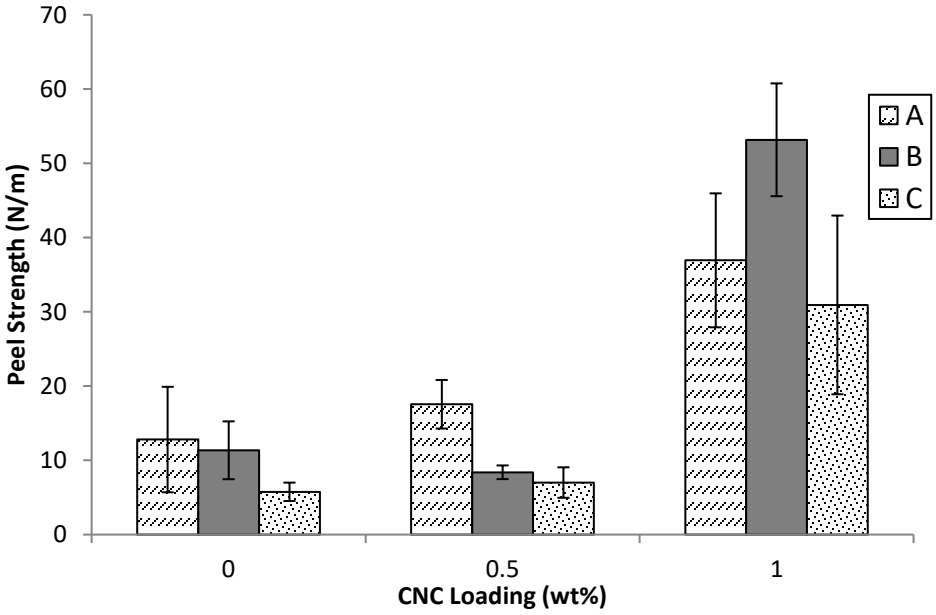

Figure 2-9: Peel strength vs. CNC content for the three latex formulations

The shear strength increased dramatically for all formulations with increasing CNC content (Figure 2-10). The shear was so high with 1 wt% CNC content that films were removed after ~115 h because they had not dropped. Formulation A exhibited the largest increase in shear strength with CNC loading; this was consistent with its higher T_g. Harder monomers and polymers with higher T_gs exhibit higher shear strength due to the increase in cohesive strength.[4] For increasing gel content, shear strength would be expected to increase but peel strength and tack would be expected to decrease.[37] The results for formulation C are consistent with this idea. However, formulations A and B did not show significant increases in gel content (Figure 2-6) and thus the increased shear strength suggests that the CNCs are contributing to cohesive strength not due to a cross-linking mechanism but rather with increased association (grafting or hydrogen bonding) with the polymer matrix. The use of hard monomers (having a higher T_g) will combat the effect of gel content as seen for all three adhesive properties. Therefore, since the gel content is not varying much based on formulation, the difference in T_g is the dominant effect on the PSAs produced here.

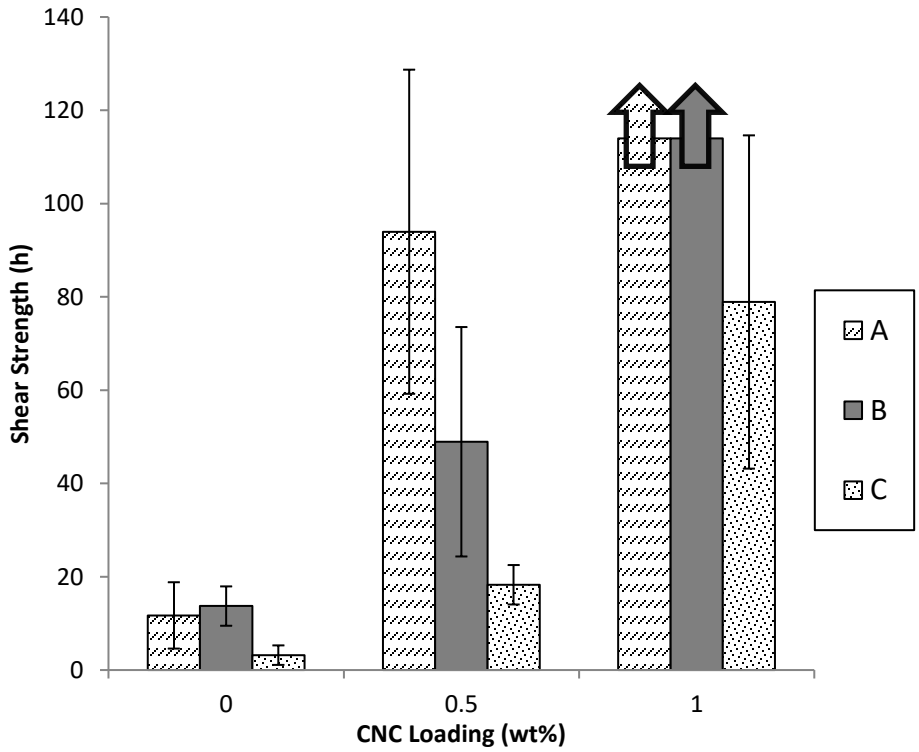

Figure 2-10: Shear strength vs. CNC content for the three latex formulations

Using CNCs, all three adhesive properties have been improved simultaneously. In most emulsion-based PSA studies, when shear strength is improved, it results in a weaker peel strength and loop tack and vice-versa.[37] Thus, the CNCs appear to be playing a dual role of increasing association of CNCs to the polymer matrix to increase shear strength and increasing wettability of the PSA films resulting in improved tack and peel strength. The significance of this finding cannot be understated.

Dynamic Mechanical Analysis

DMA was used to observe the effect of CNCs on the viscoelastic properties of the adhesive. For all formulations, increasing the CNC content increased storage modulus (G'), increased loss modulus (G'') and slightly lowered tan δ. Examples are shown for formulation B (Figure 2-11 to Figure 2-13). G' represents the elastic portion while G'' represents the viscous portion of the material's response. In all cases, regardless of CNC content or formulation, the G' was higher than G'' indicating that the properties are dominated by elastic behaviour. The increase in G' can be explained by the CNCs ability to limit motion within the polymer chain. This increase is known to occur when using any type of nanofiller as the nanoparticles will restrict polymer chain movement.[37]–[41] Tan δ is the ratio between energy lost to energy stored. For all formulations, the change in tan δ was minor compared to that in G' and G''. Typically, tan δ will decrease with increasing filler content because a stiff particle is being added to a softer polymer matrix.[38], [42] Results for formulations A and C showed similar results (Appendix A).

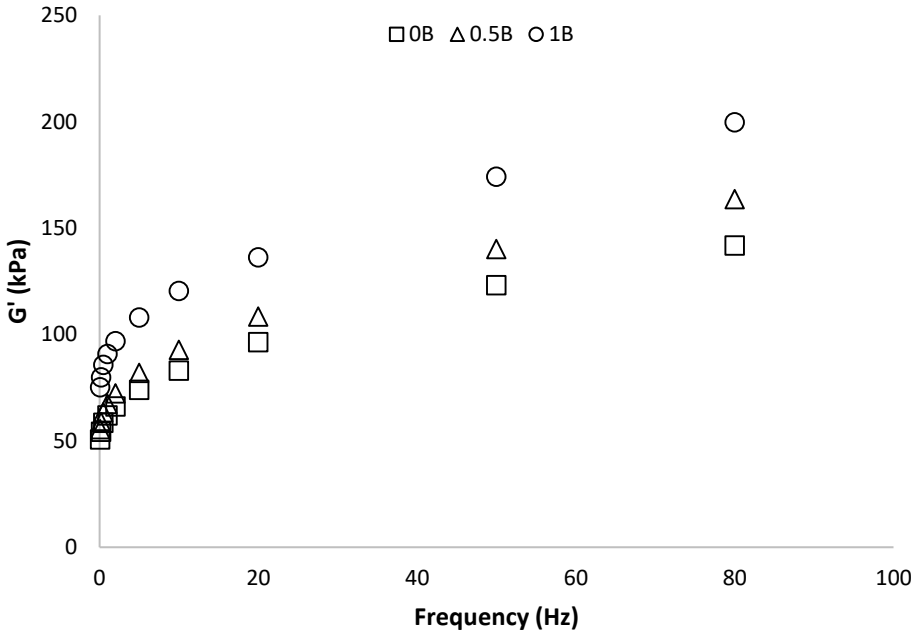

Figure 2-11: Storage moduli for formulation B at 23 °C

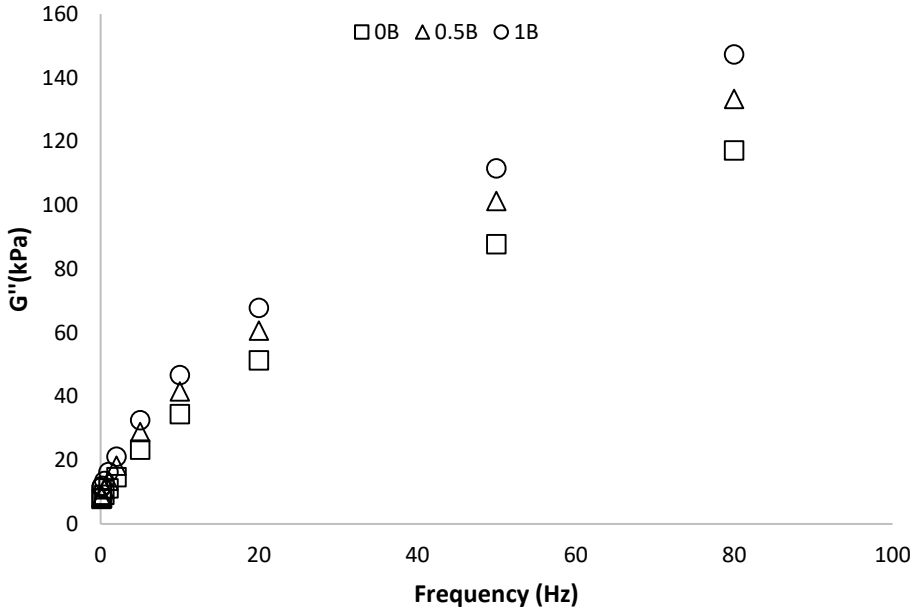

Figure 2-12: Loss moduli for formulation B at 23 °C

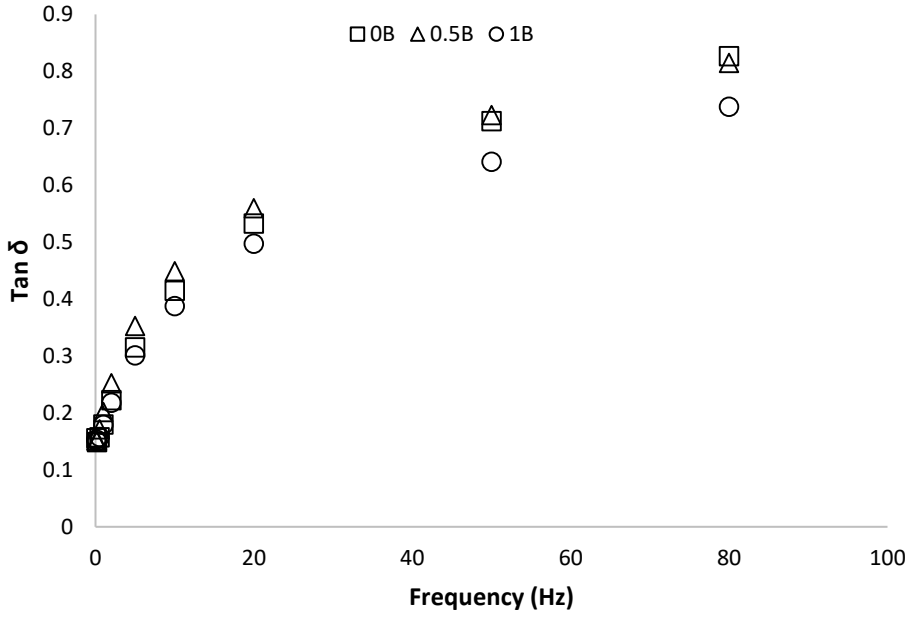

Figure 2-13: Tan δ for formulation B at 23 °C

Because the application of adhesives does not require frequencies above 10 Hz, for practical reasons, all samples were compared at this frequency (Table 2-6).[41] No significant differences were seen in tack between the different formulations (Figure 2-7). Based on the DMA results, formulation C had the lowest G' and G'' and therefore should have had the highest tack because an increase in G' indicates a more rigid PSA. In general, adhesives with lower G' and G'' should have higher tack.[4] This is also what would be expected based on T_g. Formulation A had the highest tan δ and highest peel strength, regardless of CNC content (Figure 2-9). Peel strength typically decreases with increasing tan δ.[37] All A formulations had the highest G' when CNCs were added and therefore also exhibited the highest shear strength. This was expected as formulation A had the highest T_g (Figure 2-10). Shear strength is normally highest for the PSA with the highest G', which is an indication of increased polymer rigidity.[43] This is synonymous with improved cohesive strength, which is the main measure of shear strength.

The DMA results do not follow the expected trends when comparing them to the adhesive results for the runs using CNCs. For all formulations, when CNC content was increased, the G' and G'' also increased, indicating the formation of a more rigid PSA. The tack, peel strength and shear strength of each formulation increased simultaneously with increasing CNC content (Figures 2-7,

2-9 and 2-10). The DMA results alone would indicate that the tack and peel strength should have decreased with increasing CNC content while the shear strength should have increased. Again, this is what would typically be observed when attempting to manipulate the adhesive properties using a nanoparticle. As discussed in the adhesive results, the improvement of the peel strength and tack is attributed to the increase in the work of adhesion between the PSA and the stainless-steel testing panel due to the presence of polar hydroxyl groups on the CNCs as well as the potential for hydrogen bonding.[35], [36]

Table 2-6: DMA results for all samples at 10 Hz and 23 ºC

Sample	G' (kPa)	G" (kPa)	tan δ
0A	34	21	0.61
0.5A	102	66	0.64
1A	156	96	0.62
0B	83	34	0.41
0.5B	93	42	0.45
1B	120	47	0.39
0C	66	19	0.29
0.5C	63	18	0.28
1C	79	19	0.24

Blending vs. In Situ

We have shown that adding CNCs via in situ polymerization had a significant influence on the adhesive properties. An important question relates to the necessity of using an in situ technique as opposed to a more straightforward blend of a latex with a CNC dispersion. Thus, a blend technique was tested and factors such as heating, mixing time and the presence of initiator were investigated. All tests were done using formulation B and a 1 wt% CNC loading.

In this work, the base case latex was blended in a beaker for 30 min, using a magnetic stirrer at room temperature, with the CNC suspension to achieve 1 wt% CNCs and 40% solids (i.e., a "non-heated blend"). In previous work, it was found that CNC latex blending at room temperature did

not improve adhesive properties to the same level as did the in situ runs.[23] To test if it was the heating and mixing of the in situ conditions which resulted in adhesive performance improvements and perhaps the presence of the initiator in the polymerization mixture, a "heated blend" was performed.. The heated blend consisted of adding CNCs directly to the reactor at the end of the base case polymerization and continuing mixing at 250 rpm for 2 h at 60˚C. Lastly, to eliminate the possibility of additional shear influencing the adhesive results of the heated blend, the same heated blend experiment was performed on a base case formulation with no CNC addition ("extended base case") to identify if there were any rheological effects from the additional mixing/heating process. That base case was polymerized and then allowed to mix and be heated for an additional 2 h.

Comparison of the in situ films' adhesive properties to that of the non-heated blend, showed significantly better tack, peel strength and shear strength for the in situ case (Table 2-7). For both the in situ and non-heated blend cases, all adhesive properties were superior to that of the base case run. For the heated blend, the tack and peel strength results were not significantly different from those of the in situ run (Table 2-7). However, shear strength was higher for the in situ run. A decrease in viscosity was noted in the heated blend; this decrease was due to the formation of coagulum within the latex. Coagulum formation may be an indication of CNC aggregation due to poor dispersion.

To distinguish whether the additional heating and mixing treatments were affecting the base latex or the mixture of latex and CNCs, the extended based case run was performed. The extended base case run exhibited comparable tack, higher peel strength and lower shear strength than those of the in situ run. Although the different approaches yielded similar tack and peel strength, the in situ CNC case provided the best shear strength. In any case, a heated blend approach would not be preferred because of the additional time required to perform the procedure, which would make it impractical on a commercial scale.

Table 2-7: Blend vs. in situ adhesive results for formulation B

Run	CNC Loading (wt%)	Tack (N/m)	Peel Strength (N/m)	Shear (h)	Viscosity (cP)
Base Case	0	90±25	11±4	13±4	177
In Situ	1	256±90	53±7	*114+	231
Non-Heated Blend	1	201±56	37±12	63±17	78
Heated Blend	1	215±37	40±15	86±20	154
Extended Base Case	0	242±2	108±46	24±6	142

* Samples were removed at 114 h and had not fallen.

Conclusions

CNCs were successfully added in situ to an emulsion polymerization to synthesize a PSA nanocomposite. The resulting PSAs were stable and the CNCs showed some interaction with the PSAs (and were not aggregating) as indicated by TEM images as well as a narrow PSD from particle size analysis. Using CNC loadings from 0 to 1 wt%, it was possible to improve all adhesive properties (tack, peel strength and shear strength) without the use of harsh additives. As was shown in the adhesive performance section, the CNC/latex nanocomposite films outperformed the base case formulations in all respects.

Viscosity significantly increased with increasing CNC content. The viscosity of the 1 wt% CNC formulations were almost three times higher than the base case at the same solids content. Also, the addition of CNCs increased the storage and loss moduli. The CNCs significantly improved the PSA's elasticity, as indicated by the high storage modulus. The improvement in mechanical properties is attributed to the CNCs ability to form hydrogen bonds with the latex polymer, the potential for CNC grafting due to the presence of KPS and the potential for reinforcement due to the high surface area of the CNCs.

Significant improvements have been made to PSAs using only a small amount of CNCs. CNCs are non-toxic, renewable additives and can open doors to the development of a more sustainable polymer product.

Acknowledgements

Financial support for this work through the Natural Science and Engineering Research Council (NSERC) of Canada, CelluForce and NSERC, CelluForce, and FPInnovations is greatly acknowledged.

References

[1] K. Leja and G. Lewandowicz, "Polymer biodegradation and biodegradable polymers - a review," *Polish J. Environ. Stud*, vol. 19, no. May, pp. 255–266, 2010.

[2] W. P. Flauzino Neto, M. Mariano, I. S. V. da Silva, H. A. Silvério, J. L. Putaux, H. Otaguro, D. Pasquini, and A. Dufresne, "Mechanical properties of natural rubber nanocomposites reinforced with high aspect ratio cellulose nanocrystals isolated from soy hulls," *Carbohydr. Polym.*, vol. 153, pp. 143–152, 2016.

[3] R. J. Young and P. A. Lovell, *Introduction to Polymers*, Third. Boca Raton: CRC Press, 2011.

[4] R. Jovanovic and M. A. Dubé, "Emulsion-based pressure-sensitive adhesives : A review," *J. Macromol. Sci.*, vol. C44, no. 1, pp. 1–51, 2004.

[5] F. Chivrac, E. Pollet, and L. Avérous, "Progress in nano-biocomposites based on polysaccharides and nanoclays," *Mater. Sci. Eng. R Reports*, vol. 67, no. 1, pp. 1–17, 2009.

[6] A. Dufresne, *Nanocellulose*. Saint Martin D'Heres cedex: De Gruyter, 2012.

[7] S. Spinella, G. Lo Re, B. Liu, J. Dorgan, Y. Habibi, P. Leclère, J. M. Raquez, P. Dubois, and R. A. Gross, "Polylactide/cellulose nanocrystal nanocomposites: Efficient routes for nanofiber modification and effects of nanofiber chemistry on PLA reinforcement," *Polym. (United Kingdom)*, vol. 65, pp. 9–17, 2015.

[8] Y. Habibi, L. A. Lucia, and O. J. Rojas, "Cellulose nanocrystals : chemistry , self-

assembly , and applications," *Chem. Rev.*, vol. 110, no. 6, pp. 3479–3500, 2010.

[9] S. J. Eichhorn, A. Dufresne, M. Aranguren, N. E. Marcovich, J. R. Capadona, S. J. Rowan, C. Weder, W. Thielemans, M. Roman, S. Renneckar, K. Abe, W. Gindl, S. Veigel, J. Keckes, H. Yano, M. Nogi, A. N. Nakagaito, A. Mangalam, J. Simonsen, A. S. Benight, T. Peijs, A. Bismarck, and L. A. Berglund, "Review : current international research into cellulose nanofibres and nanocomposites," *J. Mater. Sci.*, vol. 45, pp. 1–33, 2010.

[10] Y. Habibi, "Key advances in the chemical modification of nanocelluloses," *Chem. Soc. Rev.*, vol. 43, no. 5, pp. 1519–1542, 2014.

[11] V. Favier, G. R. Canova, J. Y. Cavaillé, H. Chanzy, A. Dufresne, and C. Gauthier, "Nanocomposite materials from latex and cellulose whiskers," *Polym. Adv. Technol.*, vol. 6, no. 5, pp. 351–355, 1995.

[12] A. Ben Mabrouk, M. C. B. Salon, A. Magnin, M. N. Belgacem, and S. Boufi, "Cellulose-based nanocomposites prepared via mini-emulsion polymerization: Understanding the chemistry of the nanocellulose/matrix interface," *Colloids Surfaces A Physicochem. Eng. Asp.*, vol. 448, no. 1, pp. 1–8, 2014.

[13] M. S. Reid, M. Villalobos, and E. D. Cranston, "Benchmarking cellulose nanocrystals: from the laboratory to industrial production," *Langmuir*, vol. 33, no. 7, pp. 1583–1598, 2017.

[14] M. Hervy, S. Evangelisti, P. Lettieri, and K. Y. Lee, "Life cycle assessment of nanocellulose-reinforced advanced fibre composites," *Compos. Sci. Technol.*, vol. 118, pp. 154–162, 2015.

[15] R. J. Moon, A. Martini, J. Nairn, J. Youngblood, A. Martini, and J. Nairn, "Cellulose nanomaterials review : structure , properties and nanocomposites," *Chem. Soc. Rev.*, vol. 40, no. 6, pp. 3941–3994, 2011.

[16] C. E. Meree, G. T. Schueneman, J. C. Meredith, and M. L. Shofner, "Rheological behavior of highly loaded cellulose nanocrystal/poly(vinyl alcohol) composite

suspensions," *Cellulose*, vol. 23, no. 5, pp. 3001–3012, 2016.

[17] C. Miao and W. Y. Hamad, "In-situ polymerized cellulose nanocrystals (CNC) poly(L-lactide) (PLLA) nanomaterials and applications in nanocomposite processing," *Carbohydr. Polym.*, vol. 153, pp. 549–558, 2016.

[18] J. Yang, J. J. Zhao, and X. M. Zhang, "Modification of cellulose nanocrystal-reinforced composite hydrogels: effects of co-crosslinked and drying treatment," *Cellulose*, pp. 3487–3496, 2014.

[19] N. Girouard, G. T. Schueneman, M. L. Shofner, and J. C. Meredith, "Exploiting colloidal interfaces to increase dispersion, performance, and pot-life in cellulose nanocrystal/waterborne epoxy composites," *Polymer (Guildf).*, vol. 68, pp. 111–121, 2015.

[20] F. Bettaieb, R. Khiari, A. Dufresne, M. F. Mhenni, and M. N. Belgacem, "Mechanical and thermal properties of Posidonia oceanica cellulose nanocrystal reinforced polymer," *Carbohydr. Polym.*, vol. 123, pp. 99–104, 2015.

[21] M. Roman and W. T. Winter, "Cellulose nanocrystals for thermoplastic reinforcement : effect of filler surface chemistry on composite properties," in *Cellulose Nanocomposites Processing, Characterization and Properties*, K. Oksman and M. Sain, Eds. Washington, D.C.: Oxford University Press Inc., 2006, pp. 99–113.

[22] Y. Zhang and M. A. Dubé, "Green emulsion polymerization technology," in *Advances in Polymer Science*, Berlin, Heidelberg: Springer, 2017, pp. 1–36.

[23] Z. Dastjerdi and M. A. Dubé, "Cellulose nanocrystals : renewable property modifiers for pressure sensitive adhesives," University of Ottawa, 2017.

[24] A. Li and K. Li, "Pressure-sensitive adhesives based on soybean fatty acids," *RSC Adv.*, vol. 4, no. 41, pp. 21521–21530, 2014.

[25] P. Ghosh, D. Dev, and A. K. Samanta, "Graft copolymerization of acrylamide on cotton cellulose in a limited aqueous system following pretreatment technique," *J. Appl. Polym. Sci.*, vol. 58, no. 10, p. 1727, 1995.

[26] G. Gürdag and S. Sarmad, “Cellulose graft copolymers: synthesis, properties, and applications,” in *Polysaccharide Based Graft Copolymers*, S. Kalia and M. W. Sabaa, Eds. Berlin, Heidelberg: Springer Berlin Heidelberg, 2013, pp. 15–57.

[27] K. B. Anoop, S. Kabelac, T. Sundararajan, and S. K. Das, “Rheological and flow characteristics of nanofluids: Influence of electroviscous effects and particle agglomeration,” *J. Appl. Phys.*, vol. 106, no. 3, 2009.

[28] Gaganpreet and S. Srivastava, “Influence of particle shape on viscosity of nanofluids,” *AIP Conf. Proc.*, vol. 1512, no. 2013, pp. 984–985, 2013.

[29] M. C. Li, Q. Wu, K. Song, S. Lee, Y. Qing, and Y. Wu, “Cellulose nanoparticles: structure-morphology-rheology relationships,” *ACS Sustain. Chem. Eng.*, vol. 3, no. 5, pp. 821–832, 2015.

[30] E. V. Timofeeva, J. L. Routbort, and D. Singh, “Particle shape effects on thermophysical properties of alumina nanofluids,” *J. Appl. Phys.*, vol. 106, no. 1, 2009.

[31] Y. C. Ching, M. Ershad Ali, L. C. Abdullah, K. W. Choo, Y. C. Kuan, S. J. Julaihi, C. H. Chuah, and N. S. Liou, “Rheological properties of cellulose nanocrystal-embedded polymer composites: a review,” *Cellulose*, vol. 23, no. 2, pp. 1011–1030, 2016.

[32] C. Qiao, G. Chen, J. Zhang, and J. Yao, “Structure and rheological properties of cellulose nanocrystals suspension,” *Food Hydrocoll.*, vol. 55, pp. 19–25, 2016.

[33] H.-Y. Yu, Z.-Y. Qin, C.-F. Yan, and J.-M. Yao, “Green nanocomposites based on functionalized cellulose nanocrystals: a study on the relationship between interfacial interaction and property enhancement,” *ACS Sustain. Chem. Eng.*, vol. 2, no. 4, pp. 875–886, 2014.

[34] E. Erbas Kiziltas, A. Kiziltas, S. C. Bollin, and D. J. Gardner, “Preparation and characterization of transparent PMMA-cellulose-based nanocomposites,” *Carbohydr. Polym.*, vol. 127, pp. 381–389, 2015.

[35] C. Fang, Y. Jing, Y. Zong, and Z. Lin, “Effect of N , N-dimethylacrylamide (DMA) on the comprehensive properties of acrylic latex pressure sensitive adhesives,” *Int. J. Adhes.*

Adhes., vol. 71, pp. 105–111, 2016.

[36] S. Sohn and S. Yang, “On the work of adhesion and peel strength between pressure sensitive adhesives and the polymeric films used in LCD devices,” *J. Adhes. Sci. Technol.*, vol. 17, no. 7, pp. 903–915, 2017.

[37] L. Qie and M. A. Dubé, “Performance improvement of latex-based PSAs using polymer microstructure control,” University of Ottawa, 2011.

[38] Z. Dastjerdi, E. D. Cranston, and M. A. Dubé, “Synthesis of poly (n -butyl acrylate / methyl methacrylate)/ CNC latex nanocomposites via in situ emulsion polymerization,” *Macromol. React. Eng.*, pp. 1–8, 2017.

[39] J. Kajtna and U. Šebenik, “Novel acrylic / nanocellulose microsphere with improved adhesive properties,” *Int. J. Adhes. Adhes.*, vol. 74, no. November 2016, pp. 100–106, 2017.

[40] N. E. Marcovich, M. I. Auad, N. E. Bellesi, S. R. Nutt, and M. Aranguren, “Cellulose micro / nanocrystals reinforced polyurethane,” *J. Mater. Res.*, vol. 21, no. 4, pp. 870–881, 2006.

[41] M. Khalina, M. Sanei, H. S. Mobarakeh, and A. Reza, “Preparation of acrylic / silica nanocomposites latexes with potential application in pressure sensitive adhesive,” *Int. J. Adhes. Adhes.*, vol. 58, pp. 21–27, 2015.

[42] V. G. Gregoriou, G. Kandilioti, and S. T. Bollas, “Chain conformational transformations in syndiotactic polypropylene / layered silicate nanocomposites during mechanical elongation and thermal treatment,” *Polymer (Guildf).*, vol. 46, pp. 11340–11350, 2005.

[43] E. P. Chang, “Viscoelastic properties of pressure- sensitive adhesives,” *J. Adhes.*, vol. 60, pp. 233–248, 1997.

Chapter 3: Effect of Monomer Water Solubility on CNC Nanocomposites for Adhesive Applications via In Situ Semi Batch Emulsion Polymerization

Alexandra Ouzas[1], Elina Niinivaara[2], Emily D. Cranston[2], Marc A. Dubé[1]

[1]Department of Chemical and Biological Engineering
Centre for Catalysis Research and Innovation
University of Ottawa
161 Louis Pasteur Pvt.
Ottawa, Ontario K1N 6N5, Canada

[2]Department of Chemical Engineering
McMaster University
1280 Main Street West
Hamilton, Ontario L8S 4L7, Canada

Cellulose from various plant sources can be used to make cellulose nanocrystals (CNCs) which are designated safe and green, hydrophilic nanoparticles. CNCs were added in situ during a semi-batch 2-ethyl hexyl acrylate (EHA)/n-butyl acrylate (BA)/methyl methacrylate (MMA) emulsion polymerization. Results were compared to the previously investigated isobutyl acrylate (IBA)/BA/MMA system. The adhesive properties (loop tack, peel strength and shear strength) of the IBA/BA/MMA system were previously shown to improve with increasing CNC loading. For the EHA/BA/MMA system, the reinforcing effect of the CNCs was inhibited because of the hydrophobicity of EHA relative to IBA. Shear strength was improved for the EHA/BA/MMA system using CNCs, but the observed effect was not as significant as that for the IBA/BA/MMA system. Both systems showed similar trends for conversion, latex particle size, pH, viscosity, polymer glass transition temperature (T_g), and gel content. Microscopy was used to confirm a poor dispersion of CNC in the EHA/BA/MMA system. Comparison of the in situ polymerized nanocomposites to their blended counterparts was also made.

Keywords: 2-ethyl hexyl acrylate, butyl acrylate, isobutyl acrylate, methyl methacrylate, cellulose nanocrystals, nanocomposites, emulsion polymerization, pressure sensitive adhesives

Introduction

The polymer industry is actively seeking ways to make polymerization reactions and products more sustainable. This can include replacing monomers and other polymer additives with renewable (or bio-sourced) components.[1] Over 140 million tonnes of synthetic polymers are synthesized per year.[2] The use of bio-sourced monomers as replacements to the synthetic components often necessitates additional effort to maintain polymer application properties.[3] There is significant interest in finding a way to use these monomers without sacrificing performance. This is often accomplished by the use of additives such as chain transfer agents and crosslinkers to modify the polymer microstructure and thus affect the polymer performance properties in a positive direction. Ideally, these additives would themselves be renewable and non-toxic.

A pressure sensitive adhesive (PSA) is a polymer that remains permanently tacky at room temperature and adheres to a surface with a light application of pressure.[4] PSAs are made by co-polymerizing a monomer with a low polymer glass transition temperature (T_g), such as n-butyl acrylate (BA), with a high homopolymer T_g monomer, such as methyl methacrylate (MMA). This is done to balance the adhesive properties and tune the copolymer T_g for the appropriate application temperature. The adhesive properties in question include tack, peel strength and shear strength. Tack describes how well the adhesive bonds with a surface and peel strength is a measure of the force needed to remove the adhesive from that surface. Shear strength is the cohesive force of the adhesive polymer. Often, improving the shear strength results in decreases to peel strength and tack.[5] In particular, low shear strength is commonly an issue for emulsion-based PSAs compared to their solution-based counterparts. Due to the compartmentalized nature of emulsion polymerization, achieving a continuous gel network in the final PSA film (cast from a latex dispersion) is challenging. As a result, the cohesive forces are reduced and this leads to a lower shear strength compared to the solution case, in which a continuous gel network is formed.[6]

Nanomaterials are often used to improve polymer properties (e.g., tensile strength) as a nanocomposite with a polymer matrix. Nanoparticles can significantly affect polymer properties due to their high surface area and thus, act as reinforcing agents. Some nanoparticles such as carbon black and silica, which are traditionally used for natural rubber reinforcement, require high energy consumption for their production.[7] Less energy intensive and “greener” nanoparticles such as starch, cellulose and chitin are also available for use in nanocomposites.[8] One such nanoparticle

type is cellulose nanocrystals (CNCs), which are isolated from natural cellulose, the most abundant polymer on earth. CNCs are a "green" alternative to common reinforcing agents and have many other potential applications as rheological modifiers and interface stabilizers.[9] CNCs form colloidally stable dispersions in water and can easily be incorporated/processed in water-based systems, eliminating the need for organic solvents.[7] Cellulose contains a large number of hydroxyl groups which are capable of hydrogen bonding; the combination of cellulose's potential to crystallize and hydrogen bond makes it a strong, rigid and generally insoluble material. To dissolve cellulose or improve its compatibility with hydrophobic polymers, cellulose can be derivatized or nanocellulose can be surface modified.[10] Modifications of CNCs are possible due to the presence of hydroxyl groups.[11] The most common method to produce CNCs is through acid hydrolysis with sulfuric acid; this process preferentially degrades the disordered cellulose regions and leaves behind the crystalline CNCs with grafted anionic sulfate half ester groups.[9] The resulting nanoparticles are whisker-shaped and have a high aspect ratio.[11] CNCs provide composite material reinforcement in the range of other nanomaterials. [9], [11]

In the past, CNCs have been blended with polymers and significant strength improvements were noted[8, 13-20]. This was the case for styrene-BA polymer films cast with CNCs.[12] Others have reported improved storage moduli for CNC-reinforced polylactide and natural rubber.[7], [13] CNC nanocomposites have also been produced using in situ polymerization methods. L-lactide ring opening polymerization in the presence of CNCs resulted in improved barrier properties of poly (lactic acid).[14] CNCs have also been incorporated via in situ methods in the synthesis of poly(acrylamide) hydrogels. Tensile strength and elongation ratios were both improved in that case.[15] Most recently, we have produced CNC nanocomposites using batch and semi-batch emulsion polymerization. Using BA and MMA, both storage and loss moduli were improved with increasing CNC content.[16] When incorporating a hydrophilic particle, such as starch, into a hydrophobic polymer matrix, the polymer-particle interface presents a weakness.[8] Because CNCs are hydrophilic nanoparticles, challenges are encountered in emulsion polymerization formulations. In previous work, CNCs were successfully integrated into latexes using MMA, BA, and isobutyl acrylate (IBA) each of which possess moderate water solubility. It is also well known that the more the CNCs (or nanocomposites in general) are well-dispersed within a latex, the better is the reinforcing effect.[17], [18] In this work, 2-ethyl hexyl acrylate (EHA), a highly hydrophobic monomer, is used in the formulation. Comparisons of EHA/BA/MMA (henceforth referred to as

the EHA system) adhesive film performance are made to films previously produced using IBA/BA/MMA terpolymers (henceforth referred to as the IBA system) (Chapter 2).

Experimental

Materials

BA, EHA and MMA (all >99%, Sigma Aldrich) were used as received. The initiator, potassium persulfate (KPS, ACS Reagent, >99%, Sigma Aldrich), and the anionic surfactant, sodium dodecyl sulfate (SDS, ACS Reagent >99%, Sigma Aldrich), were used with no further purification. CNCs produced by sulfuric acid hydrolysis were donated by CelluForce (Windsor, Quebec) as a spray-dried powder in the sodium salt form (183±88 × 6±2 nm)[19] and were used to create aqueous CNC dispersions. Distilled, deionized (DDI) water was used to prepare the CNC dispersions as well as the pre-emulsion and solvent for initiator. Hydroquinone ('Baker' grade, JT Baker Chemical Co.) was used as an inhibitor. Tetrahydrofuran (THF, ACS grade, Sigma Aldrich) was used as supplied for gel content analysis.

CNC Redispersion

CNC dispersions were prepared by mixing CNC powder with DDI water on a magnetic stir plate with a stirring bar for 1-3 h until all powder was dispersed. The dispersion was sonicated (Fisher Scientific 550 sonic dismembrator) for 5 min at 75% amplitude while submerged in an ice bath. It was left to rest for 5 min and the cycle was repeated for a total of 3 times. The dispersion was vacuum filtered (110 mm, particle retention of >2.7 μm) to ensure no contaminants remained. It was filtered three times and then stored at room temperature.

Emulsion Polymerization

All polymerization reactions were performed in a 1.25 L stainless steel Mettler Toledo LabMax Automatic Lab Reactor equipped with an anchor stirrer, cooling jacket, condenser and feed lines for both the initiator and pre-emulsion. A nitrogen blanket was maintained throughout all reactions. A semi-batch procedure was used where an initial seed was prepared in the reactor followed by a feeding phase and final cook stage.

Three formulations (Table 3-1) were tested at three CNC loadings (0, 0.5 and 1 wt% based on total monomer) for a total of nine runs. The general recipe and water allocation can be found in Table 3-2 and 3. The composition was varied to achieve a range of T_gs suitable for PSA applications.[20],

[21] A modified recipe is shown for the base case in Table 3-4; to ensure proper film formation, the base case was made using a higher solids content.

Table 3-1: Monomer composition and theoretical T_g values of formulations A, B and C

Run*	EHA/BA/MMA (wt%)	EHA/BA/MMA (mol%)	T_g (°C)
E-A	29/41/30	20/41/39	-18
E-B	39/41/20	29/28/43	-30
E-C	49/41/10	39/46/15	-40

*Runs were identified by composition and CNC wt%; e.g., E-0.5B represents EHA/BA/MMA composition B with 0.5 wt% CNC.

Table 3-2: General recipe for seeded semi-batch polymerization

Component	Seed Stage (g)	Feed Stage (g)
CNC	0, 1.1 or 2.2	-
Monomer	22	198
KPS	0.06	0.54
SDS	0.7	2.6
Water	208*	122**

*Includes KPS solution, SDS solution and CNC dispersion (if used). Exact distribution varied depending on if CNCs were used (Table 3-3).
**54 g for KPS solution and 68 g for pre-emulsion (monomer, SDS and water).

Table 3-3: Water allocation in solution/dispersion for seed stage

Solution/dispersion	Water [0 wt% CNC] (g)	Water [0.5 wt% CNC] (g)	Water [1 wt% CNC] (g)
CNC	0	110	165
KPS	3	3	3
SDS	205	95	40

Table 3-4: Higher solids recipe for base case film formation

Component	Seed Stage (g)	Feed Stage (g)
Monomer	22	198
KPS	0.06	0.54
SDS	0.43	2.6
Water	115/3*	122

* 115 g of water was used to prepare the surfactant solution and 3 g was used to prepare the initiator solution. The water distribution for the feed stage is as described in Table 3-2.

Seed Stage

The reactor was initially charged with SDS solution. If the run included CNCs, the CNC dispersion was charged to the reactor as a shot at this time. The reactor was heated for 30 min to 60 ˚C and the stirrer set to 250 rpm. During this time, the reactor was purged with nitrogen gas (Linde Canada). Once at the set point, the monomer was added and allowed to heat and mix for 3 min. Then, an initiator solution was added and reacted for 30 min.

Feed Stage

Once the seed stage was complete, the feed phase began. The pre-emulsion was fed at 1.3 g/min for 210 min and the initiator solution was fed at 0.22 g/min for 240 min. The temperature of 60 ˚C was held constant throughout the entire reaction. Samples (~10 g) were collected periodically. Upon completion of the feed stage, the reaction was continued for a 20 min cook stage. The final latex was stored at room temperature for characterization.

Characterization

Conversion by gravimetry, particle size by dynamic light scattering (DLS), and pH were measured for all samples and final latexes. Final latexes were further characterized for viscosity, gel content, and T_g using differential scanning calorimetry (DSC). The adhesive properties (tack, peel strength and shear strength) of the films were measured using standard Pressure Sensitive Tape Council (PSTC) methods. Selected latexes were analyzed by Transmission Electron Microscopy (TEM). All error bars presented represent the standard deviation of the measurement (only used when repeat measurements were performed).

Conversion

The overall conversion for each sample was calculated based on the total dried polymer using standard gravimetric techniques. The instantaneous conversion was calculated on the basis of monomer fed at the sampling time whereas overall conversion was calculated based on the monomer content in the entire reaction formulation.

Particle Size

Using DLS (Malvern NanoS Zetasizer), the particle size and particle size distribution (PSD) were measured for all samples and final latexes. A double dilution (to ca. 10,000x) was used on one drop of sample in ~2 g of DDI water and was placed in a cuvette. Each sample was tested 3 times at an angle of 176 º.

pH

The pH of all samples and final latexes was measured using a pH probe (Fisher Scientific/ Accumet Research AR50 Dual Channel pH/Ion/ Conductivity meter).

Viscosity

The viscosity of all final latexes was measured using a Thermo Scientific HAAKE Viscotester (Model D). The shear speed was 200 rpm and the correct spindle was chosen to provide enough drag to perform the measurement.

Glass Transition Temperature (T_g)

~20 mg of sample was prepared and tested by DSC (TA Instruments, Model Q100). Only final latexes were characterized for T_g. The system was calibrated and a nitrogen blanket was maintained throughout the measurement. Samples were initially heated to 100 ˚C at 10 ºC/min and then cooled to -80 ºC. Samples were then reheated at 10 ºC/min to 20 ºC. The T_g was calculated at the inflection point of the reverse heat flow curve.

Gel Content

Gel content was measured for all final latexes. Approximately 0.2 g of polymer was placed in a PVDF (poly(vinylidene fluoride)) Durapore (Millipore) membrane pouch with a pore size of 0.5 μm and a diameter of 47 mm and heat sealed. Each pouch was then soaked in THF for 12 h and then gently shaken for an additional 12 h. Each pouch was dried to a constant weight and the gel content was calculated.

Adhesive Properties

A #50 Meyer rod was used to cast latexes onto 12” x 14” corona treated Mylar sheets. Films were dried in a humidity (50±5 % relative humidity) and temperature (23±2 ˚C) controlled room for 48 h. These conditions were also used during adhesive testing.

Loop tack for all latexes was measured using the PSTC-16 standard. Using a 1” x 5” piece of sample, a loop was formed with the adhesive side on the outside. A piece of masking tape was used to secure the sample. The sample was secured in the Instron tester and then lowered at 2 mm/s until a 1” by 1” contact area was obtained on the stainless-steel test panel. The sample was then removed at 5 mm/s and the maximum force required was reported as the tack. A minimum of 3 samples were tested per film.

Peel strength of all latexes was measured using the PSTC-101 standard using Test A for 180^o peel. Strips of 1” x 12” from the film were cut and a piece of masking tape was attached to one end of the sample. This was to add extra grip so the Instron tester could hold the sample. With the adhesive side down, the sample was rolled onto a stainless-steel plate with a 2040 ± 45 g steel roller. The

roller was rolled at 10 mm/s and the sample was rolled twice in each direction. A minimum of 5 samples were tested per film.

Shear strength was obtained using the PSTC-107A standard. Test strips of 0.5" x 5" were cut from the film. The sample was rolled onto a stainless-steel plate using the same steel roller as described above, ensuring the contact area was 0.5" x 0.5" (Normally, a testing area of 1" x 1" is used but this was reduced to 0.5" x 0.5" due to the very high shear strengths for our samples). A rolling speed of 10 mm/s was used to roll the sample twice in both directions. Shear strength was measured by hanging a 1 kg weight from the sample; the time required for the weight to fall was reported as well as the failure mechanism (adhesive or cohesive failure).

Water Contact Angle

Water contact angle measurements were performed using a VCA Optima (AST Productions Inc.). A 1.8 mm thick sample of polymer was prepared on silicon release paper. The samples were dried for 1-2 days at ambient conditions. They were heated to 35 ˚C under vacuum for 5-7 days. A 1 µL water droplet was dropped onto the surface followed by immediate measurement of the contact angle. Contact angle was calculated by VCA OptimaXE software. At least 3 measurements per sample were performed.

Microscopy

TEM was used to image selected latex samples. A drop casting method was used. The latex was dropped on Formvar coated copper TEM grids and was air dried for 24 h. A JEOL 1200 EX TEMSCAN microscope using 80 kV collected the TEM images. No staining was used.

Results and Discussion

The goal of this study was to investigate the effect of the addition of CNCs on adhesive properties for a comonomer system containing a significant amount of a highly hydrophobic component (i.e., EHA). In a previous study, we investigated the IBA/BA/MMA system, for which all components exhibit a certain water solubility (Table 3-5). The IBA/BA/MMA study demonstrated a reinforcing effect when CNCs were added to the formulation (Chapter 2). In that case, the monomer formulation differed in that the MMA content was held constant (Table 3-6). However, the procedure and amounts of the other components in the latex formulations were the same (Chapter 2). Results from the EHA/BA/MMA runs were compared to the IBA/BA/MMA system. As noted above, part of the motivation for using EHA instead of IBA in the formulation was to

modify the overall water solubility of each recipe and to investigate the effect of a highly hydrophobic monomer on the property enhancements afforded by the CNCs. The apparent solubility of each system in water was estimated using the respective solubility of each monomer as a mass-weighted average (Table 3-7). Although the EHA content was changed, the overall solubility of the formulations was dominated by the MMA content, MMA being significantly more soluble than the other monomers (Table 3-5). For the IBA system, the solubility remained relatively constant between formulations. The apparent solubility of two of the EHA latexes (i.e., E-A, E-B) was higher than that of the IBA system whereas the E-C system was less soluble overall (Table 3-7).

Table 3-5: Solubility of monomers in water

Monomer	Solubility in water at 20˚C (g/L)
BA	1.4
MMA	15.9
IBA	2
EHA	<0.001

Table 3-6: Compositions of IBA/BA/MMA system from Chapter 2

Run*	IBA/BA/MMA (wt%)	IBA/BA/MMA (mol%)
I-A	70/20/10	68/20/12
I-B	39/51/10	38/50/12
I-C	8/82/10	8/80/12

*As in Table 3-1, runs were identified by composition and CNC wt%; e.g., I-0.5C represents IBA/BA/MMA composition C with 0.5 wt% CNC.

Table 3-7: Apparent water solubility of IBA and EHA formulations

Formulation	Solubility (g/L)
I-A	3.30
I-B	3.11
I-C	2.93
E-A	5.34
E-B	3.75
E-C	2.16

Conversion

The overall conversion for runs for all formulations and CNC loadings followed the same trends; the addition of CNCs did not impact the overall reaction rate (Figure 3-1). Previously reported results with the IBA system followed the same trends (Chapter 2). The instantaneous conversion was also calculated (Figure 3-2). All runs followed similar trends and starved feed conditions were not achieved as was the case for the previously reported IBA system; instantaneous conversions above, say 80%, would indicate a starved feed condition. Figures for E-B and E-C have been included in Appendix A.

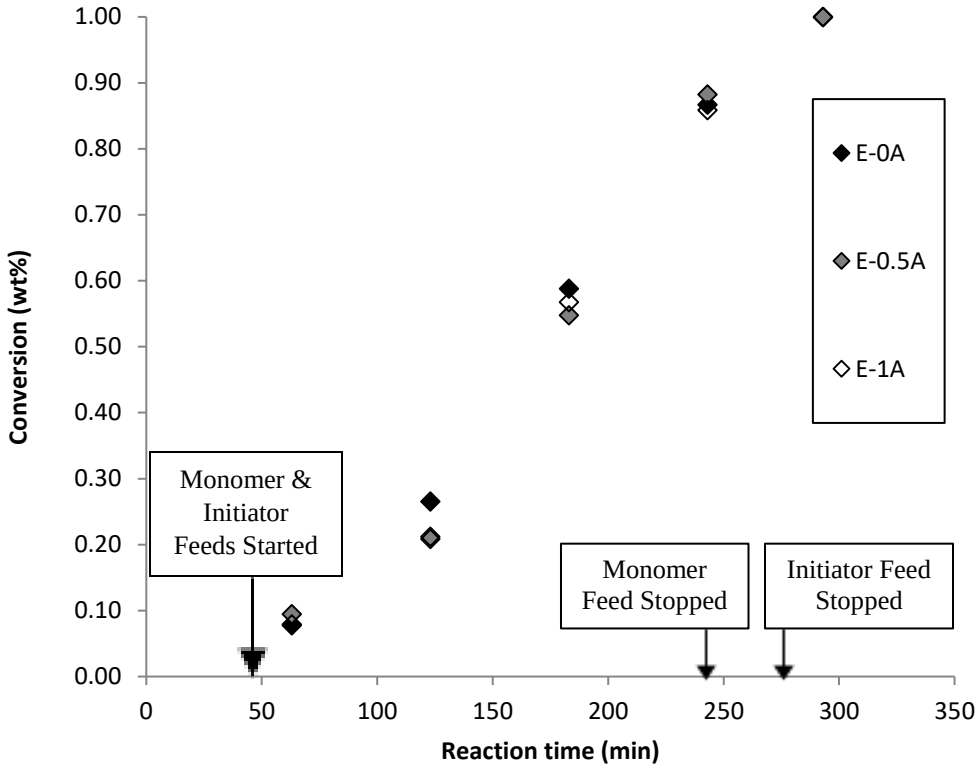

Figure 3-1: Overall conversion for E-A runs

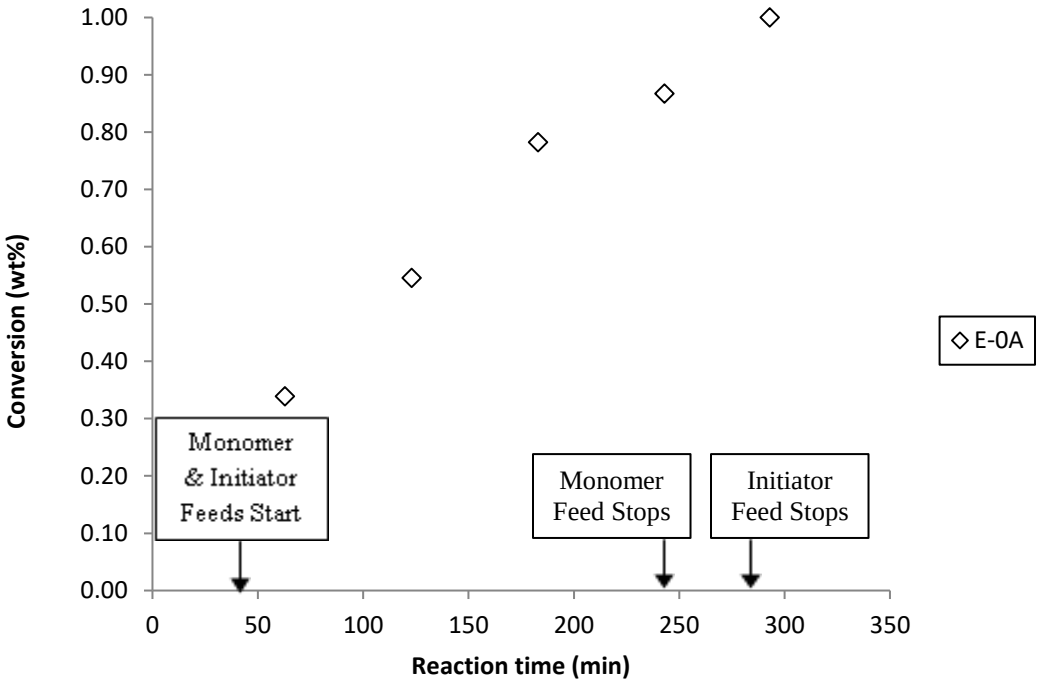

Figure 3-2: Instantaneous conversion for runs E-0A

Particle Size

CNCs did not significantly impact the size of the final latex (Figures 3-3 and 3-4). The final latex particle sizes ranged from 148-161 nm. For all formulations except E-0.5C and E-1C, all samples were considered mono-dispersed as the PSD was below 0.1. For formulations E-0.5C and E-1C, the first samples were not mono-dispersed and had a wide PSD. This effect was likely due to the hydrophilic nature of CNCs and how they interacted with a hydrophobic monomer; the E-C formulations were the most hydrophobic and contained the most EHA (Table 3-7). Thus, CNCs had no impact on particle nucleation, which concurs with the conversion data. For the E-C formulations with CNCs, the first samples taken showed higher particle sizes and a wide PSD of 0.148 and 0.190 for E-0.5C and E-1C, respectively (Figure 3-4). This would suggest that CNCs may have been forming aggregates within the reaction media at the initial stages of polymerization. However, as the reaction progressed, the PSD narrowed and the final latex particle sizes normalized. Formulation E-B followed the same trend (Appendix A). For the previously reported IBA system, the final particle size was in the same range as the EHA system with values ranging from 140-157 nm (Chapter 2). In both systems, the CNCs did not impact particle nucleation and it was surmised that CNCs were likely not located within the latex particles but were rather near the particle–water interface. No effects were observed on the final latex particle size when CNCs were used.

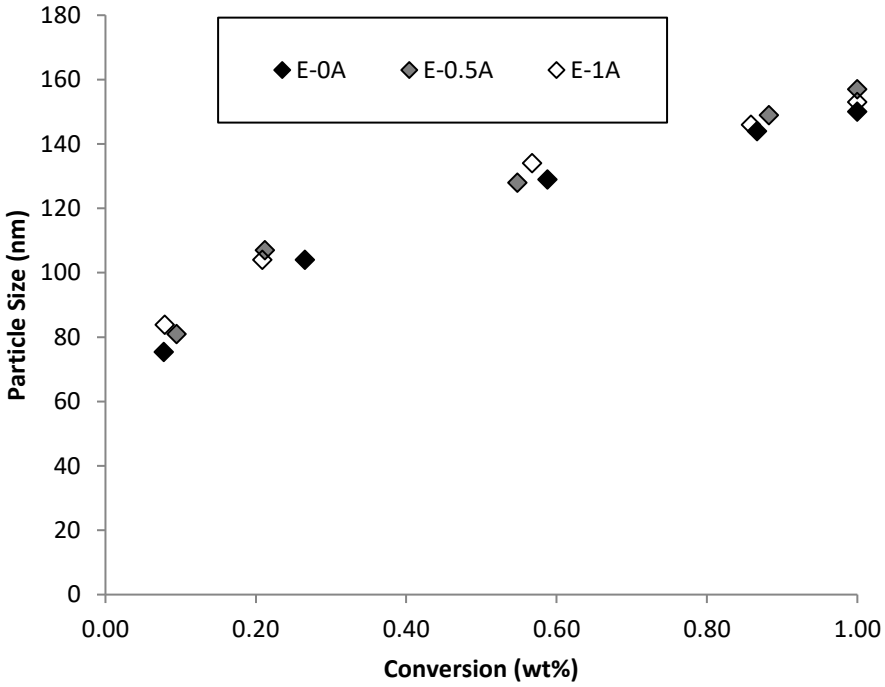

Figure 3-3: Particle size of E-A runs

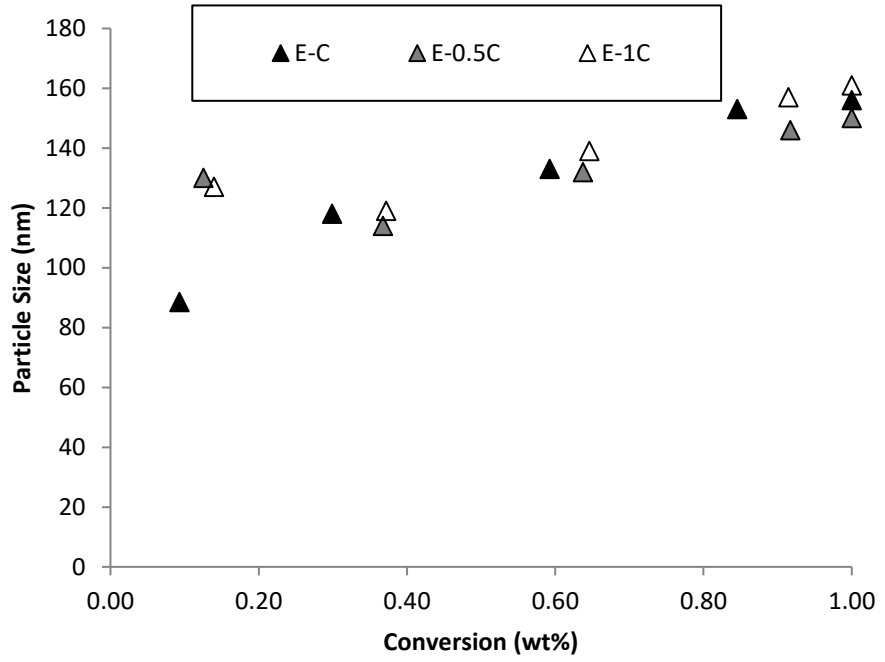

Figure 3-4: Particle size of E-C runs

Viscosity

Coagulation is an issue when using CNCs in emulsion polymerization; high CNC contents (>2 wt%) can lead to CNC aggregate formation and destabilization of the latex.[16] An indicator of the CNC loading limit is the viscosity of the final latex. All base case formulations were similar in viscosity (Figure 3-5). With increasing CNC loading, the viscosity increased markedly. Similar effects were noted in the IBA system. The E-C formulations, i.e., the ones with the most EHA, showed the greatest increase in viscosity.

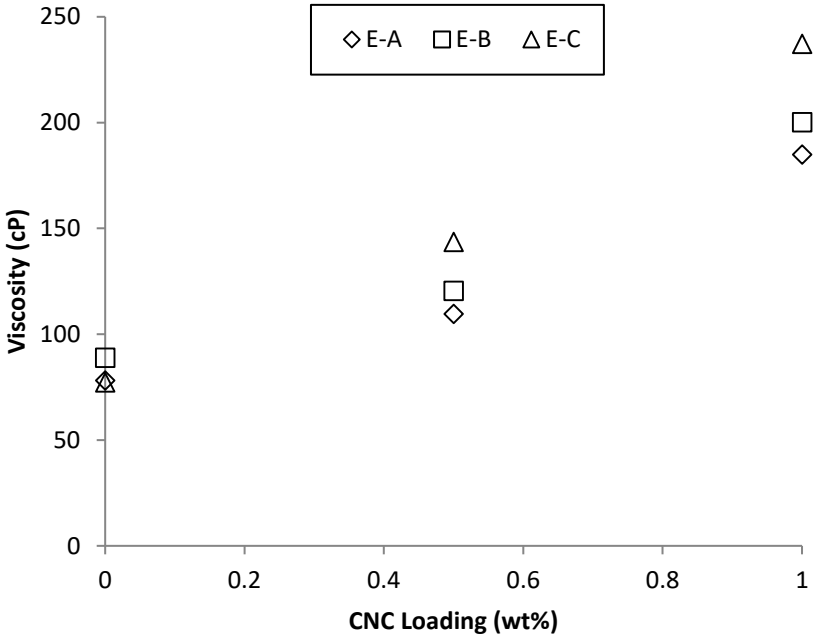

Figure 3-5: Viscosity of all final latexes

Recalling that CNCs have a high aspect ratio and are whisker-like in shape, explains the viscosity increases observed. In general, as the sphericity of a particle decreases, the viscosity of the fluid will increase.[22] High aspect ratios result in less efficient particle packing, but result in a larger surface area and an increased likelihood of particle interactions.[22]–[25] CNC rheology has been thoroughly investigated and as expected, as the aspect ratio or concentration increases, so does the viscosity.[22] Thus, it is expected that the viscosity of the nanocomposite will be higher than that of the neat latex.[26] Results for the IBA system were similar and indicated that CNCs influenced

the rheological properties of the latex (Chapter 2). Thus, CNCs could be crosslinking with the polymer, which would lead to the increased latex viscosity.[26]

pH

For all EHA formulations, the initial pH ranged from 3.9-4.2. As the reaction continued, the pH decreased to a range of 3.6-3.9 for the final latex. This behavior is what is normally expected in a non-buffered emulsion polymerization. The addition of CNCs did not have a noticeable effect on pH as, at most, only 2.2 g were added to the reaction formulations. Similar results for the pH in the IBA system were previously reported (Chapter 2).

Glass Transition Temperature

The addition of CNCs did not have a significant effect on the T_g of the resulting polymer for either the IBA or EHA system (Table 3-8). In this case, the comonomer composition of each formulation provided the main influence on T_g (compositions were provided in Tables 3-1 and 3-6). Comparisons based on the effect of CNC content showed that the results were within the error of the T_g measurement. It was previously suggested that CNCs could increase T_g via grafting and the formation of a more reinforced polymer causing the immobilization of polymer chains.[27], [28]

Table 3-8: Glass transition temperatures of EHA runs

EHA Formulation	T_g [ºC]	IBA Formulation	T_g [ºC]
E-0A	-21	**I-0A**	-22
E-0.5A	-19	**I-0.5A**	-21
E-1A	-21	**I-1A**	-20
E-0B	-34	**I-0B**	-29
E-0.5B	-35	**I-0.5B**	-28
E-1B	-34	**I-1B**	-26
E-0C	-48	**I-0C**	-35
E-0.5C	-48	**I-0.5C**	-36
E-1C	-47	**I-1C**	-37

Gel Content

Like the IBA system previously studied, the gel content of the EHA system was high (Figure 3-6). The amount of gel in a system is usually an indicator on degree of crosslinking. The base case formulations, without the addition of CNCs, already displayed high gel contents and any increases due to the addition of CNCs were not observed.

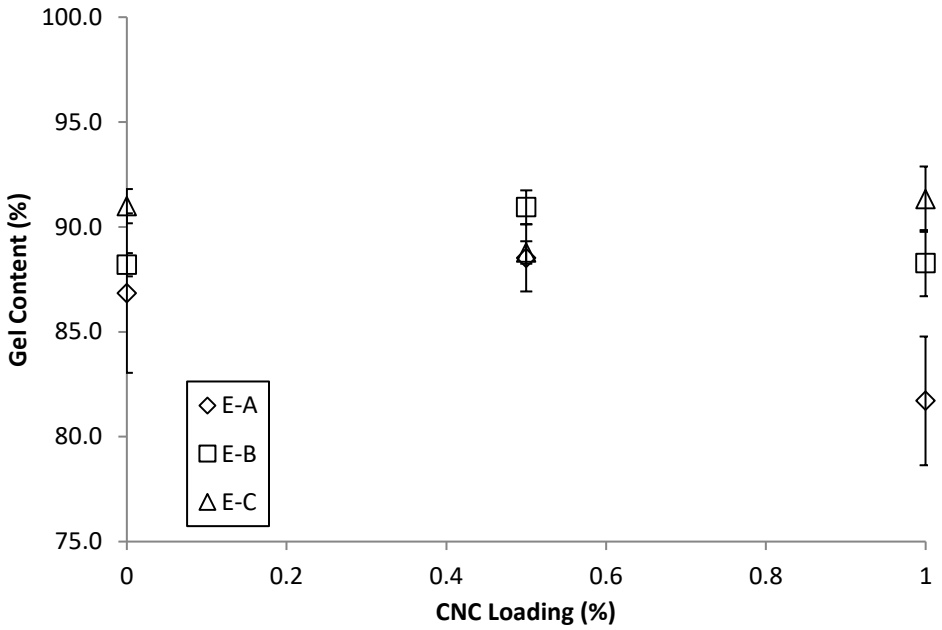

Figure 3-6: Gel content of EHA/BA/MMA system

Adhesive Performance

For the EHA system, no statistically significant change was seen in tack with increasing CNC loading (Figure 3-7). Nonetheless, for the E-B and E-C formulations, the trends were increasing. For the EHA system, the increasing variability in tack results could be an indication of poor film formation due to a non-uniform CNC distribution. In contrast, results from the IBA system showed a significant effect of CNC loading on tack (IBA results are shown in Figure 3-7 as points designated by I-A, I-B and I-C). The IBA results were attributed to improved wettability of the PSA films due to the hydrophilicity of the CNCs; this was further confirmed using contact angle measurements. For the EHA formulations with CNCs, it was not possible to achieve a reproducible water contact angle measurement on any film. Depending on where the water droplet was placed on the dried latex, the contact angle changed significantly. Thus, the significant contact angle variability within a film is consistent with the variability in tack that was observed. These results

could also indicate the agglomeration of CNCs, or at the very least, the repulsion of CNCs by the hydrophobic EHA chains.

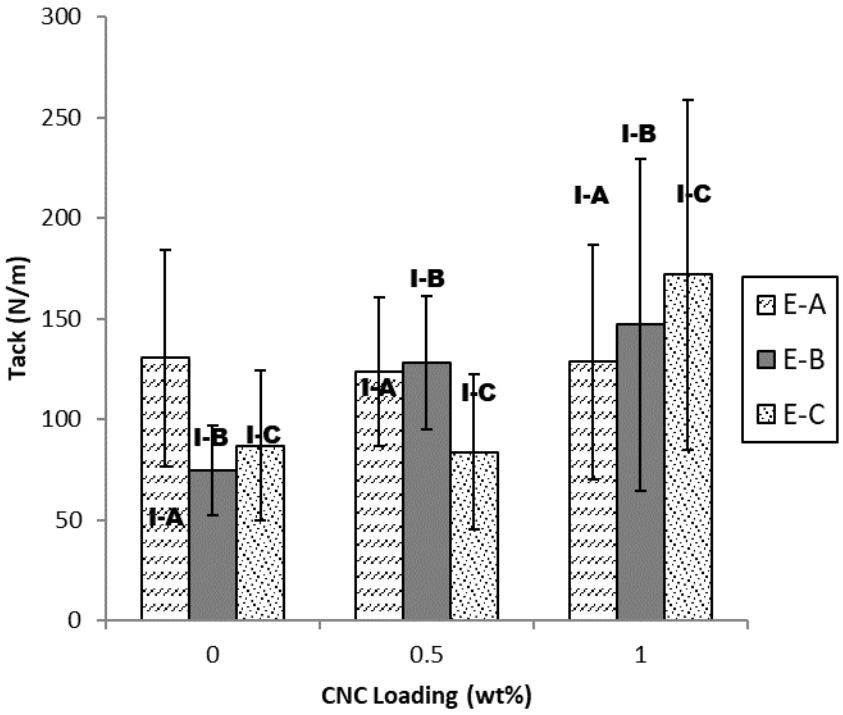

Figure 3-7: Tack results EHA/BA/MMA system with an overlay of tack results from the IBA system denoted as points labelled I-A, I-B and I-C

Peel strength increased with increased CNC loading for formulations E-A and E-C (Figure 3-8). Given the MMA content of the EHA system (Table 3-1), the peel strength would be expected to decrease from formulation E-A to E-B to E-C. A high T_g monomer will increase the peel strength to a maximum because it provides greater stiffness to the film at room temperature.[5] In this respect, the results are consistent at the base case level (i.e., 0 wt% CNC loading) but not at the highest CNC loading (1 wt%). It is noteworthy that the E-C formulation showed significant variability in peel strength. In comparison, the increase in peel strength with CNC loading for the IBA system was significant and consistent.

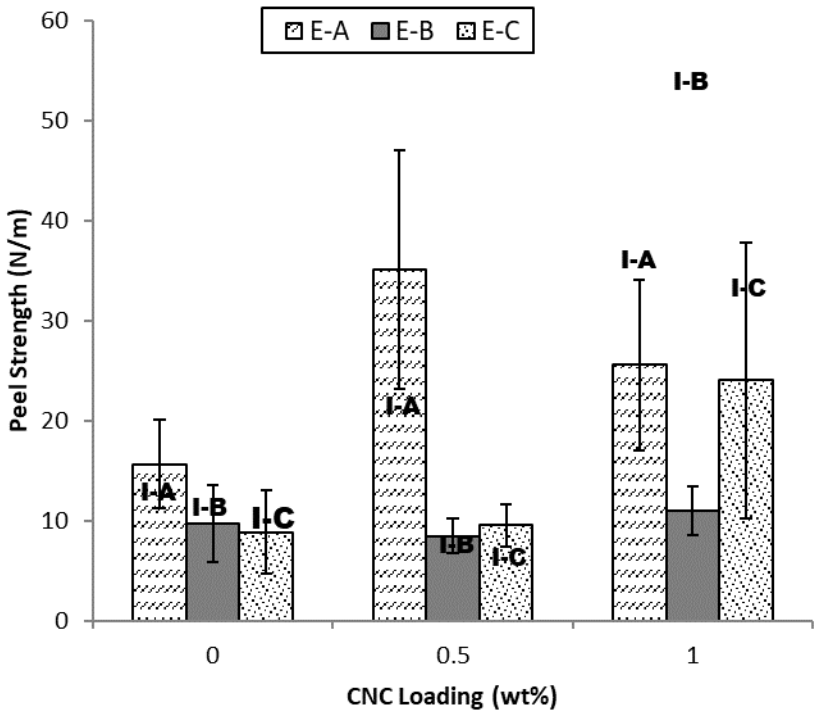

Figure 3-8: Peel strength results EHA/BA/MMA system with an overlay of peel strength results from the IBA system denoted as points labelled I-A, I-B and I-C

The addition of a nanoparticle to a polymer matrix, usually results in increased shear strength. This is because the cohesive strength of a material will improve when a stiff filler is inserted in between otherwise non-linked particles.[5] It was therefore no surprise that the shear strength improved in each system (Table 3-9) (compositions were provided in Tables 3-1 and 3-6). Within the EHA system, the variability in shear strength from formulation to formulation differed because of the changing MMA content. For the E-A formulations with CNCs, the samples were taken down as they would not fall and are indicated with a "+" to indicate the shear strength was likely higher than the value reported. The same was true for the I-A and I-B systems at 1 wt% CNC.

Table 3-9: Shear strength for EHA/BA/MMA system

EHA Formulation	Shear Strength (h)	IBA Formulation	Shear Strength (h)
E-0A	293±210	**I-0A**	12±7
E-0.5A	385+	**I-0.5A**	94±35
E-1A	850+	**I-1A**	114+
E-0B	10±4	**I-0B**	14±4
E-0.5B	32±9	**I-0.5B**	49±25
E-1B	39±29	**I-1B**	114+
E-0C	1.3±0.4	**I-0C**	3.2±2.1
E-0.5C	1.7±0.4	**I-0.5C**	18±4
E-1C	4.2±1.0	**I-1C**	79±36

CNCs had a limited influence on adhesive properties for the EHA system compared to the significant effects shown for the IBA system. The variability in the adhesive and contact angle results coupled with the system solubility suggest a poor distribution of CNCs within the polymer matrix for the EHA system.

Microscopy and Distribution of CNCs

As surmised from the adhesive testing and contact angle measurements, a relatively poor dispersion of CNCs in the EHA system was detected from selected samples analyzed by TEM. For reference, a TEM image of formulation E-0A shows the neat latex particles (Figure 3-9). Latex from formulation E-1A provides evidence that the CNCs are located outside the latex particles and that there is some aggregation (Figures 3-10 a and b). At the very least, there appear to be regions which are devoid of CNCs around the latex particles. Thus, it appears from the TEM image that the CNCs are not distributed uniformly throughout the latex dispersion. The evidence for poor CNC distribution is even stronger for formulation E-1C (Figures 3-10 c and d). In fact, the TEM image for E-1C indicates a greater number of aggregates and consequently poorer distribution. As discussed above, E-1C films gave highly variable adhesive testing results compared to E-1A films. The poor distribution of CNCs would explain that variability. In stark comparison, TEM images from formulation I-1A suggest a much more uniform distribution of CNCs in the latex (Figures 3-

11 a and b). This also explains the more consistent and less variable adhesive test results for the IBA system. The performance of the PSA (or any polymer composite) is impacted by the level of dispersion within the polymer matrix; it is therefore not surprising that the EHA system underperformed given the suspected poor dispersion of CNCs.[17], [18] Additional figures have been provided in Appendix A.

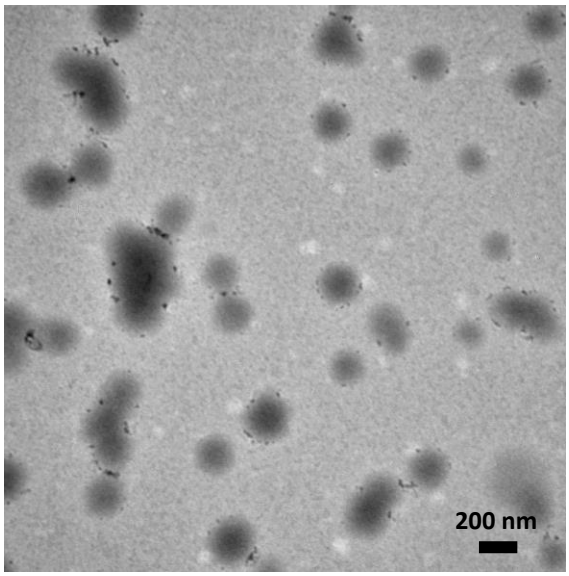

Figure 3-9: TEM image of E-0A latex

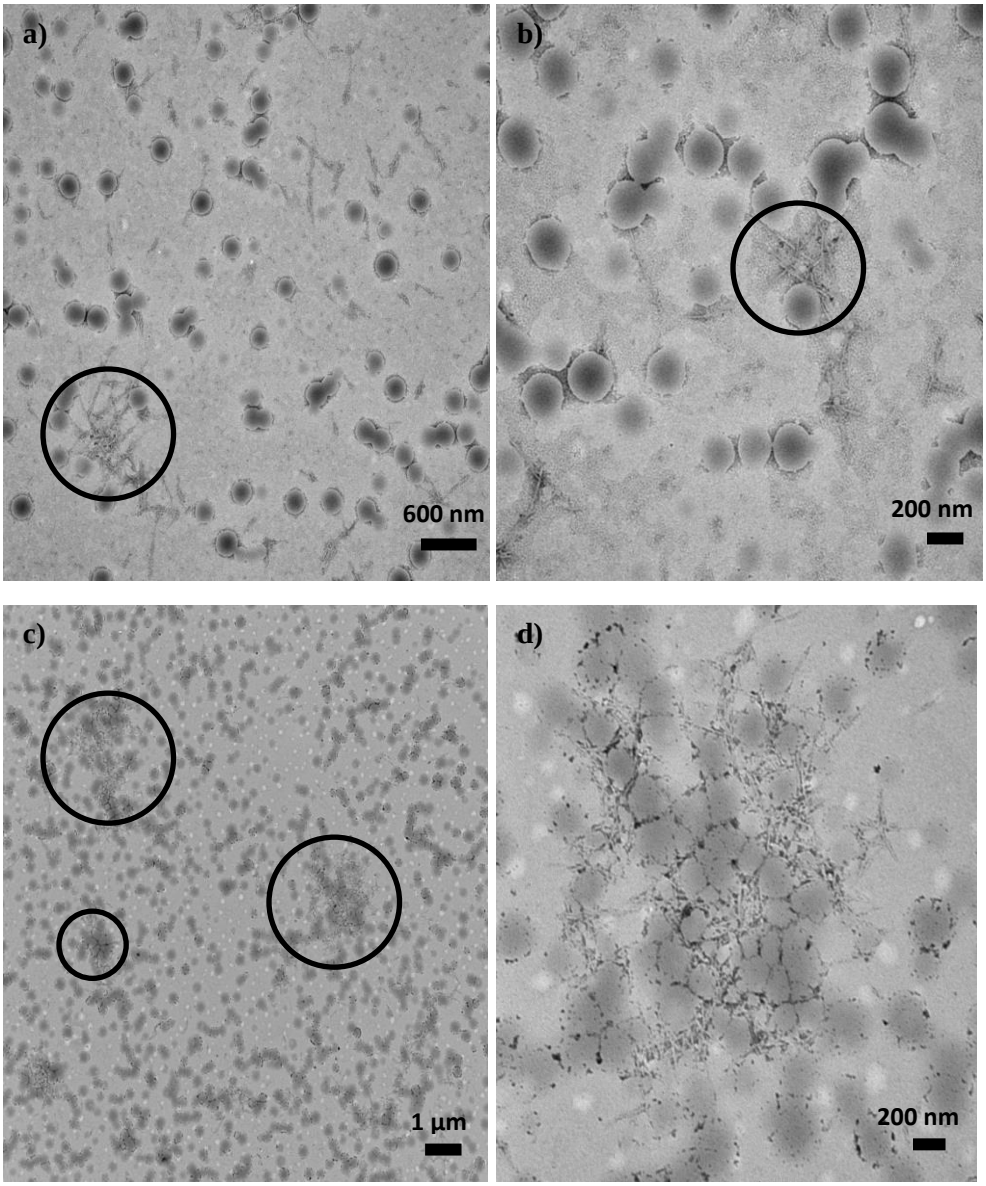

Figure 3-10: TEM image of E-1A latex (a, b), E-1C (c, d). CNC rich areas are circled.

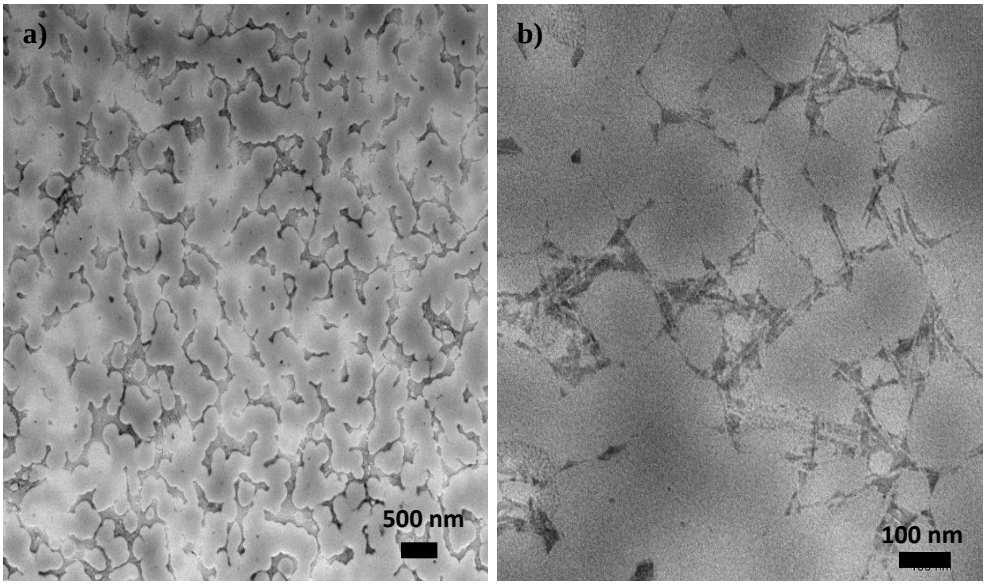

Figure 3-11: TEM image of I-1A latex

For both the EHA and IBA systems, the conversion, particle size and latex viscosities were similar. The biggest difference lay in the hydrophobicity (or solubility) of the monomers. This led to differences in the distribution of CNCs within each latex dispersion and consequently, differences in adhesive testing variability. One would expect a certain degree of polymer grafting from CNC via hydrogen abstraction from the hydroxyl groups when initiator is present.[29] Higher amounts of grafting have been reported when KPS was used as initiator.[30] Once abstracted, a radical forms on the CNC and can act as the reactive center in the polymerization. CNCs may not induce grafting when a highly hydrophobic monomer is present. It is therefore possible that the EHA acted as a repulsive barrier to the CNCs, reducing the possibility for grafting. This would also explain the improved behavior of the IBA system.

Blend vs. in situ polymerization

For both systems, additional testing was done to compare in situ composite preparation to blending. The E-B and I-B base case latexes were each mixed with a CNC dispersion and mixed for 30 min at room temperature. In previous work, it was shown that blends did not achieve the same improvement in adhesive performance.[31] However, the in situ cases involve heating and extended mixing unlike the simple, room temperature blend approach. Thus, “heated blends”

where the CNC dispersion was added at the completion of a base case polymerization and mixed at 250 rpm and 60 ˚C for an additional 2 h in the reactor, were prepared.

For the EHA system, because of the high variability in results, statistically significant differences were not seen (Table 3-10). However, trends were certainly evident. Tack was not significantly improved using CNCs in situ, but the non-heated and heated blends showed slight improvements over the base case. For the IBA system, tack was improved almost to the level of the in situ run using both blending methods (Table 3-11). Peel strength showed no significant differences for either the EHA or IBA system when comparing in situ to blend techniques. For the shear strength, the EHA system showed better performance for the blending methods compared for the in situ one. It is likely that less aggregation occurred during blending compared to the in situ case. For the IBA system, in situ outperformed the blend cases. Evidence of greater CNC-latex particle interaction appears in the viscosity data (Tables 3-10 and 3-11). The in situ cases clearly show higher viscosities than the blend cases. Therefore, there must be some interaction occurring between CNCs and the polymer induced by the in situ runs; most likely there is grafting in the event of a better dispersion of CNCs within the latex.[18]

Table 3-10: EHA/BA/MMA system blend adhesive results

Run	CNC Loading (wt%)	Tack (N/m)	Peel Strength (N/m)	Shear (h)	Viscosity (cP)
Base Case	0	75±22	10±4	10±4	235*
In Situ	1	147±83	11±2	39±29	200
Non-Heated Blend	1	181±40	34±24	67±40	81
Heated Blend	1	221±76	27±6	130±63	191

* increased solids run used

Table 3-11: IBA/BA/MMA system blend adhesive results

Run	CNC Loading (wt%)	Tack (N/m)	Peel Strength (N/m)	Shear (h)	Viscosity (cP)
Base Case	0	90±25	11±4	13±4	177*
In Situ	1	256± 90	53±7	114 +	231
Non-Heated Blend	1	201±56	37±12	63±17	78
Heated Blend	1	215±37	40±15	86±20	154

* increased solids run used

Conclusions

Comparisons were made between two emulsion polymer systems containing CNCs (0 to 1 wt%) and how they influenced PSA properties. The EHA system did not show the same improvements in adhesive properties as the IBA system. The highly hydrophobic nature of EHA seems to be responsible. The presence of a hydrophobic monomer in the latex formulation reduced the amount of latex particle-CNC interactions and led to poor distribution and aggregation of CNCs in the final latex dispersion. This conclusion is supported by the viscosity measurements, adhesive measurements and the inability to measure a reproducible contact angle for the EHA system as

well as by the comparison with the performance of the more hydrophilic IBA formulation, prepared similarly with CNCs.

The use of CNCs as PSA property modifiers has been shown to be highly effective for relatively hydrophilic systems such as IBA/BA/MMA (Chapter 2). However, the use of a hydrophobic monomer such as EHA, appears to interfere with the desired interaction of the polymer matrix with the nanoparticle and leads to poor distribution of the CNCs in the latex dispersion and ultimately, poor adhesive performance. Thus, when a polymer application calls for a more hydrophobic monomer to be used, surface modification of the CNCs may be required to improve latex-nanoparticle compatibility.

Acknowledgements

Financial support for this work through the Natural Science and Engineering Research Council (NSERC) of Canada, CelluForce and FPInnovations is gratefully acknowledged.

References

[1] S. Salehpour and M. A. Dubé, "Applying the principles of green chemistry to polymer production technology," *Macromol. React. Eng.*, no. 8, pp. 7–28, 2014.

[2] M. Shimao, "Biodegradation of plastics," *Curr. Opin. Biotechnol.*, vol. 12, no. 3, pp. 242–247, 2001.

[3] K. Leja and G. Lewandowicz, "Polymer biodegradation and biodegradable polymers - a review," *Polish J. Environ. Stud*, vol. 19, no. May, pp. 255–266, 2010.

[4] W. Maaßen, S. Oelmann, D. Peter, W. Oswald, N. Willenbacher, and M. A. R. Meier, "Novel insights into pressure-sensitive adhesives based on plant oils," *Macromol. Chem. Phys.*, vol. 216, pp. 1609–1618, 2015.

[5] R. Jovanovic and M. A. Dubé, "Emulsion-based pressure-sensitive adhesives : A review," *J. Macromol. Sci.*, vol. C44, no. 1, pp. 1–51, 2004.

[6] L. Qie and M. A. Dubé, "Performance improvement of latex-based PSAs using polymer microstructure control," University of Ottawa, 2011.

[7] W. P. Flauzino Neto, M. Mariano, I. S. V. da Silva, H. A. Silvério, J. L. Putaux, H.

Otaguro, D. Pasquini, and A. Dufresne, “Mechanical properties of natural rubber nanocomposites reinforced with high aspect ratio cellulose nanocrystals isolated from soy hulls,” *Carbohydr. Polym.*, vol. 153, pp. 143–152, 2016.

[8] K. R. Rajisha, H. J. Maria, L. A. Pothan, Z. Ahmad, and S. Thomas, “Preparation and characterization of potato starch nanocrystal reinforced natural rubber nanocomposites,” *Int. J. Biol. Macromol.*, vol. 67, pp. 147–153, 2014.

[9] A. Dufresne, *Nanocellulose*. Saint Martin D’Heres cedex: De Gruyter, 2012.

[10] F. Chivrac, E. Pollet, and L. Avérous, “Progress in nano-biocomposites based on polysaccharides and nanoclays,” *Mater. Sci. Eng. R Reports*, vol. 67, no. 1, pp. 1–17, 2009.

[11] R. J. Moon, A. Martini, J. Nairn, J. Youngblood, A. Martini, and J. Nairn, “Cellulose nanomaterials review : structure , properties and nanocomposites,” *Chem. Soc. Rev.*, vol. 40, no. 6, pp. 3941–3994, 2011.

[12] F. Bettaieb, R. Khiari, A. Dufresne, M. F. Mhenni, and M. N. Belgacem, “Mechanical and thermal properties of Posidonia oceanica cellulose nanocrystal reinforced polymer,” *Carbohydr. Polym.*, vol. 123, pp. 99–104, 2015.

[13] S. Spinella, G. Lo Re, B. Liu, J. Dorgan, Y. Habibi, P. Leclère, J. M. Raquez, P. Dubois, and R. A. Gross, “Polylactide/cellulose nanocrystal nanocomposites: Efficient routes for nanofiber modification and effects of nanofiber chemistry on PLA reinforcement,” *Polym. (United Kingdom)*, vol. 65, pp. 9–17, 2015.

[14] C. Miao and W. Y. Hamad, “In-situ polymerized cellulose nanocrystals (CNC) poly(L-lactide) (PLLA) nanomaterials and applications in nanocomposite processing,” *Carbohydr. Polym.*, vol. 153, pp. 549–558, 2016.

[15] J. Yang, C. R. Han, J. F. Duan, M. G. Ma, X. M. Zhang, F. Xu, and R. C. Sun, “Synthesis and characterization of mechanically flexible and tough cellulose nanocrystals-polyacrylamide nanocomposite hydrogels,” *Cellulose*, vol. 20, no. 1, pp. 227–237, 2013.

[16] Z. Dastjerdi, E. D. Cranston, and M. A. Dubé, “Synthesis of poly (n -butyl acrylate / methyl methacrylate)/ CNC latex nanocomposites via in situ emulsion polymerization,”

Macromol. React. Eng., pp. 1–8, 2017.

[17] F. Ansari, M. Salajkova, Q. Zhou, and L. A. Berglund, "Strong surface treatment effects on reinforcement efficiency in biocomposites based on cellulose nanocrystals in poly(vinyl acetate) matrix," *Biomacromolecules*, vol. 16, pp. 3916–3924, 2015.

[18] K. Oksman, Y. Aitomäki, A. P. Mathew, G. Siqueira, Q. Zhou, S. Butylina, S. Tanpichai, X. Zhou, and S. Hooshmand, "Review of the recent developments in cellulose nanocomposite processing," *Compos. Part A*, vol. 83, pp. 2–18, 2016.

[19] M. S. Reid, M. Villalobos, and E. D. Cranston, "Benchmarking cellulose nanocrystals: from the laboratory to industrial production," *Langmuir*, vol. 33, no. 7, pp. 1583–1598, 2017.

[20] R. J. Young and P. A. Lovell, *Introduction to Polymers*, Third. Boca Raton: CRC Press, 2011.

[21] A. Li and K. Li, "Pressure-sensitive adhesives based on soybean fatty acids," *RSC Adv.*, vol. 4, no. 41, pp. 21521–21530, 2014.

[22] E. V. Timofeeva, J. L. Routbort, and D. Singh, "Particle shape effects on thermophysical properties of alumina nanofluids," *J. Appl. Phys.*, vol. 106, no. 1, 2009.

[23] K. B. Anoop, S. Kabelac, T. Sundararajan, and S. K. Das, "Rheological and flow characteristics of nanofluids: Influence of electroviscous effects and particle agglomeration," *J. Appl. Phys.*, vol. 106, no. 3, 2009.

[24] Gaganpreet and S. Srivastava, "Influence of particle shape on viscosity of nanofluids," *AIP Conf. Proc.*, vol. 1512, no. 2013, pp. 984–985, 2013.

[25] M. C. Li, Q. Wu, K. Song, S. Lee, Y. Qing, and Y. Wu, "Cellulose nanoparticles: structure-morphology-rheology relationships," *ACS Sustain. Chem. Eng.*, vol. 3, no. 5, pp. 821–832, 2015.

[26] Y. C. Ching, M. Ershad Ali, L. C. Abdullah, K. W. Choo, Y. C. Kuan, S. J. Julaihi, C. H. Chuah, and N. S. Liou, "Rheological properties of cellulose nanocrystal-embedded polymer composites: a review," *Cellulose*, vol. 23, no. 2, pp. 1011–1030, 2016.

[27] E. Erbas Kiziltas, A. Kiziltas, S. C. Bollin, and D. J. Gardner, “Preparation and characterization of transparent PMMA-cellulose-based nanocomposites,” *Carbohydr. Polym.*, vol. 127, pp. 381–389, 2015.

[28] H.-Y. Yu, Z.-Y. Qin, C.-F. Yan, and J.-M. Yao, “Green nanocomposites based on functionalized cellulose nanocrystals: a study on the relationship between interfacial interaction and property enhancement,” *ACS Sustain. Chem. Eng.*, vol. 2, no. 4, pp. 875–886, 2014.

[29] P. Ghosh, D. Dev, and A. K. Samanta, “Graft copolymerization of acrylamide on cotton cellulose in a limited aqueous system following pretreatment technique,” *J. Appl. Polym. Sci.*, vol. 58, no. 10, p. 1727, 1995.

[30] G. Gürdag and S. Sarmad, “Cellulose graft copolymers: synthesis, properties, and applications,” in *Polysaccharide Based Graft Copolymers*, S. Kalia and M. W. Sabaa, Eds. Berlin, Heidelberg: Springer Berlin Heidelberg, 2013, pp. 15–57.

[31] Z. Dastjerdi and M. A. Dubé, “Cellulose nanocrystals : renewable property modifiers for pressure sensitive adhesives,” University of Ottawa, 2017.

Chapter 4: General Discussion and Conclusion

As shown in Chapters 2 and 3, two different systems were investigated to use cellulose nanocrystals (CNCs) in situ during semi batch emulsion polymerization to influence the adhesive properties of pressure sensitive adhesives (PSAs). The first system was isobutyl acrylate (IBA)/n-butyl acrylate (BA)/methyl methacrylate (MMA) and the second was 2-ethyl hexyl acrylate (EHA)/BA/MMA. The two systems had differing overall solubility (Table 4-1).

Table 4-1: Water solubility of IBA and EHA formulations

Formulation	Solubility (g/L)
IBA A	3.30
IBA B	3.11
IBA C	2.93
EHA A	5.34
EHA B	3.75
EHA C	2.16

Increases were seen in the viscosity for both systems with CNC addition (Figure 4-1 shows the trend for IBA/BA/MMA). EHA followed the same trend.

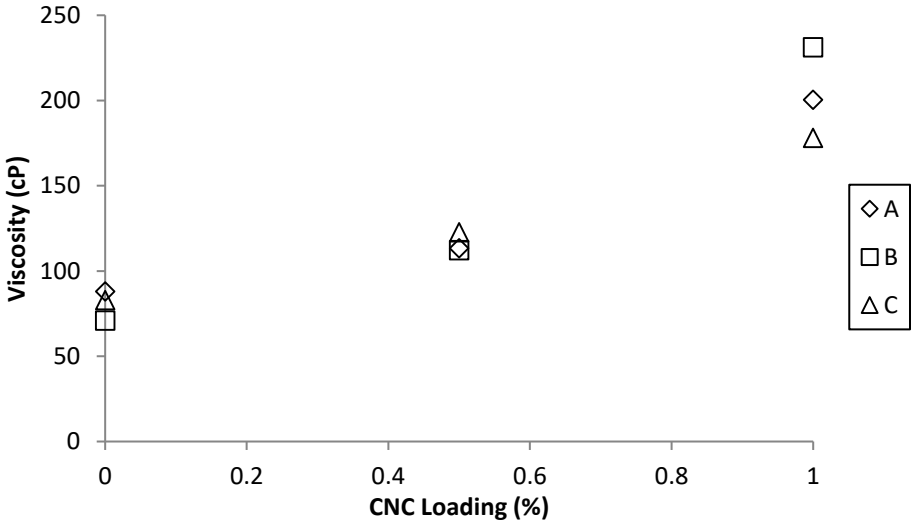

Figure 4-1: Viscosity of final latexes for all IBA formulations

Other properties which were monitored for the effect of added CNC were: conversion, particle size, pH, glass transition temperature (T_g), gel content, and polymer composition. Regardless of

CNC content, no significant effect was observed for these properties in either system. For the IBA system, dynamic mechanical analysis (DMA) was also used to characterize the viscoelastic properties of the latexes. CNCs did influence storage and loss moduli as well as tan δ. The use of CNCs had a strengthening and stiffening effect on the polymer (indicated by the DMA results) (Figure 2-11 to Figure 2-13).

CNCs are hydrophilic and our second objective was to observe the effect of hydrophilic and hydrophobic monomers. In the IBA system, the solubility did not vary based on formulation because IBA and BA are similar (slightly hydrophobic). The addition of CNCs did significantly improve all adhesive properties for System 1 (Figure 4-2 to Figure 4-4). However, the EHA system did not see the same improvement of adhesive performance. The tack did not change (significantly), peel strength slightly improved and shear strength was improved (see Figure 3-7, Figure 3-8 and Table 3-9). Although the overall apparent solubility of this system was high, the of EHA certainly presented moieties within the polymer changes that were highly hydrophobic; this is likely why only limited improvement in adhesive properties was noted. The EHA elements in the polymer matrix may have repelled the CNCs within the polymerization media. This is also surmised from TEM images which suggested a non-uniform distribution of CNCs within the latex for the EHA system (Figure 4-5). This was in direct contrast to the well-behaved IBA system, where a more uniform CNC distribution was likely (Figure 4-6).

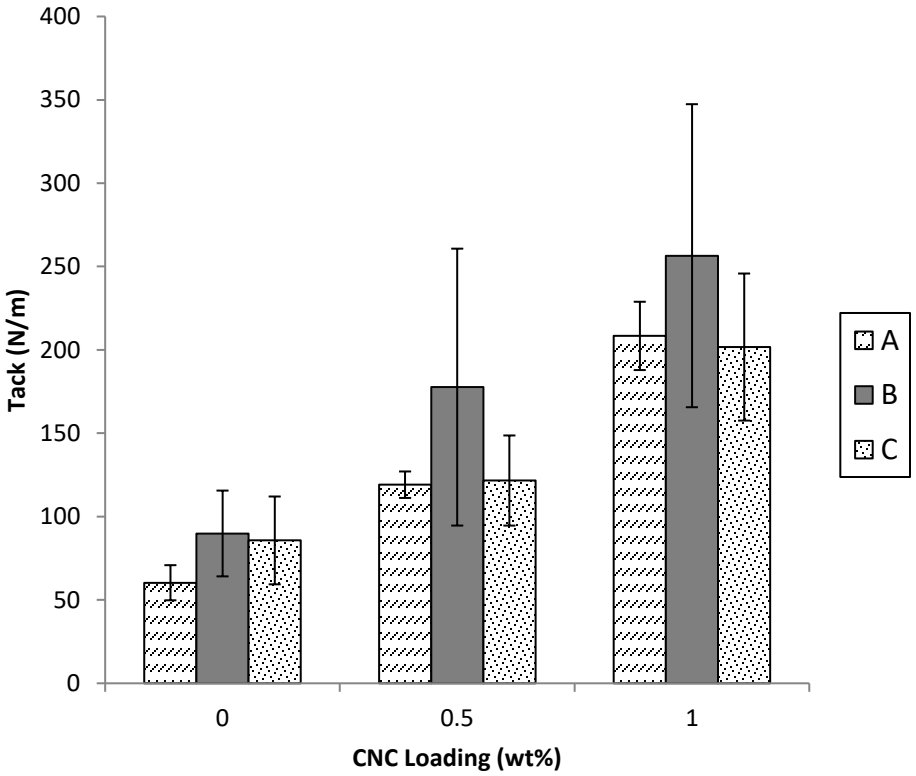

Figure 4-2: Loop tack vs. CNC content for IBA system

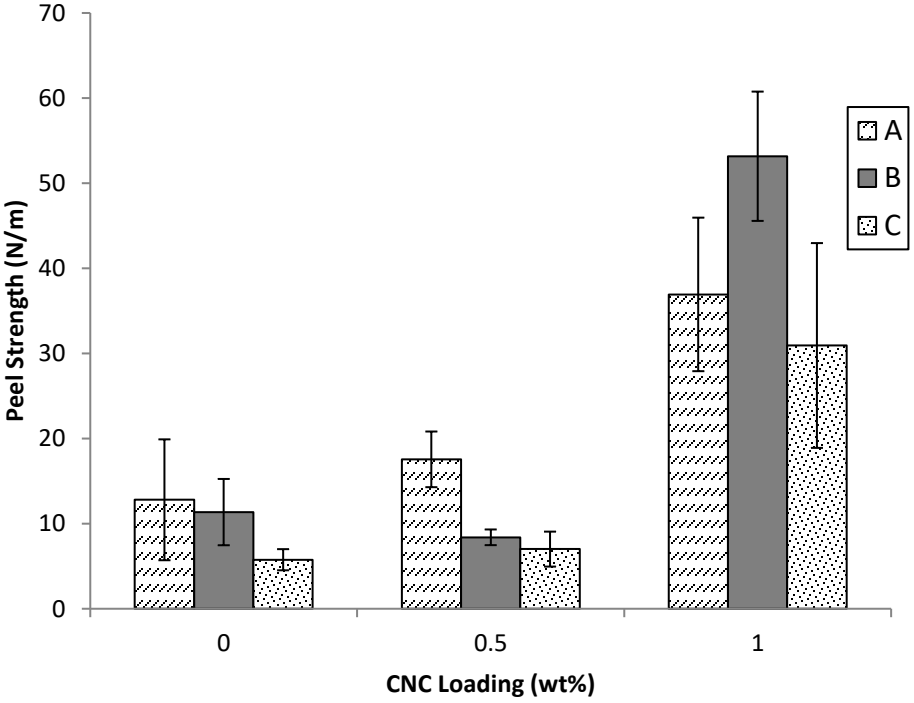

Figure 4-3: Peel strength vs. CNC content for IBA system

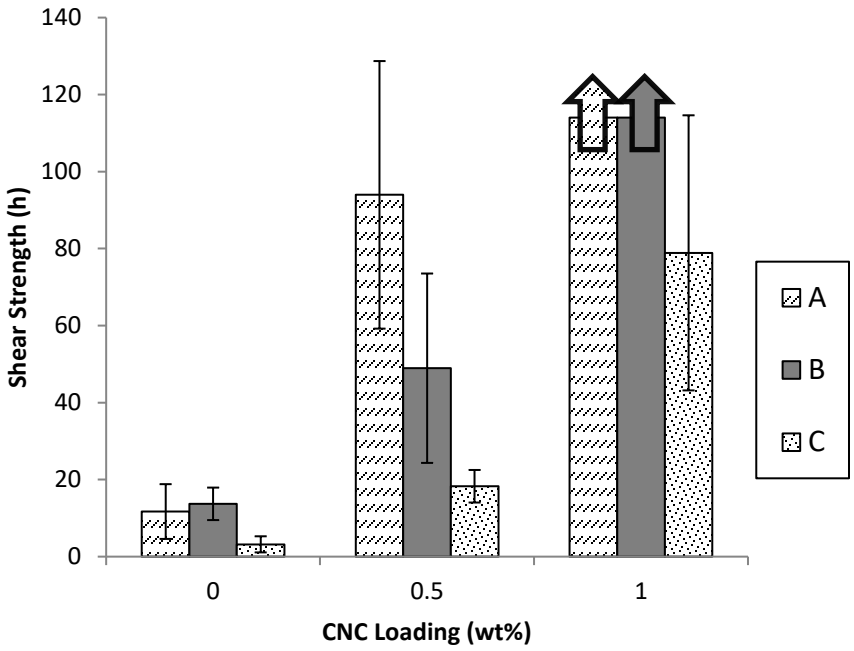

Figure 4-4: Shear strength vs. CNC content for IBA system

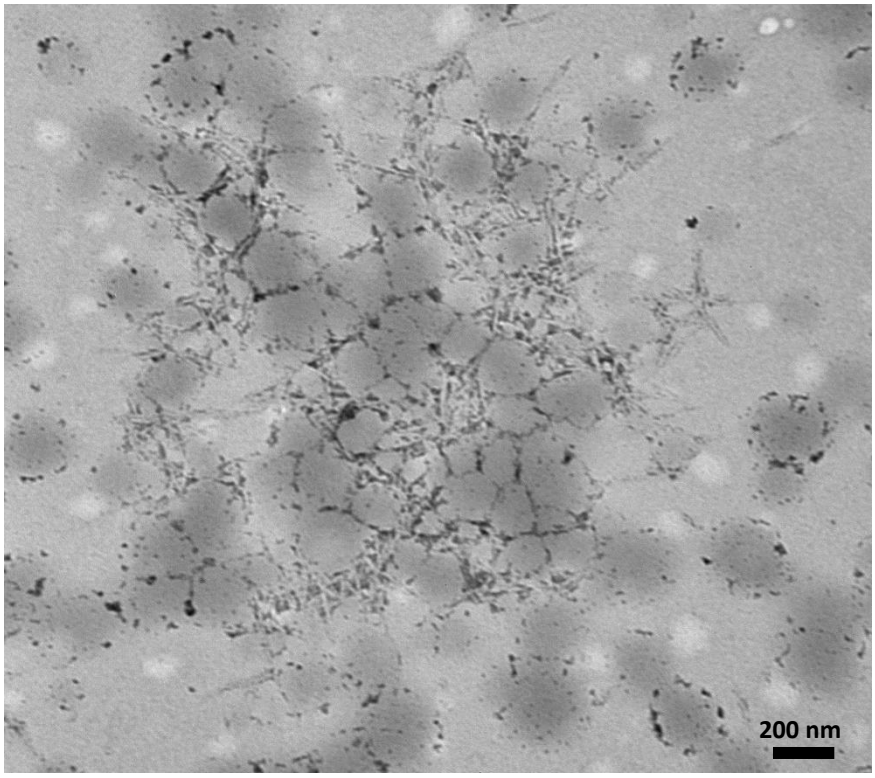

Figure 4-5: TEM image of E-1C latex zoomed in on CNC-rich area

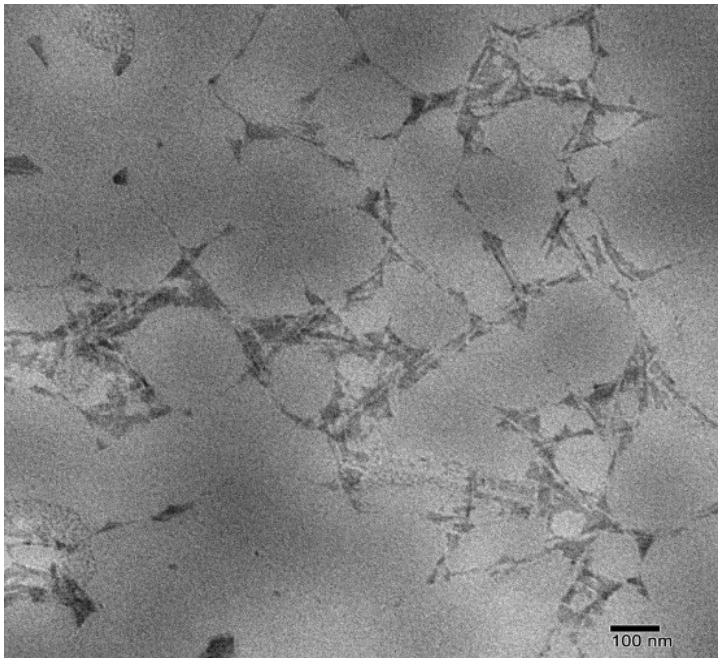

Figure 4-6: TEM image of latex from run I-1A

A legitimate question to ask is whether a more straightforward blending approach would yield the same property effects. Certainly, in the case of blending at room temperature, it was shown that adhesive properties were affected positively but not nearly as strongly as in the in situ cases. The fact that the in situ systems were exposed to prolonged heating and mixing makes the room temperature comparison somewhat questionable. Therefore, heated blends were also performed for both systems. Once again, adhesive properties were improved in both systems above the level of the base case. For the EHA system, the blends out-performed the in situ run for all adhesive properties. It is likely that the blended EHA-based nanocomposites had better distribution of the CNCs. In any case, a one-pot synthesis method would normally be preferred in a commercial setting due to time issues.

The influence of nanoparticles on nanocomposite performance is generally governed by three properties: functionalization (which can improve nanomaterial-polymer compatibility), dispersion and shape. With regards to functionalization, CNCs already possess functional groups that no doubt assisted in their compatibilization with the polymer matrix. However, there are interesting opportunities to modify the CNCs further, which is the subject of a future recommendation below. This work showed an excellent example of the impact of poor dispersion where the EHA/BA/MMA system underperformed the IBA/BA/MMA nanocomposites. The cylindrical

shape of the CNCs was assumed to play an important role in nanoparticle-polymer matrix interaction due to their higher surface area. Comparisons to spherical nanoparticles would be interesting but none of those have been designated as non-hazardous at this point.

In this thesis, groundwork has been laid for the use of CNCs in situ for adhesive property enhancement in emulsion polymerizations. Our findings lead to a number of interesting possibilities for future work:

1. Further investigation with varying hydrophilic/hydrophobic monomers can be pursued. EHA represents an extreme in hydrophobic monomers. Finding out where the limit lies for different monomers would be interesting and important for industrial applications.
2. Related to point 1 above, we demonstrated the effect of varying the monomer hydrophobicity. Rather than restrict ourselves to only hydrophilic monomers, modification of the CNC to render the nanoparticle more hydrophobic could be a more practical approach. In fact, CelluForce is soon to announce production of a more hydrophobic version of their CNC. This new material should be investigated further.
3. The range of modifications that can be made to CNCs is almost endless. Future work could be done to improve the compatibility of CNC with the polymer matrix via hydrophobic modifications (as stated in point 2) or perhaps by charge manipulation (i.e., producing cationic CNCs). Care should be taken to consider any morphological changes to the CNCs; that is, will the CNC aspect ratio become akin to a sphere?
4. One constraint that was faced in this work, was achieving a high solids content in the emulsion polymerizations due to the need to disperse the CNCs in a fairly dilute solution. Reducing the amount of water in the CNC dispersion would be of great practical value. At the same time, one could consider finding new ways to add the CNC to the latex that would also circumvent this problem.
5. In this study, we focused on PSA applications. Of course, one should not be restricted to these low T_g applications and the effect of CNCs on higher T_g applications (e.g., coatings) should also be investigated.
6. As part of the longer term focus in our laboratory towards the fully sustainable production of polymers, the use of CNCs as property modifiers with bio-based/renewable monomers would be of interest.

Conclusion

We hypothesized that CNCs can be added to adhesive polymer formulations to affect adhesive performance properties. CNCs provide a "green" and Canadian solution to the classic adhesive property issue with emulsion polymerization; shear strength can be improved while simultaneously increasing peel strength and tack. The significance of this result should not be overlooked as this type of behavior traditionally requires many extra additives which can be toxic. CNCs are therefore a "green" solution to a problem often observed in emulsion-based PSA production.

For the many cases where a slightly water-soluble monomer is used (arguably, a large percentage of the cases), the in situ approach is clearly favoured over blending. The key factors here being the preference for a one-pot synthesis and the greatly reduced processing time. For the hydrophobic monomer systems, CNC modification may be a better route.

The effect of the monomer hydrophobicity has also been demonstrated in this work. As suggested above, modification of the CNCs to be more hydrophobic would seem the next logical step in the development of CNCs as a broadly accepted polymer property modifier.

It can be argued that polymers themselves are not toxic materials. The toxicity arises in large part due to the many additives (e.g., processing aids, property modifiers) that are used in their synthesis and processing. CNCs may act as an important stepping stone towards more sustainable polymer production. This would include eliminating a toxic additive (e.g., crosslinkers) while providing even better performance. The effect of CNCs on latex viscosity and ultimately, film formation also implies that a lower solids latex could be used to achieve desired adhesive performance. Thus, less materials would be needed to achieve the same goals. At the same time, CNCs can be used with bio-based, renewable monomers, which traditionally lack strong mechanical properties.[1] Moreover, CNCs can play an important role towards increased polymer product sustainability.

References

[1] K. Leja and G. Lewandowicz, "Polymer Biodegradation and Biodegradable Polymers - A Review," *Polish J. Environ. Stud*, vol. 19, no. May, pp. 255–266, 2010.

Appendix A: Additional Figures

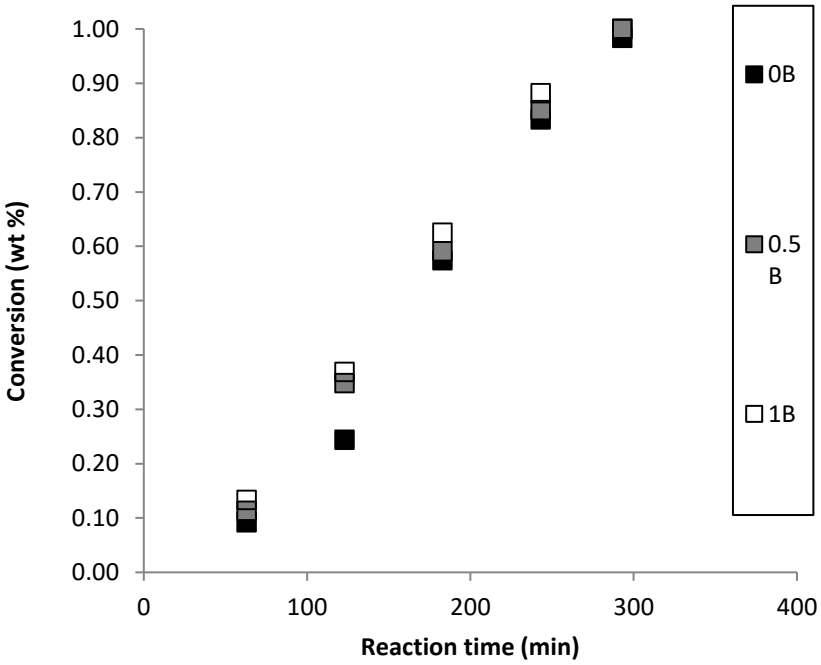

Figure A-1: Conversion vs. time formulation I-B

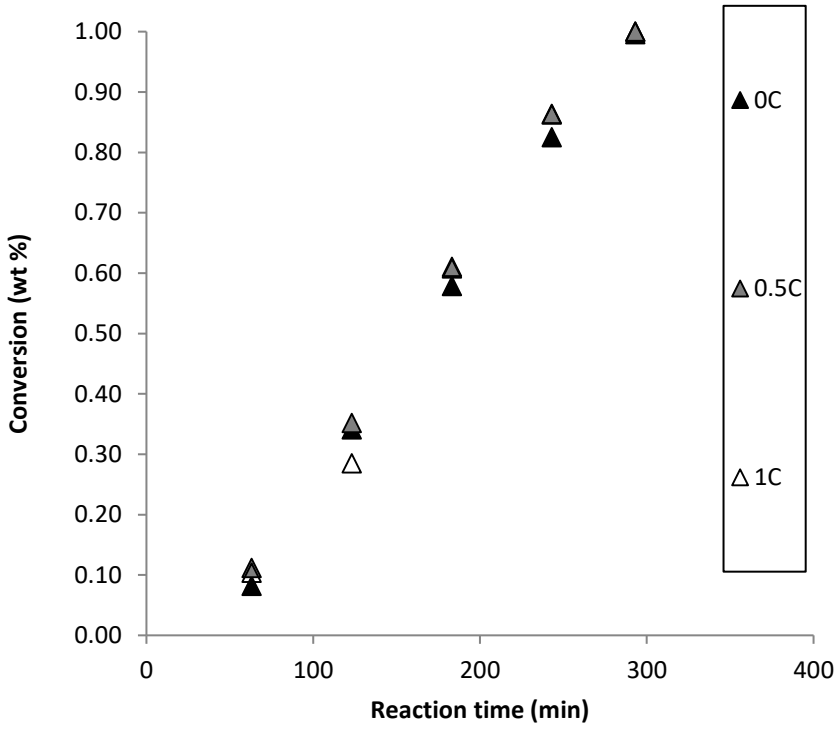

Figure A-2: Conversion vs. time formulation I-C

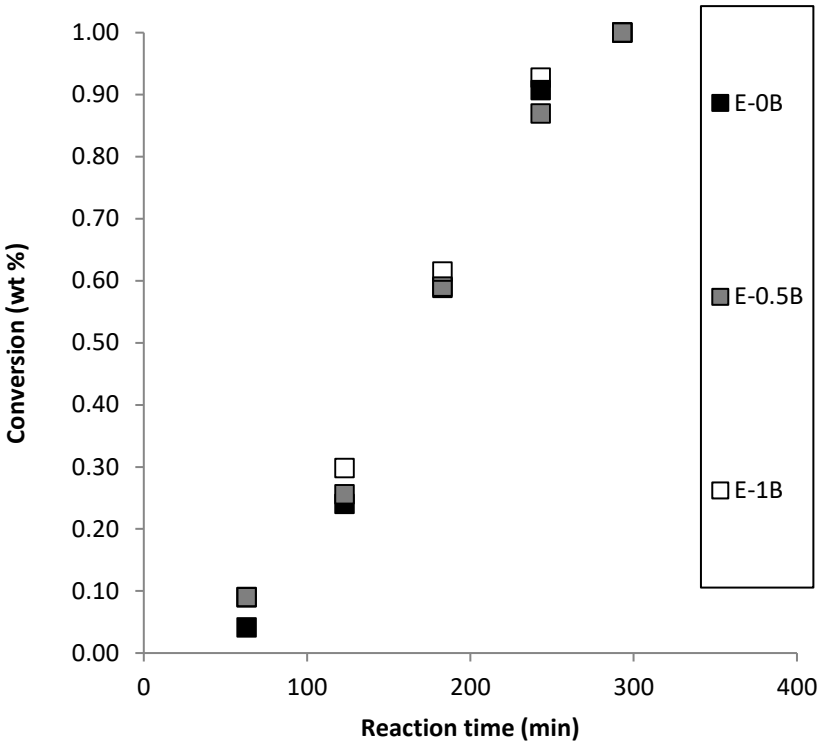

Figure A-3: Conversion vs. time formulation E-B

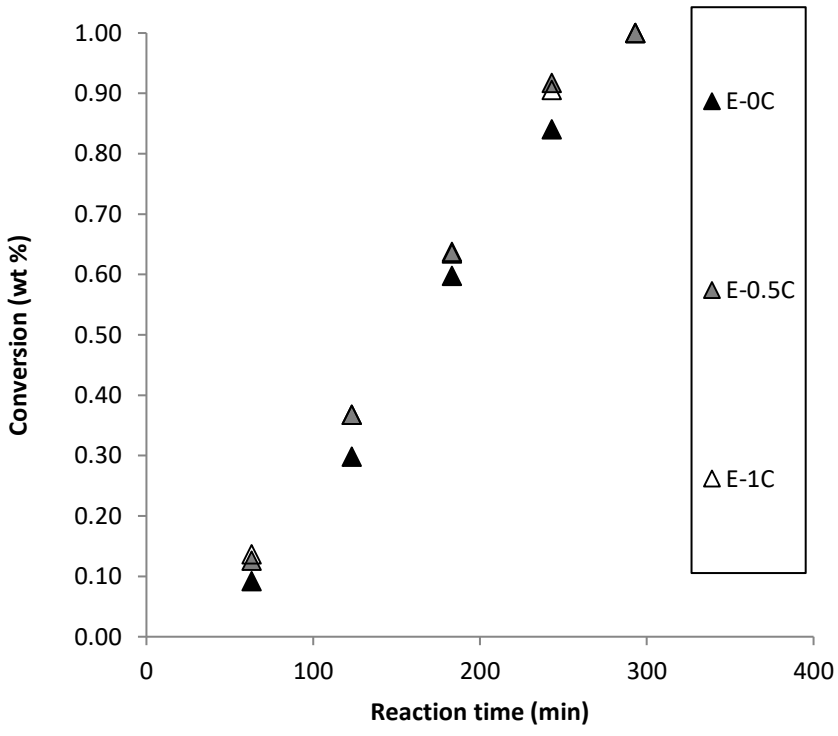

Figure A-4: Conversion vs. time for formulations E-C

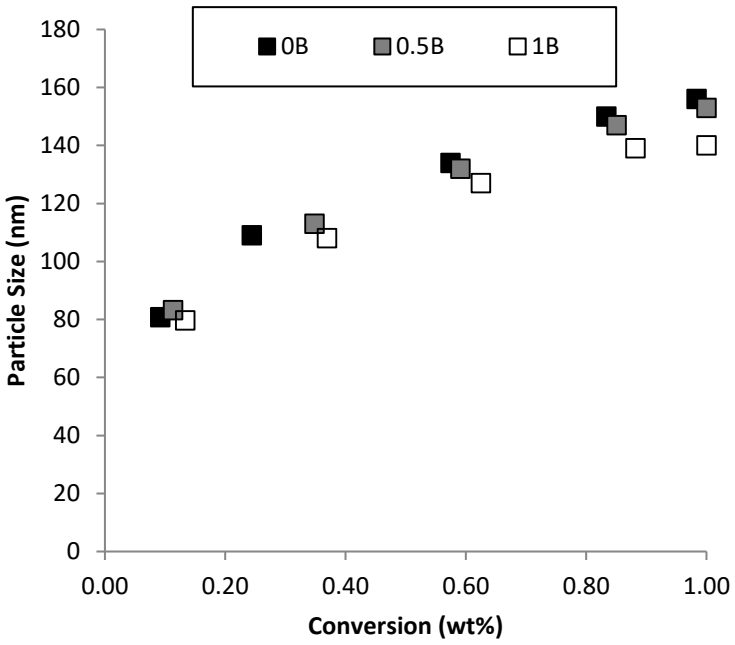

Figure A-5: Particle size vs. conversion formulation I-B

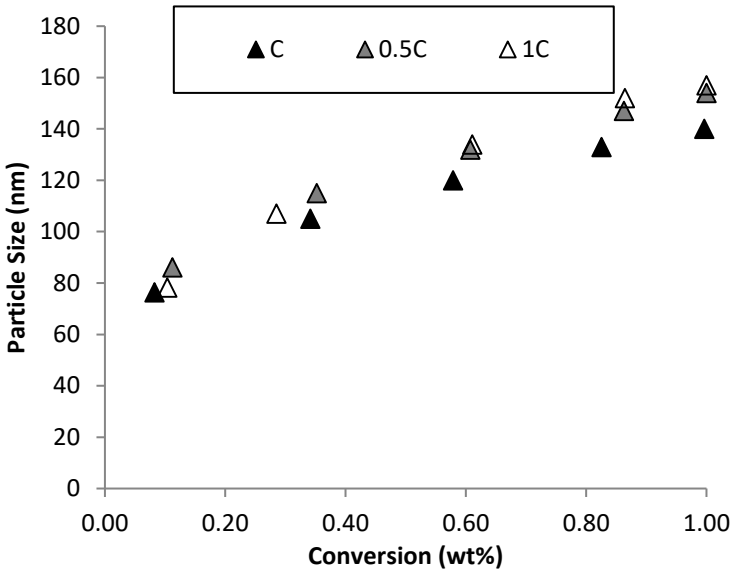

Figure A-6: Particle size vs. conversion formulation I-C

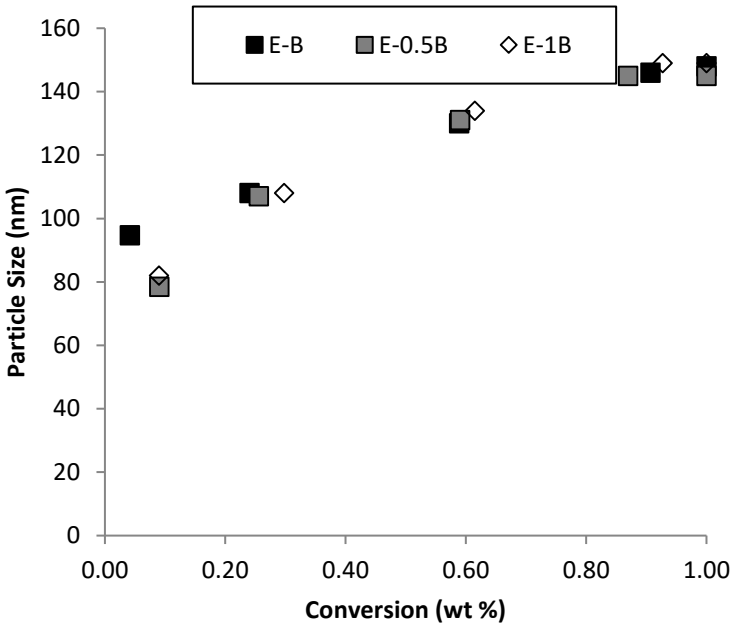

Figure A-7: Particle size vs. conversion formulation E-B

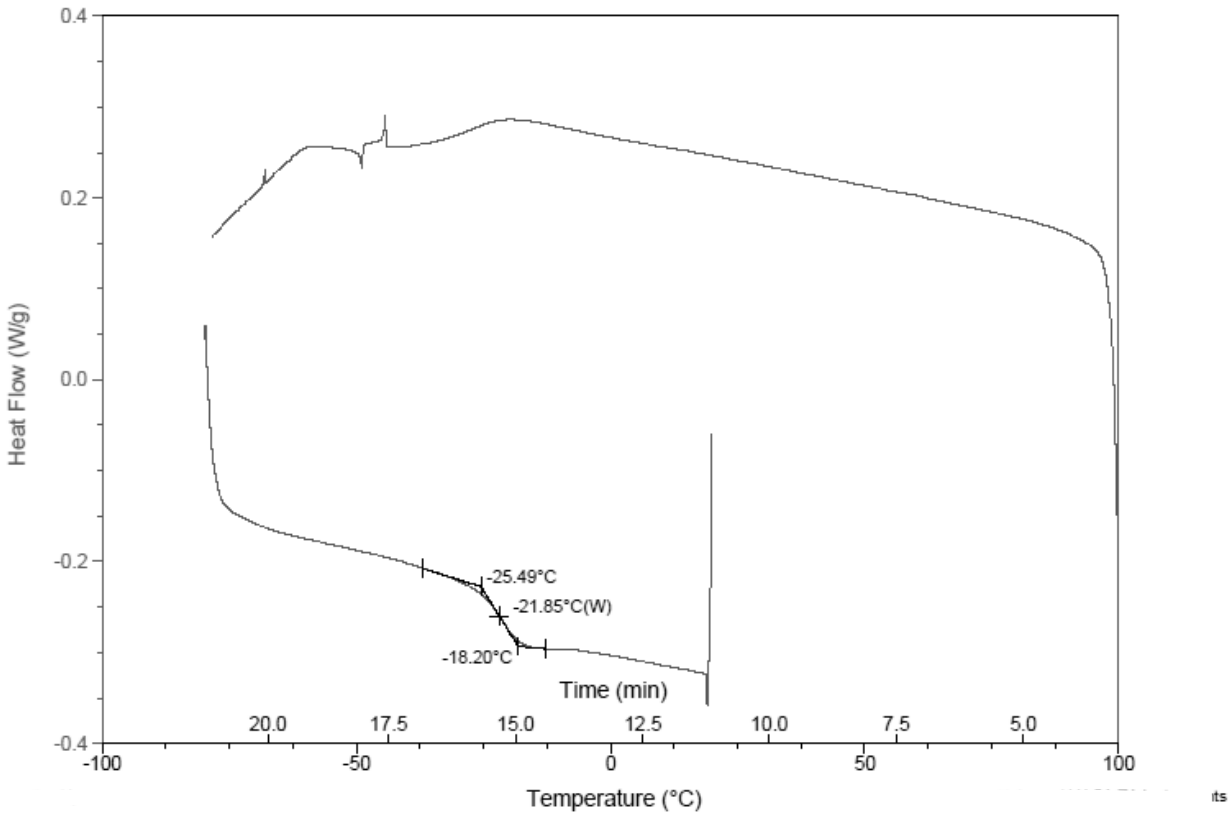

Figure A-8: Heating curve for I-0A formulation

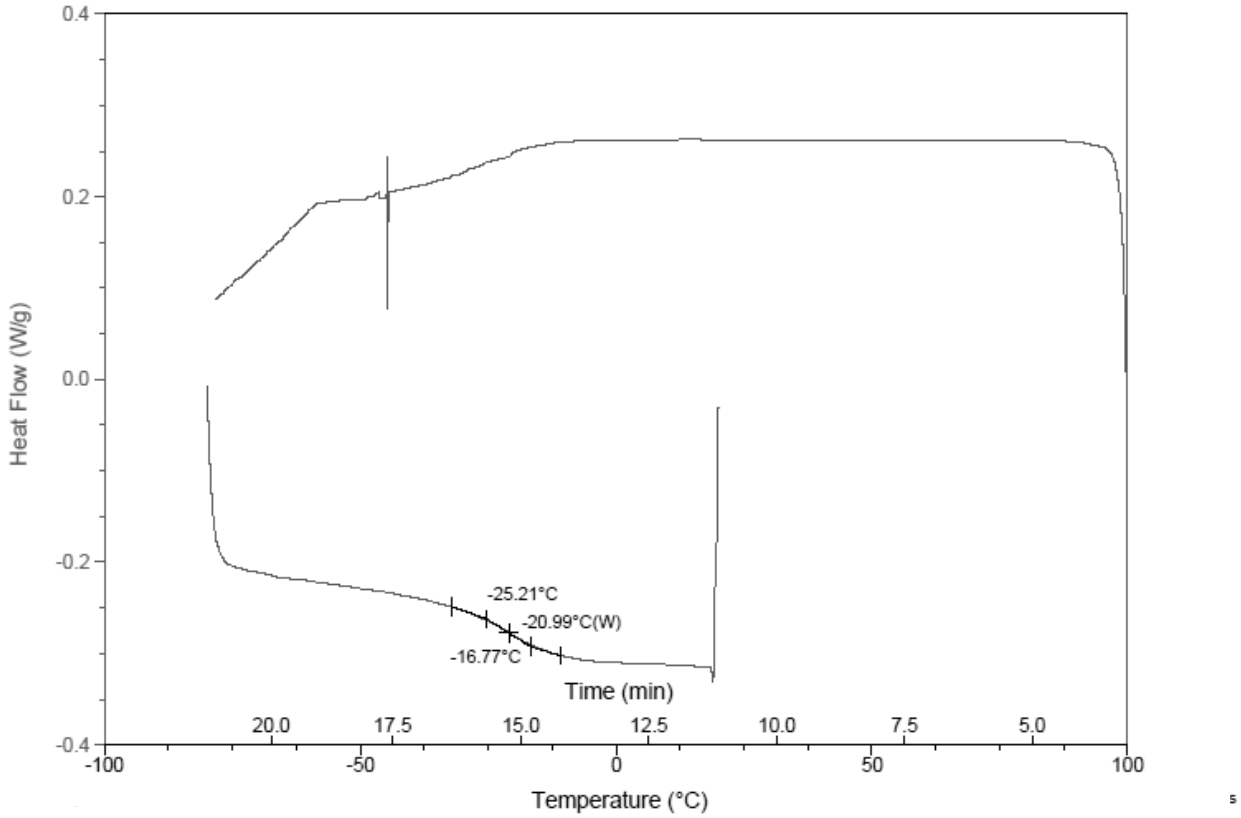

Figure A-9: Heating curve for E-1A formulation

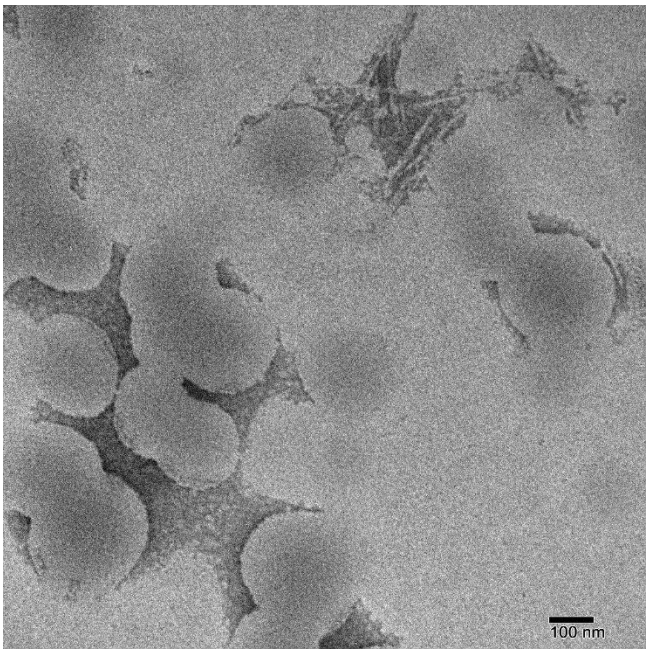

Figure A-10: TEM image of I-0.5A formulation

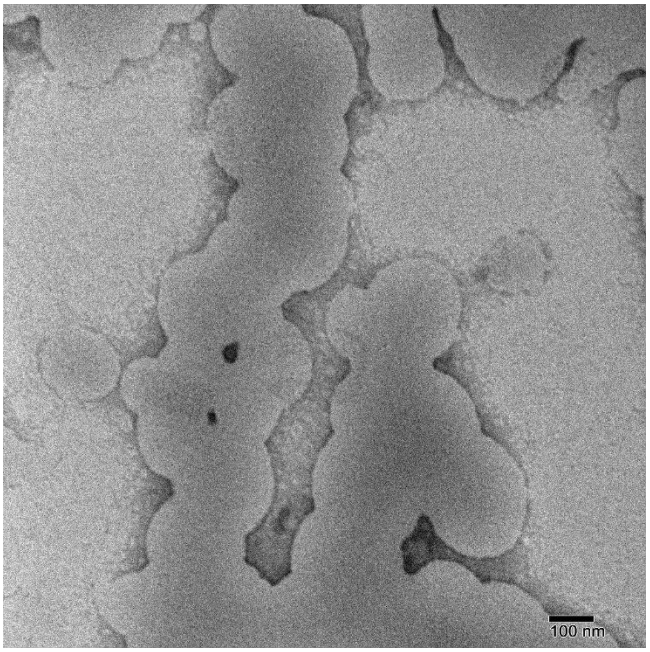

Figure A-11: TEM image of I-0B formulation

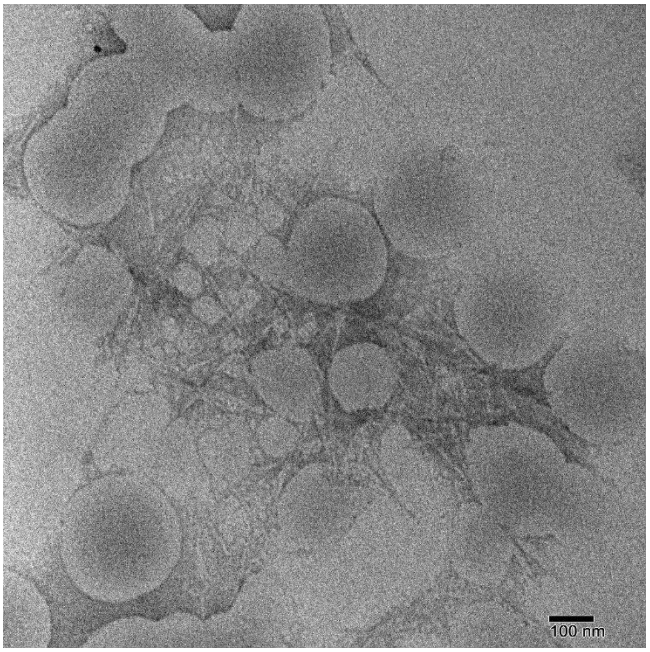

Figure A-12: TEM image I-0.5B formulation

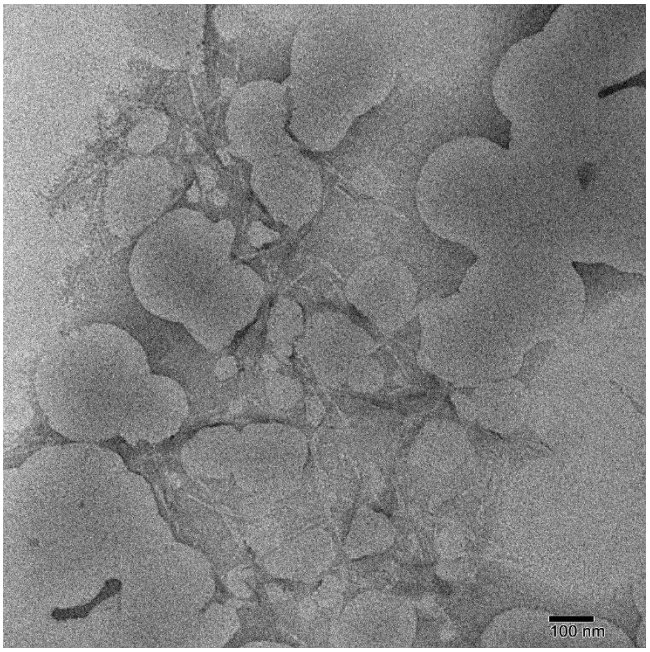

Figure A-13: TEM image of I-1B formulation

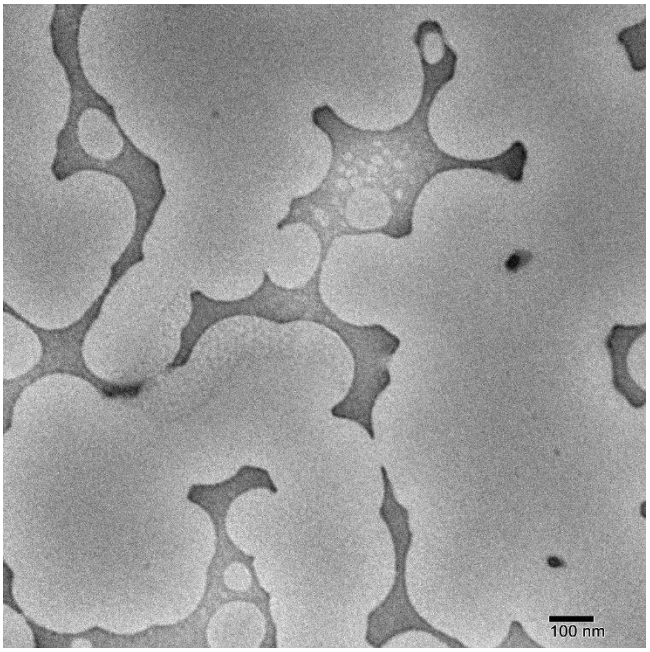

Figure A-14: TEM image of I-0C formulation

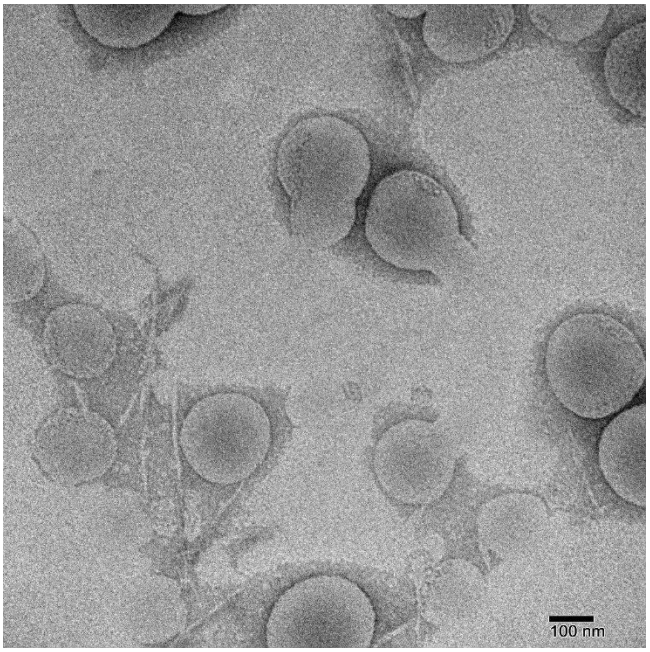

Figure A-15: TEM image of I-0.5C formulation

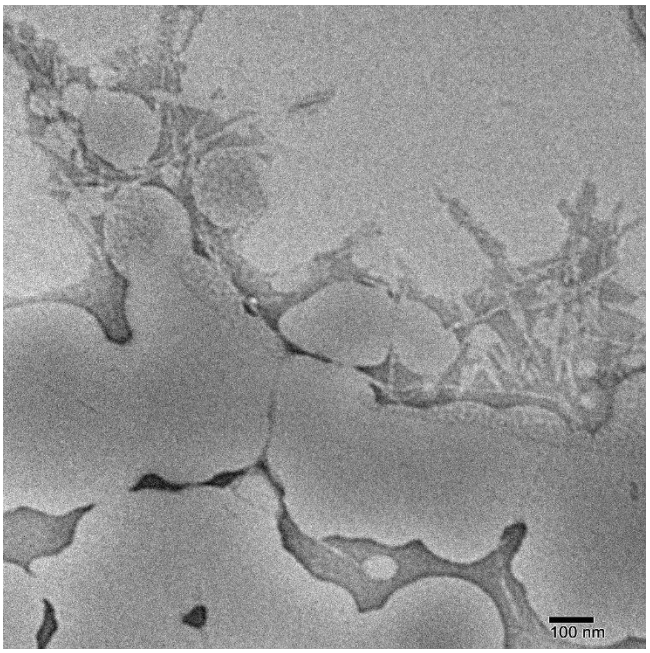

Figure A-16: TEM image of I-1C formulation

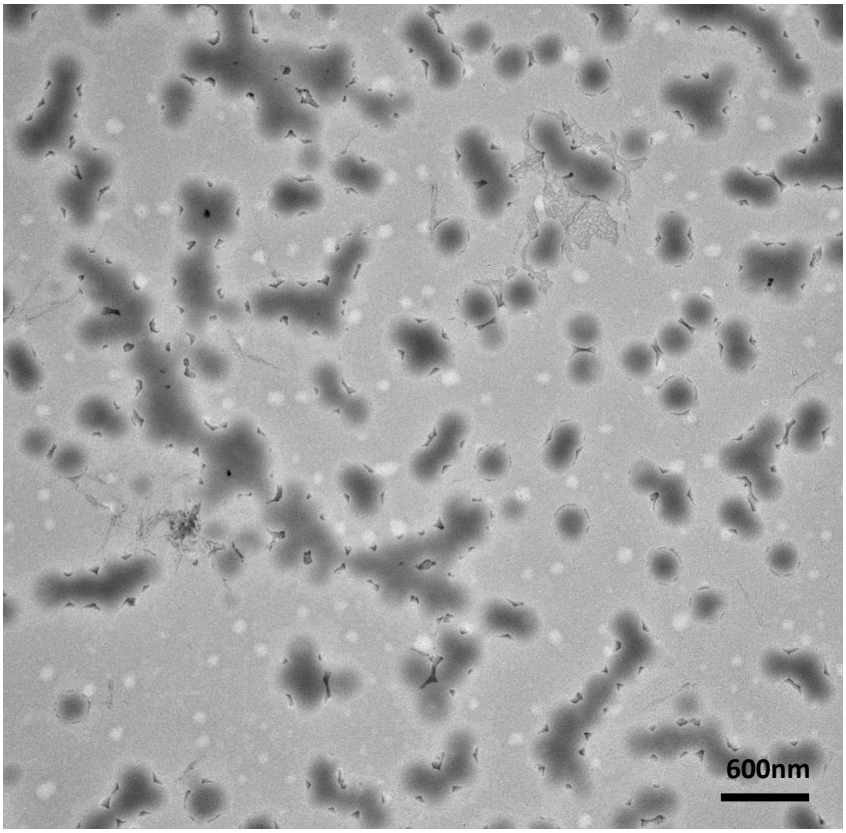

Figure A-17: TEM image of E0.5A formulation

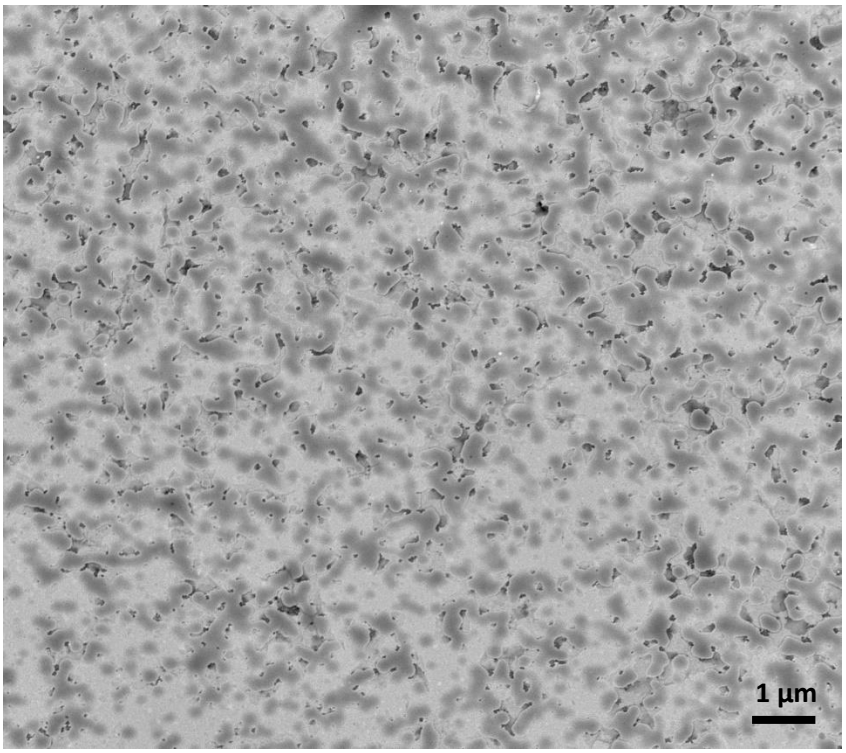

Figure A-18: TEM image of E0.5B formulation

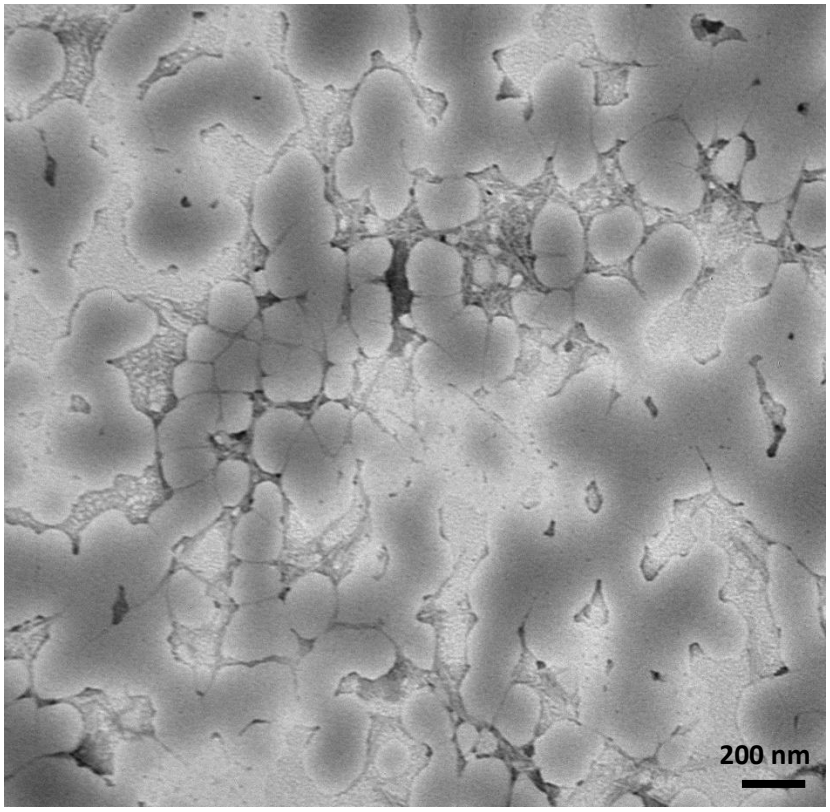

Figure A-19: TEM image of E-1B formulation

Note: Images for E-0B, E-0C and E-0.5C have not been provided due to clarity issues.

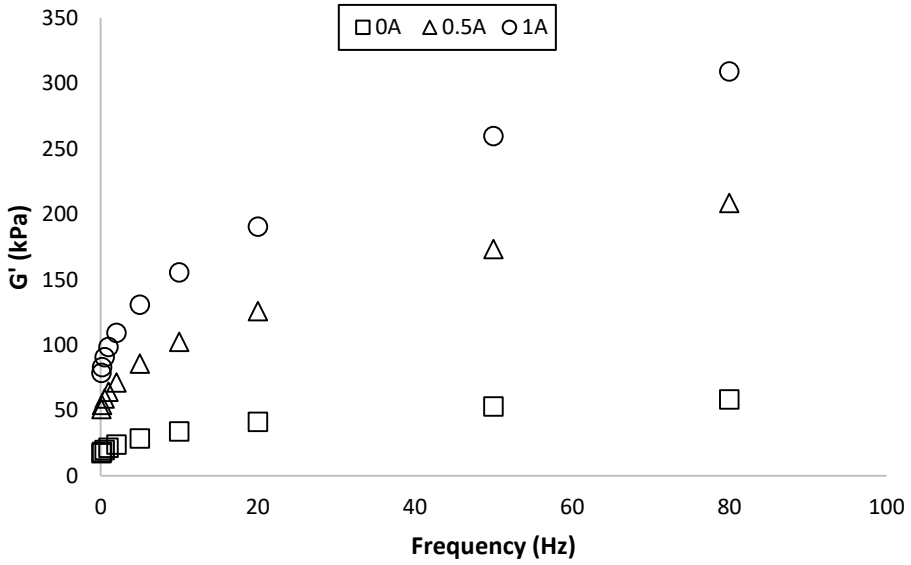

Figure A-20: Storage modulus for A formulations

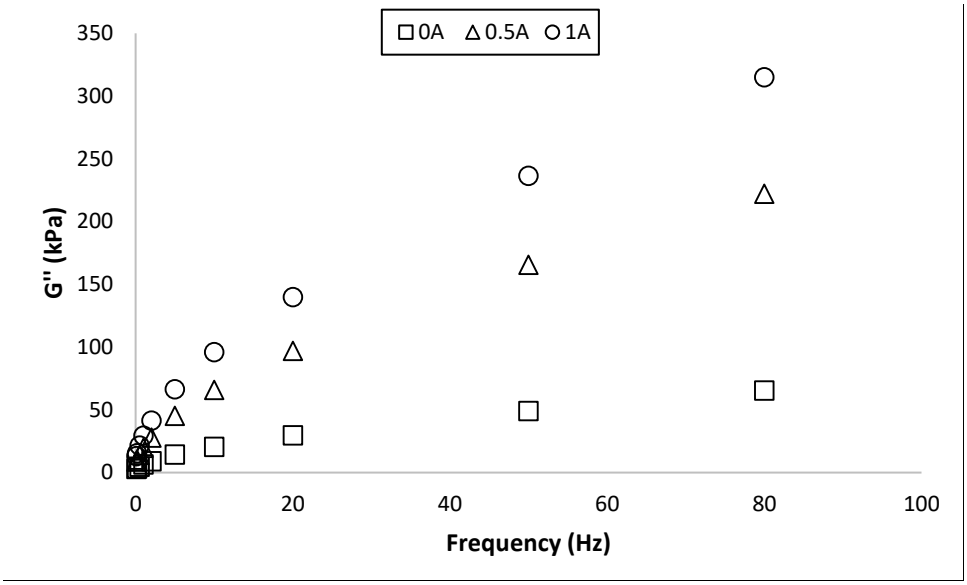

Figure A-21: Loss modulus for A formulations

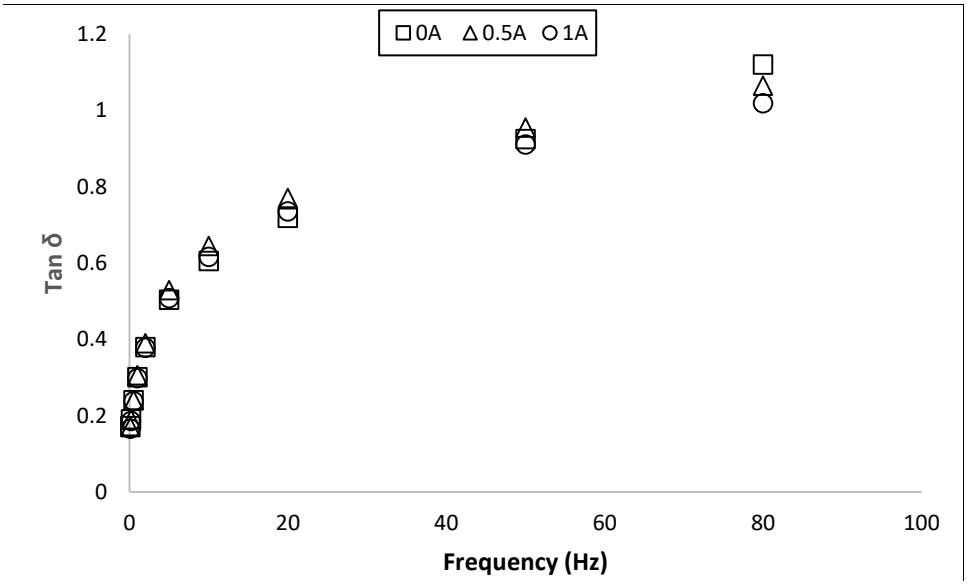

Figure A-22: Tan δ for A formulations

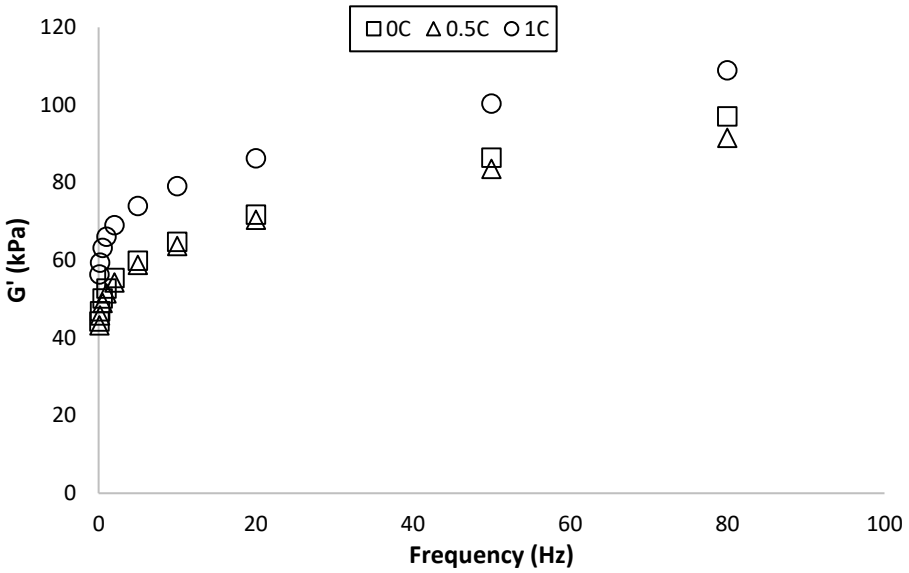

Figure A-23: Storage modulus for C formulations

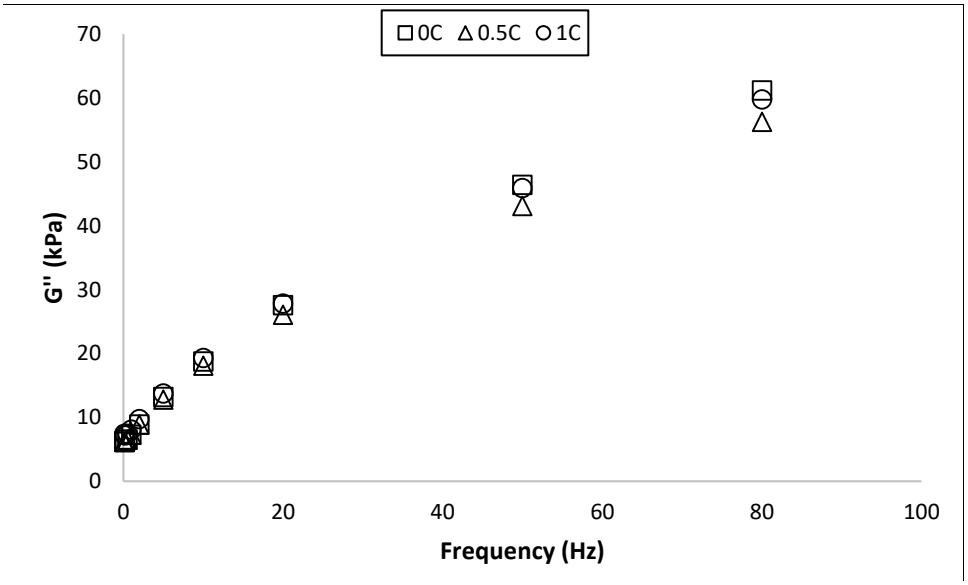

Figure A-24: Loss modulus for C formulations

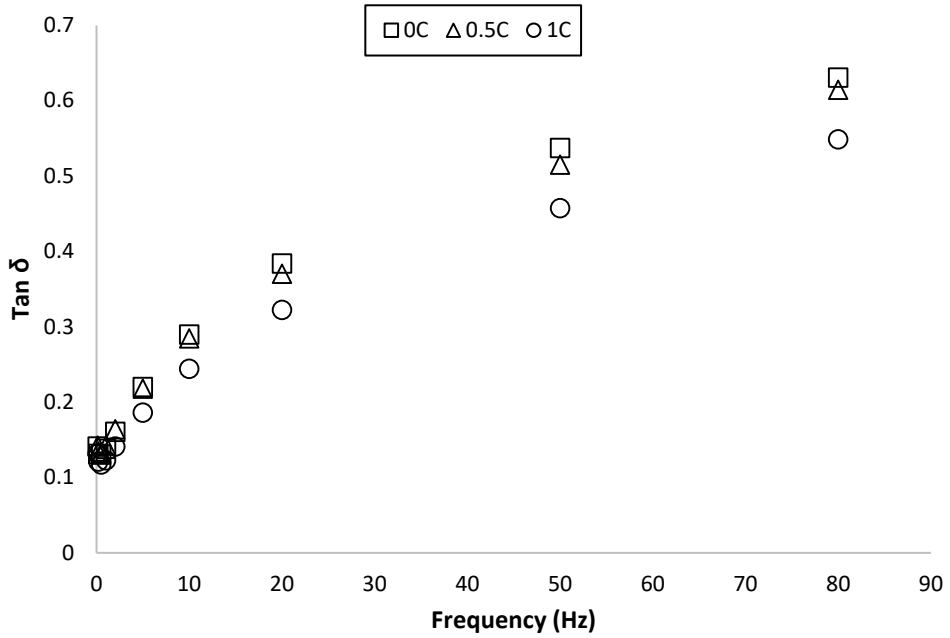

Figure A-25: Tan δ for C formulations

H-NMR Calculations

IBA/BA/MMA System

Knowing the peak assignment from 3.5-4 ppm (peaks J, D and P), it is possible to approximate the composition of the polymer. Three independent equations are known since these peaks do not overlap each other. The hydrogens assigned to each peak are outlined in Table A-1. Because the number of hydrogens is known for each peak, it is possible to calculate how many moles of each polymer are present by dividing each peak by the respective amount of hydrogens present. For example, using peak A, by dividing the integral at A by 2, the result will be the number of moles of PBA present. This can be repeated for peaks B and C. Then, the mole fractions can be calculated and therefore the overall composition is known.

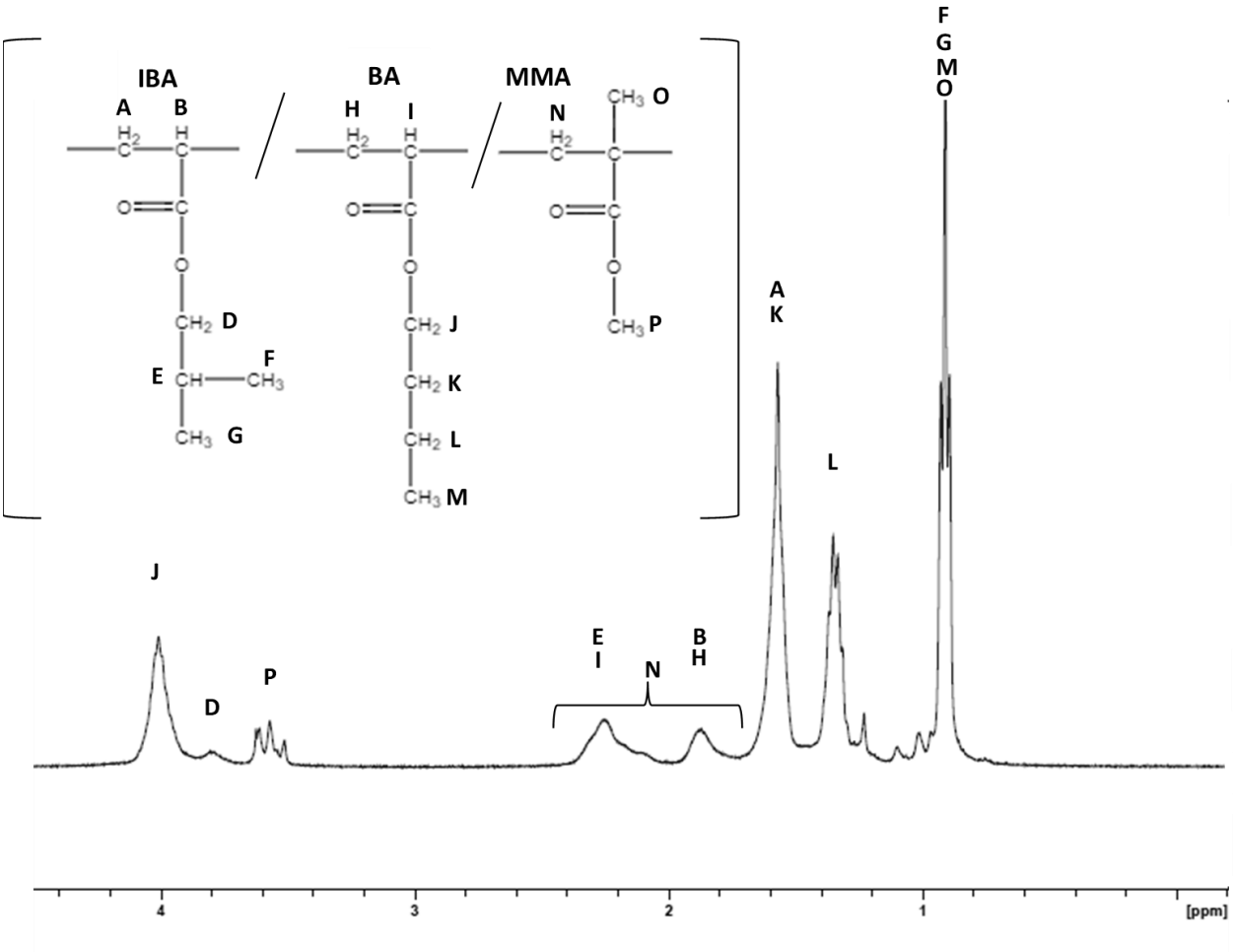

Figure A-26: NMR results for I-0C formulation

Table A-1: Peak assignments for I-0C H-NMR

Peak Label	Expected ppm	Number of Hydrogens
J	4	2
D	3.8	2
P	3.5	3

EHA/BA/MMA System

Using the obtained spectra (Figure A-27), it is possible to estimate the composition of the resulting polymer. Three equations can be built from the three integrals outlined in Table A-2. The number of moles of each species present can be determined by solving the following three equations

simultaneously, where x, y and z represent the mole fractions of EHA, BA, MMA, respectively. The mole fraction of each species can also be found.

$$I_1 = 18x + 10y + 5z$$

$$I_2 = 3z$$

$$I_3 = 2x + 2y$$

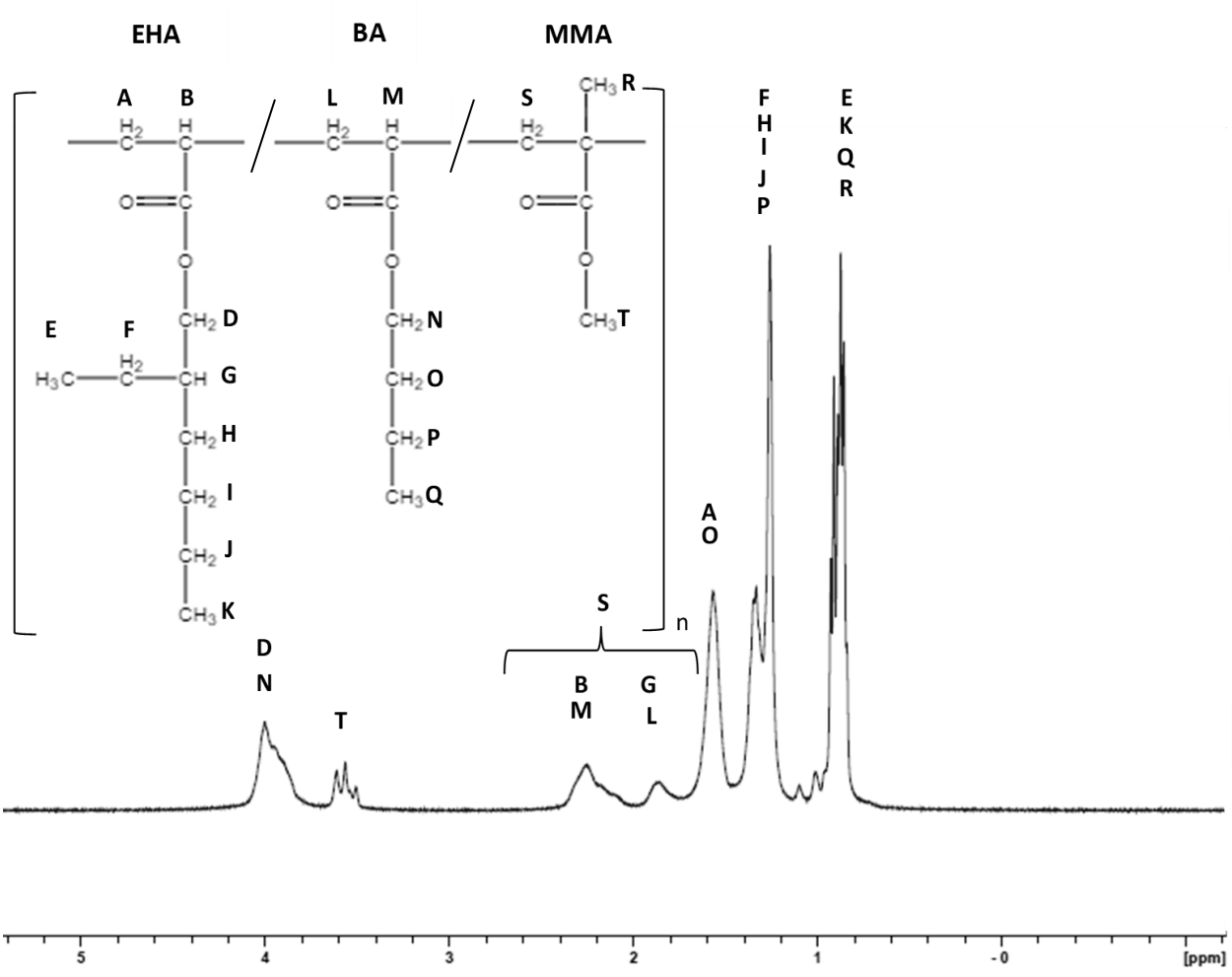

Figure A-27: NMR results for E-1C formulation

Table A-2: Peak assignments for E-1C H-NMR

Polymer	Integral [0-2.5 ppm]	Integral [3.8 ppm]	Integral [3.9-4.1 ppm]
PEHA protons	18 (B, E, F, G, H, I, J, K)	0	2 (D)
PBA protons	10 (L, M, O, P, Q)	0	2 (N)
PMMA protons	5 (R, S)	3 (T)	0

Appendix B: Health and Safety Report

Safety precautions are of utmost importance when using monomers and solvents in the laboratory. All experiments were performed safely and while wearing proper PPE (i.e., nitrile gloves, a lab coat, safety glasses and a respirator).

Pressure Extremes

Liquid nitrogen as well as gaseous nitrogen tanks were used to perform DMA and reactions, respectively. Proper handling and transfer of pressurized tanks was used.

Temperature Extremes

All reactions were conducted at 60 ˚C. Care was taken to avoid touching any hot surfaces around the reactor. Liquid nitrogen was also used for DMA; heat-resistant gloves were worn to perform DMA.

Chemical Hazards

All chemicals used in this work are summarized in Table B-1 denoting their hazards and recommended storage methods obtained from the material safety data sheets. All monomers were stored in a refrigerator and were handled inside a fume hood. Recall that CNCs are considered non-hazardous and thus are not listed.

Table B-1: Hazards and storage methods for all chemicals used in this work

Type	Compound	Hazard	Storage method	Protective measures
Monomer	Isobutyl acrylate	Toxic + irritant (skin, eyes, inhalation, ingestion)	Dry, ventilated area	PPE (i.e., nitrile gloves, a lab coat, safety glasses and a respirator).
	n-Butyl acrylate	Toxic + irritant (skin, eyes, inhalation, ingestion)	Dry, ventilated area	
	Methyl methacrylate	Toxic + irritant (skin, eyes, inhalation, ingestion)	Dry, ventilated area	
	2-Ethylhexyl acrylate	Toxic + irritant (skin, eyes, inhalation, ingestion)	Dry, ventilated area	PPE (i.e., nitrile gloves, a lab coat, safety glasses and a respirator).
Solvents	Acetone	Toxic + irritant (skin, eyes, inhalation, ingestion)	Flammables cabinet	
	THF	Acute toxicity and irritant (skin, eyes, inhalation, ingestion)	Flammables cabinet	
	Chloroform-d	Toxic, carcinogenic, irritant (skin, eyes, inhalation, ingestion)	Dark place (sensitive to light)	
Initiator	KPS	Toxic, irritant (skin, eyes, inhalation, ingestion)	Dry area, away from heat	
Surfactant	SDS	Toxic + irritant (skin, eyes, inhalation, ingestion)	Dry area	PPE (i.e., nitrile gloves, a lab coat, safety glasses and a respirator).